Summer school on cosmological numerical simulations
3rd week – FRIDAY

Helmholtz School of Astrophysics
Potsdam, July/August 2006

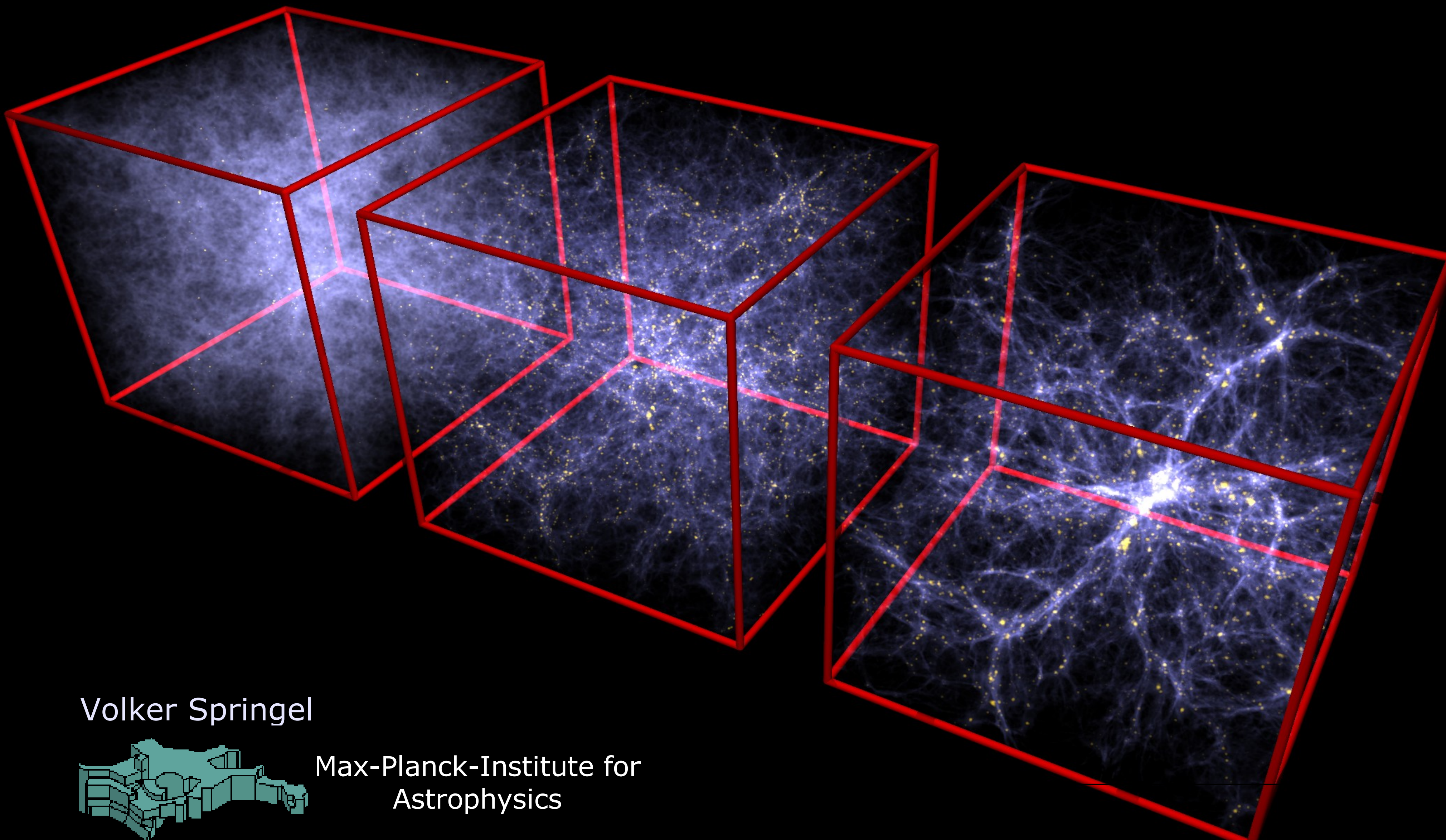

Volker Springel

Max-Planck-Institute for Astrophysics

Galaxy mergers and the role of feedback in galaxy formation

FRIDAY-Lecture of 3rd week

Volker Springel

- **First quasars**
- **History of elliptical galaxies**
- **Version control systems (CVS, subversion)**
- **Lyman-alpha forest**
- **A few WMAP3 implications**

Formation of the first quasar

In the Millennium Simulation, we can identify most massive halos/galaxies at z~6.2 as plausible Sloan quasar candidates

DARK MATTER AND GALAXY DISTRIBUTION AROUND THE GALAXY WITH THE LARGEST STELLAR MASS AT Z=6.2

$M_h = 5.3 \times 10^{12}\ h^{-1} M_\odot$

$M_* = 8.2 \times 10^{10}\ h^{-1} M_\odot$ SFR = 235 $M_\odot$ / yr

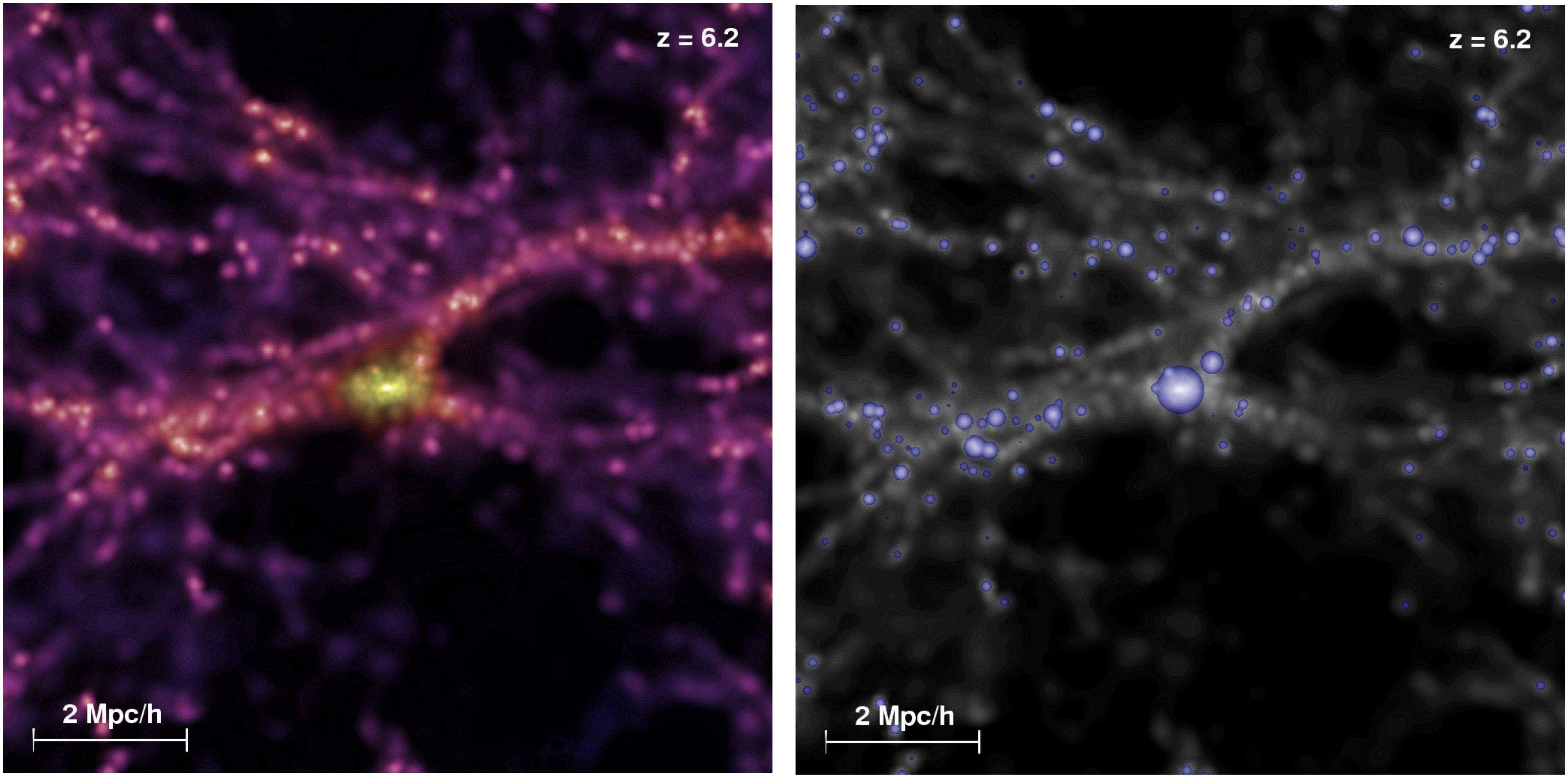

Springel et al. (2005)

The quasars end up as cD galaxies in rich galaxy clusters today

TRACING GALAXIES OVER COSMIC TIME

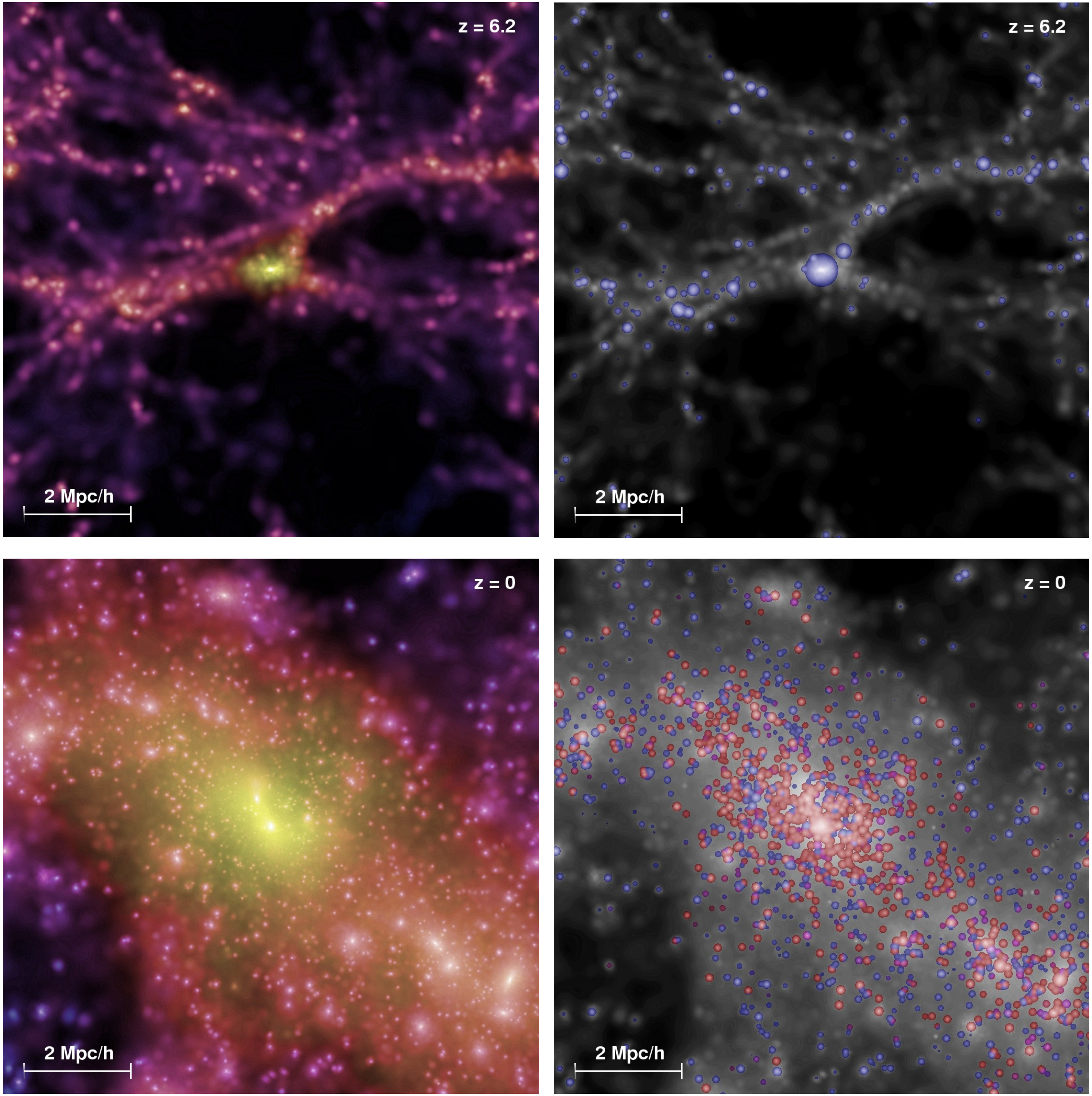

The rareness of high-z quasars requires a huge volume for the selection of a suitable host halo

RESIMULATING A SLOAN QUASAR

Yuexing Li et al. (2006)

Parent sim: 1000 h^{-1}Mpc, 400^3

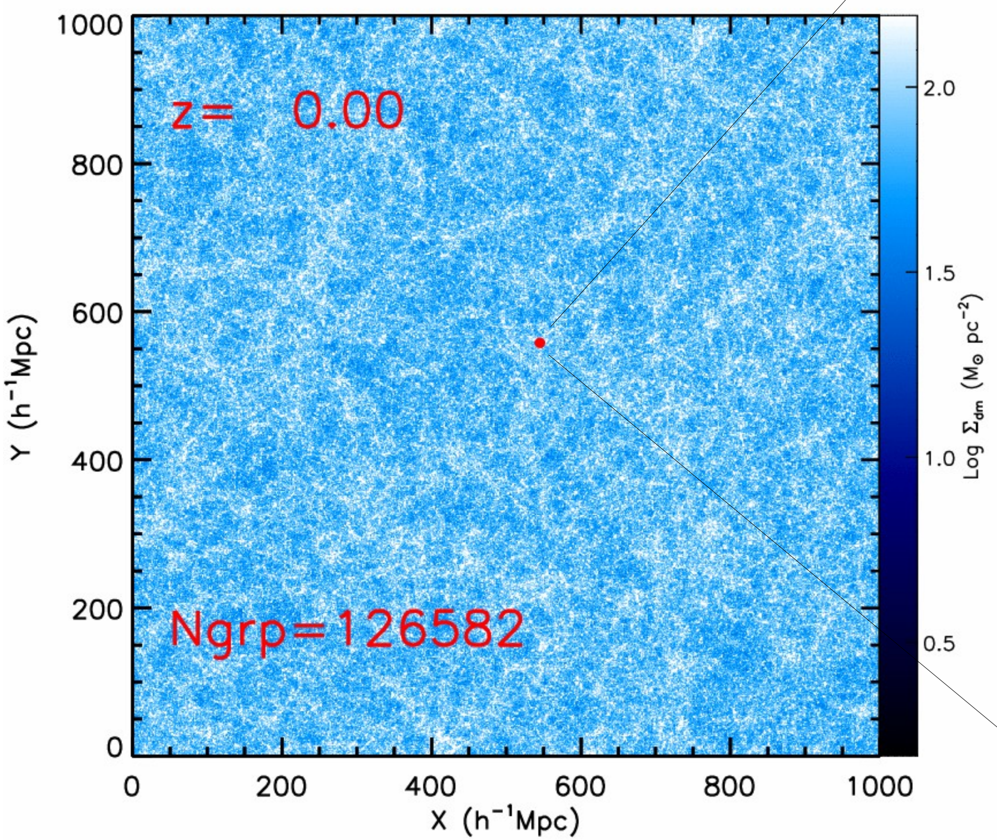

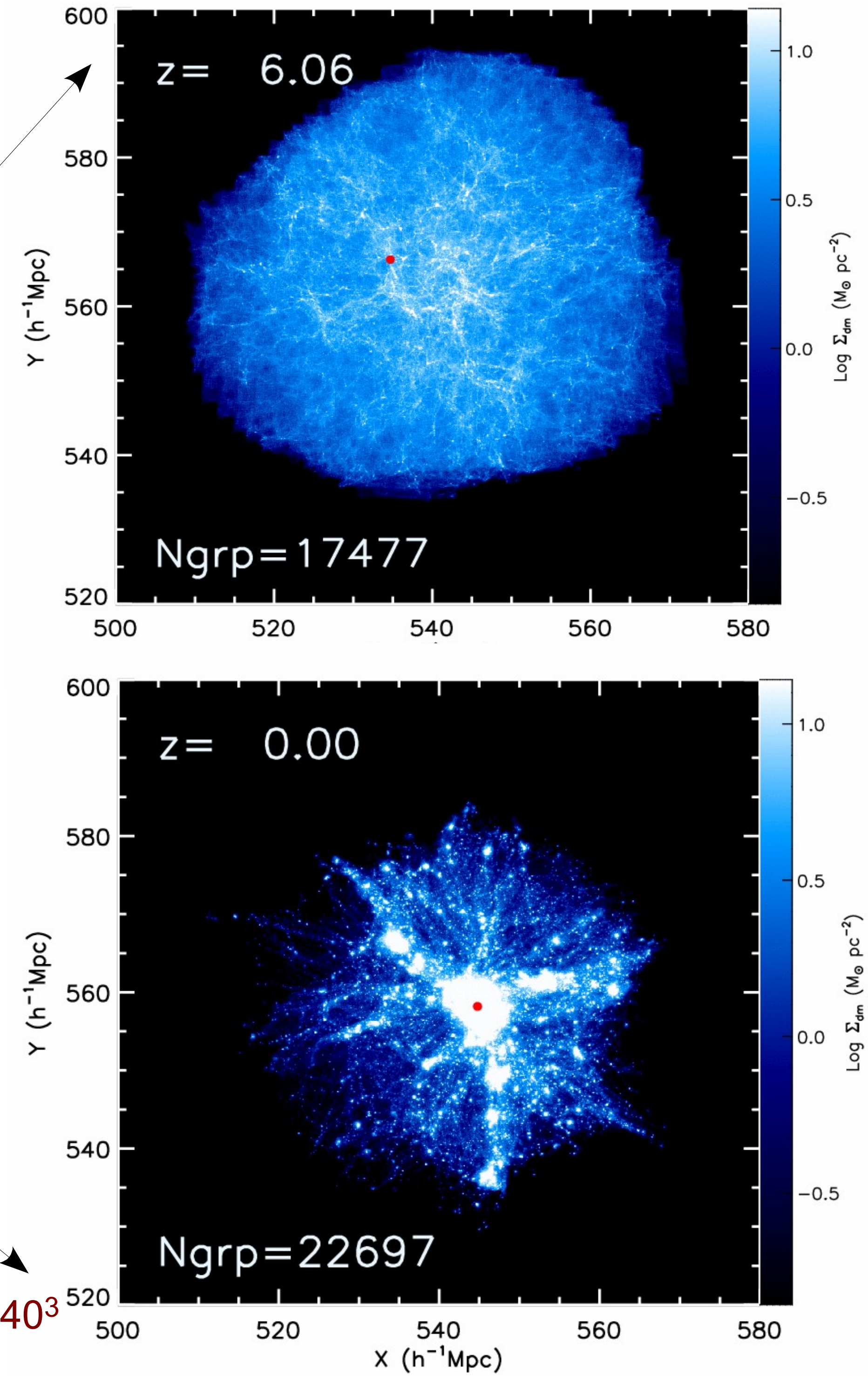

Zoom: HR-region ~30 h^{-1}Mpc, 340^3

A measurement of the merger tree in the dark matter simulation is used to set-up a hydrodynamical multi-merger reconstruction of the formation history of the halo

DETAILS OF THE PROGENTOR SET-UP

Li et al. (2006)

BH seeds are assumed to have grown at Eddington from 200 $M_\odot$ at z=30 to the time they enter the calculation.

The total seed BH mass is less than 1% of the final BH mass.

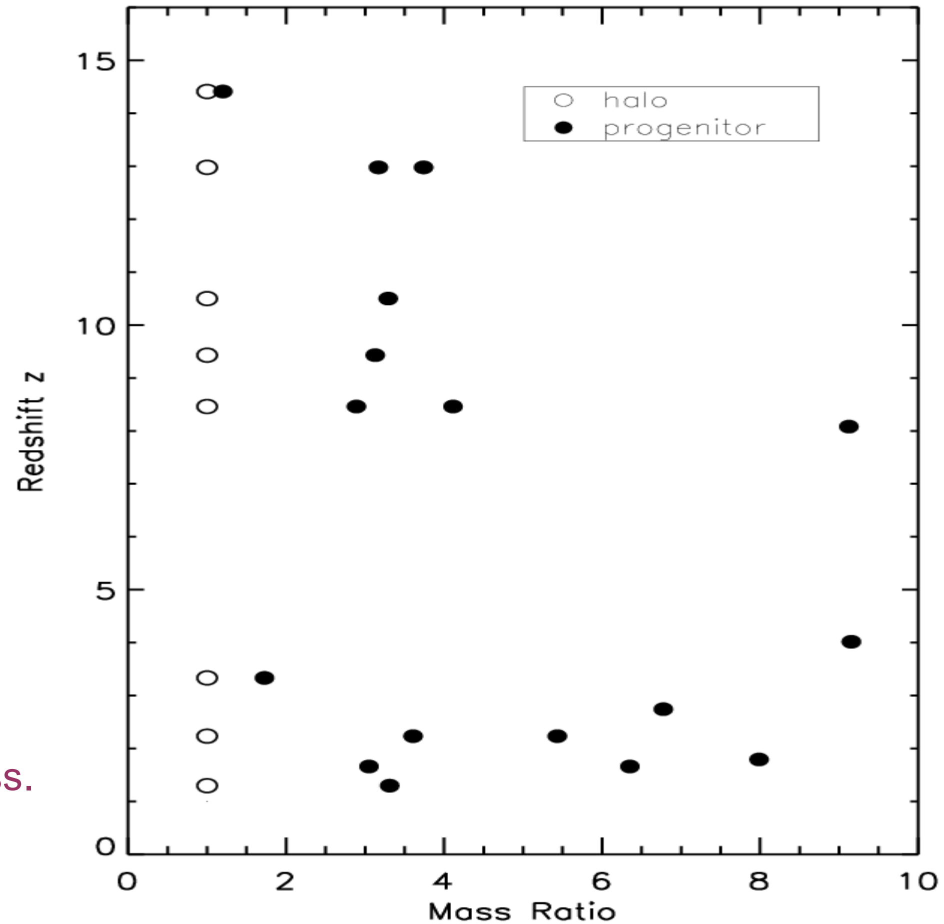

Galaxy[1]	z[2]	M_{vir}[3] $[10^{10} M_\odot]$	V_{vir}[4] [km/s]	f_{gas}[5]	M_{BH}[6] $[10^5 M_\odot]$	θ_1[7]	ϕ_1[8]	θ_2[9]	ϕ_2[10]	R_p[11] [kpc]	R_0[12] [kpc]
G1	14.4	9.0	234.1	1.0	0.21	–	–	–	–	–	–
G2	14.4	7.5	220.3	1.0	0.21	128.7	34.6	144.9	24.0	0.2	7.1
G3	13.9	21.4	297.8	1.0	0.51	38.3	93.9	94.2	119.6	0.2	8.5
G4	13.9	25.3	314.6	1.0	0.51	68.3	319.5	115.2	99.0	0.3	10.7
G5	10.5	70.1	401.0	1.0	3.56	81.7	230.2	87.8	198.9	0.4	11.3
G6	9.4	113.7	448.6	0.9	16.4	61.4	49.9	41.2	80.4	0.5	18.2
G7	8.5	228.5	540.4	0.9	88.2	86.6	93.4	21.6	43.3	0.7	25.2
G8	8.5	296.7	589.5	0.9	88.2	113.3	259.1	80.0	343.3	1.0	34.5

Hydro-simulation of the hierarchical build-up of an early Sloan quasar

TIME EVOLUTION OF THE PROJECTED GAS DISTRIBUTION

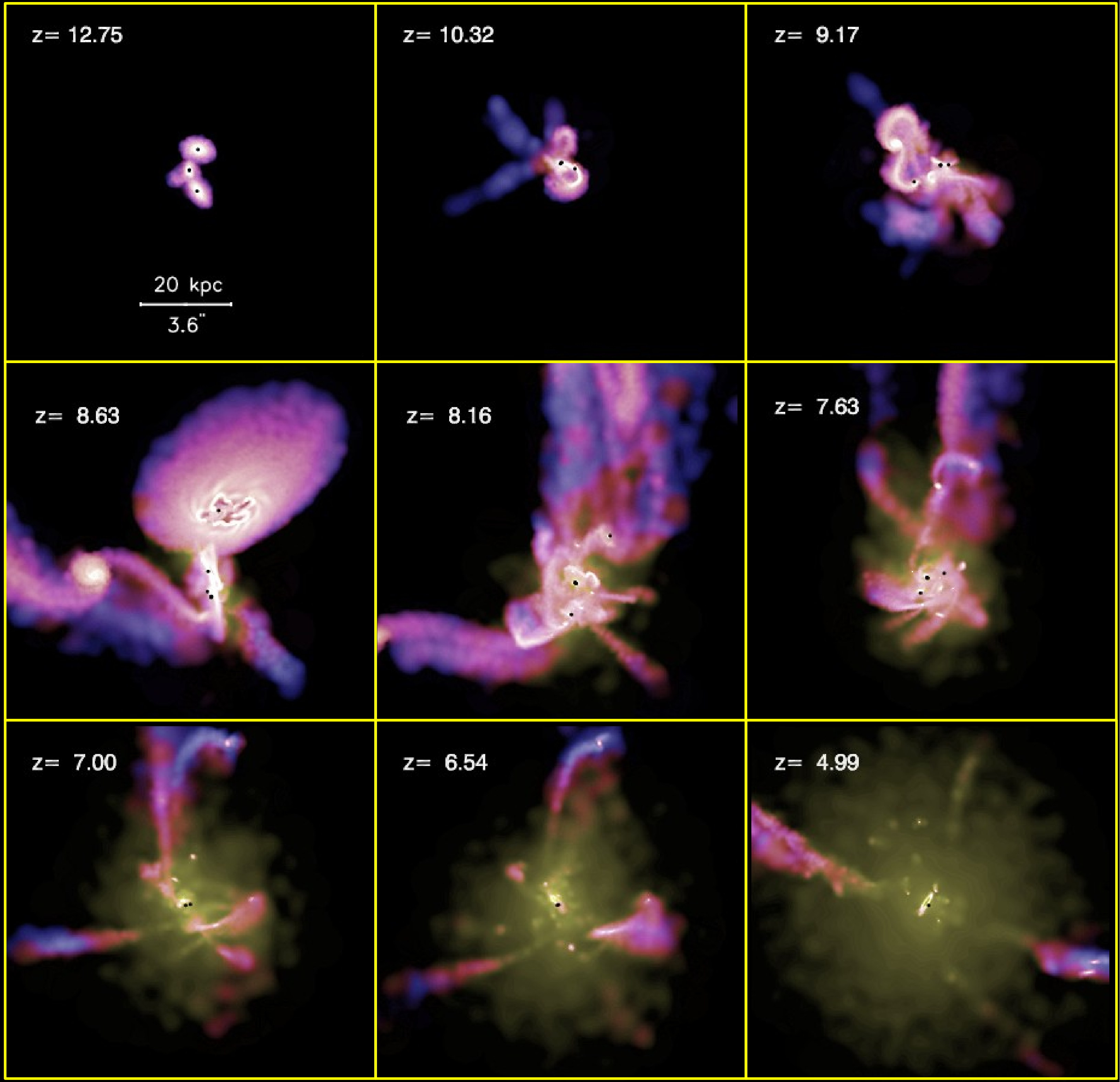

Li et al. (2006)

Hydro-simulation of the hierarchical build-up of an early Sloan quasar

TIME EVOLUTION OF THE PROJECTED STELLAR MASS

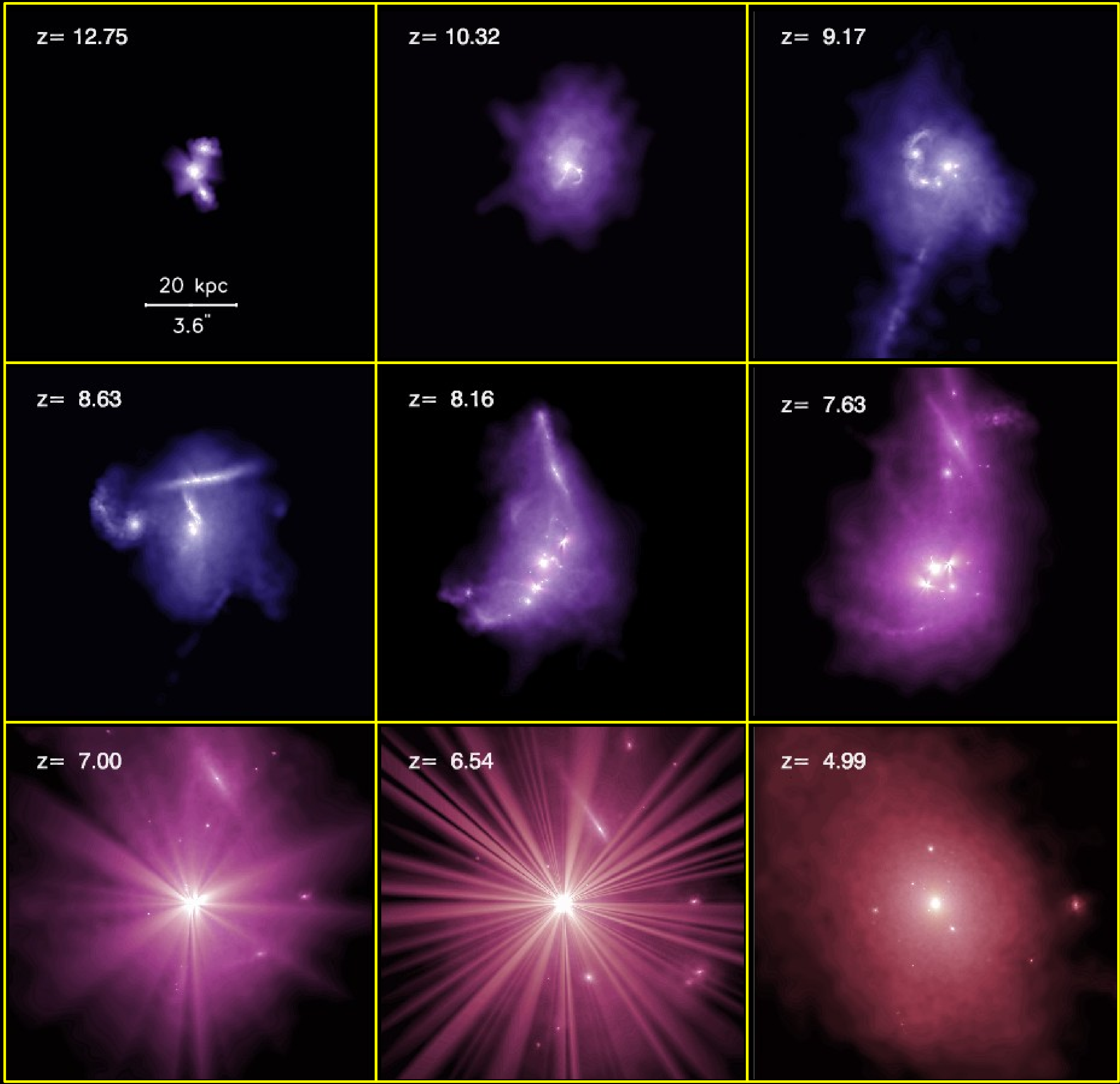

Li et al. (2006)

The black holes of the quasar progenitors have grown at ~50% of their liftetime at the Eddington luminosity, and show a high variability of their SFR

TIME EVOLUTION OF THE BH GROWTH AND THE HOST'S SFR

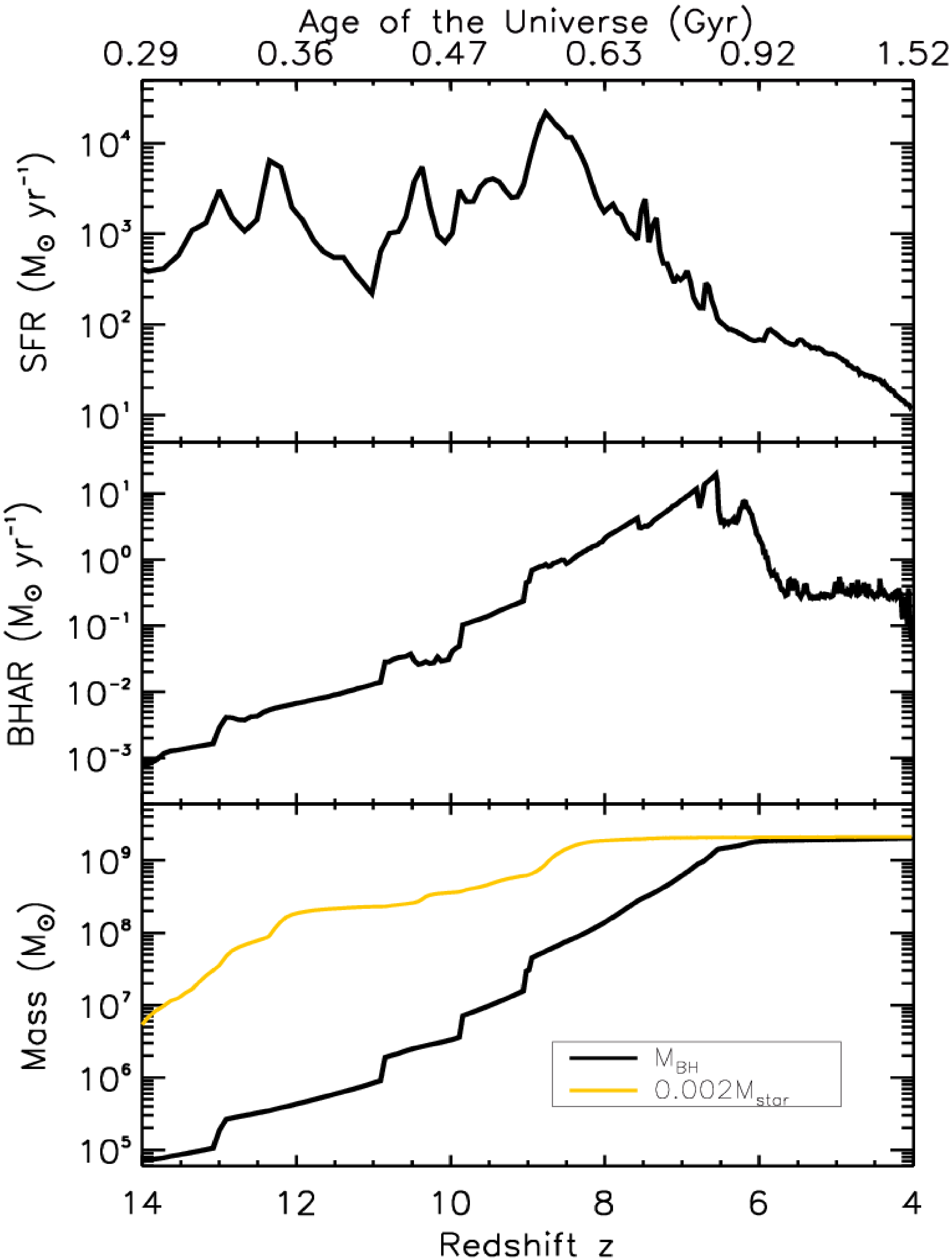

SFR peaks at >1000 $M_\odot$/yr at z~9, but drops to ~100 $M_\odot$/yr when the quasar is most luminous. Stellar mass at that time is 10^{12} $M_\odot$

Li et al. (2006)

The luminosity of the BH shows large variability and substantial line-of-sight dependence due to the obscuring gas distribution

LUMINOSITY EVOLUTION OF THE QUASAR AND THE HOST GALAXY

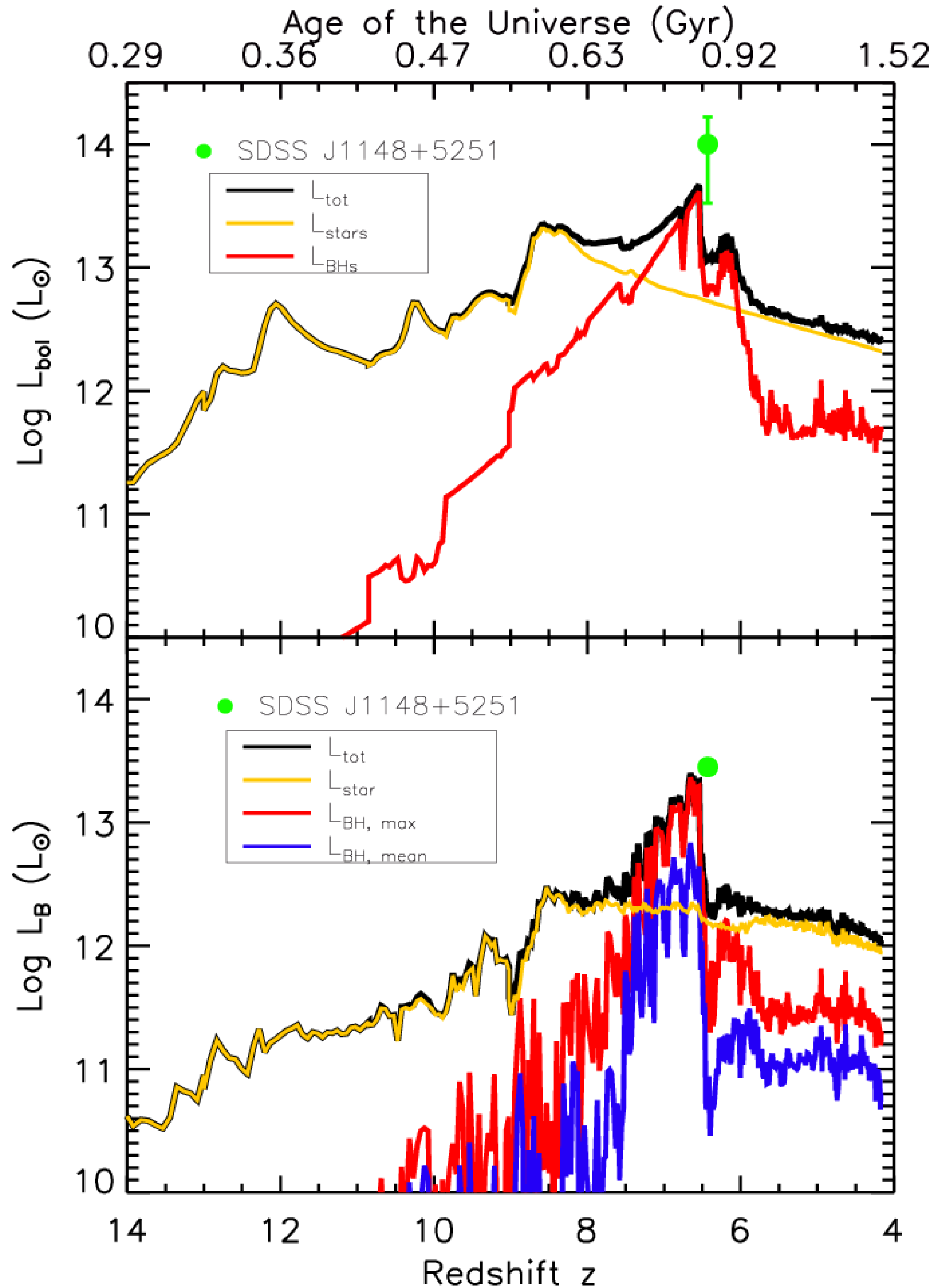

System is intrinsically bright can can power a ULRIG with $L > 10^{12}\ L_\odot$ for most of the simulation.

For the B-band luminosity, the obscuring gas column has been taken into account. The quasar would be visible as optically bright for ~160 million years between z=7.5 and z=6.4.

Li et al. (2006)

Using mergers of high-z galaxies, one can predict the evolution of the M_{BH} dispersion relationship

BH MASS – VELOCITY DISPERSION RELATIONSHIP AT DIFFERENT EPOCHS

Robertson et al. (2006)

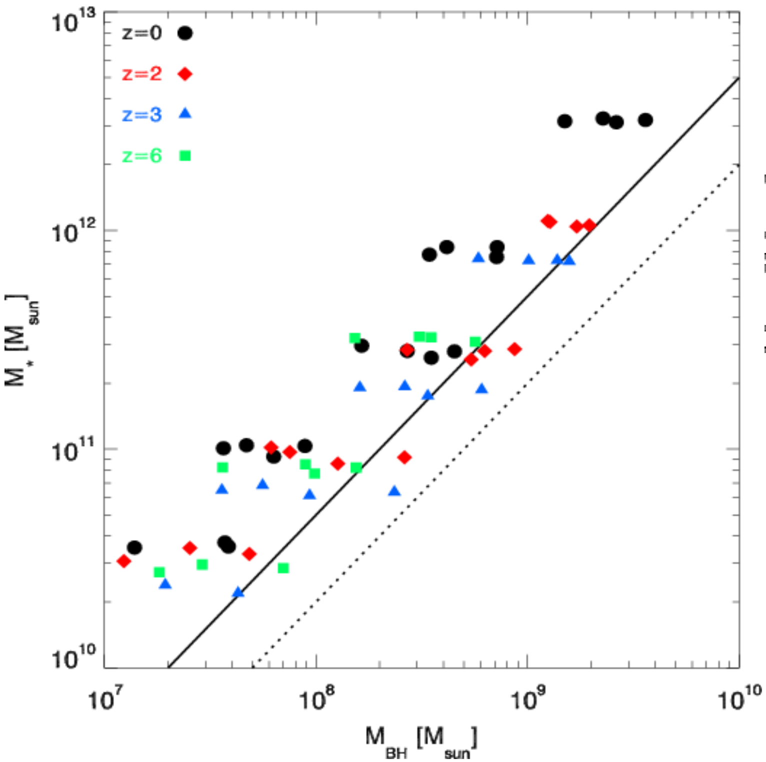

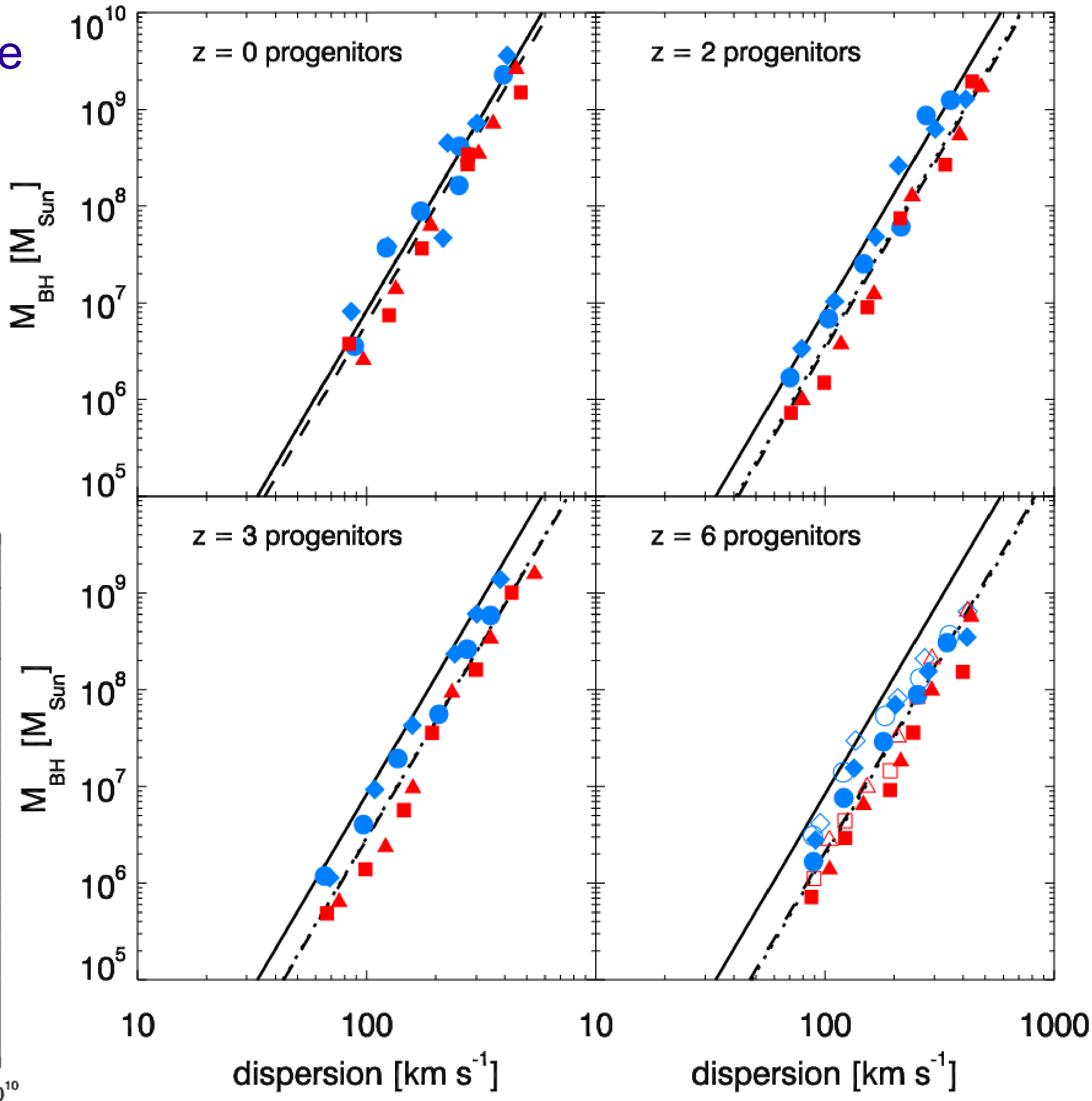

Black holes in semi-analytic models for galaxy formation

Dark matter simulations can now track the growth of all luminous galaxies in a representative piece of the universe

MILLENNIUM SIMULATION

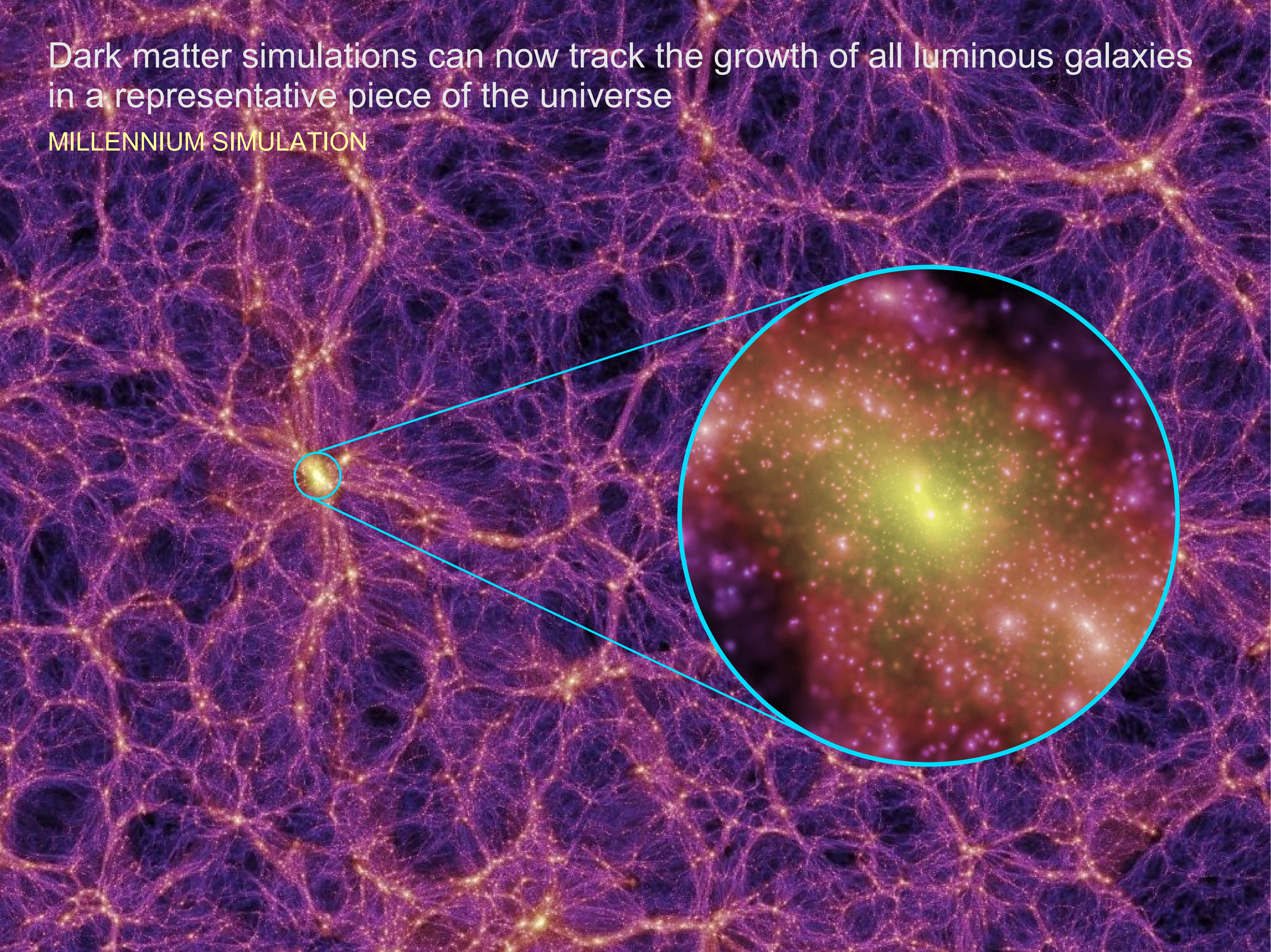

The merger-tree of the Millennium Run connects about 800 million subhalos

SCHEMATIC MERGER TREE

- The trees are stored as self-contained objects, which are the input to the semi-analytic code
- Each tree corresponds to a FOF halo at z=0 (not always exactly)
- The collection of all trees (a whole forest of them) describes all the structures/galaxies in the simulated universe

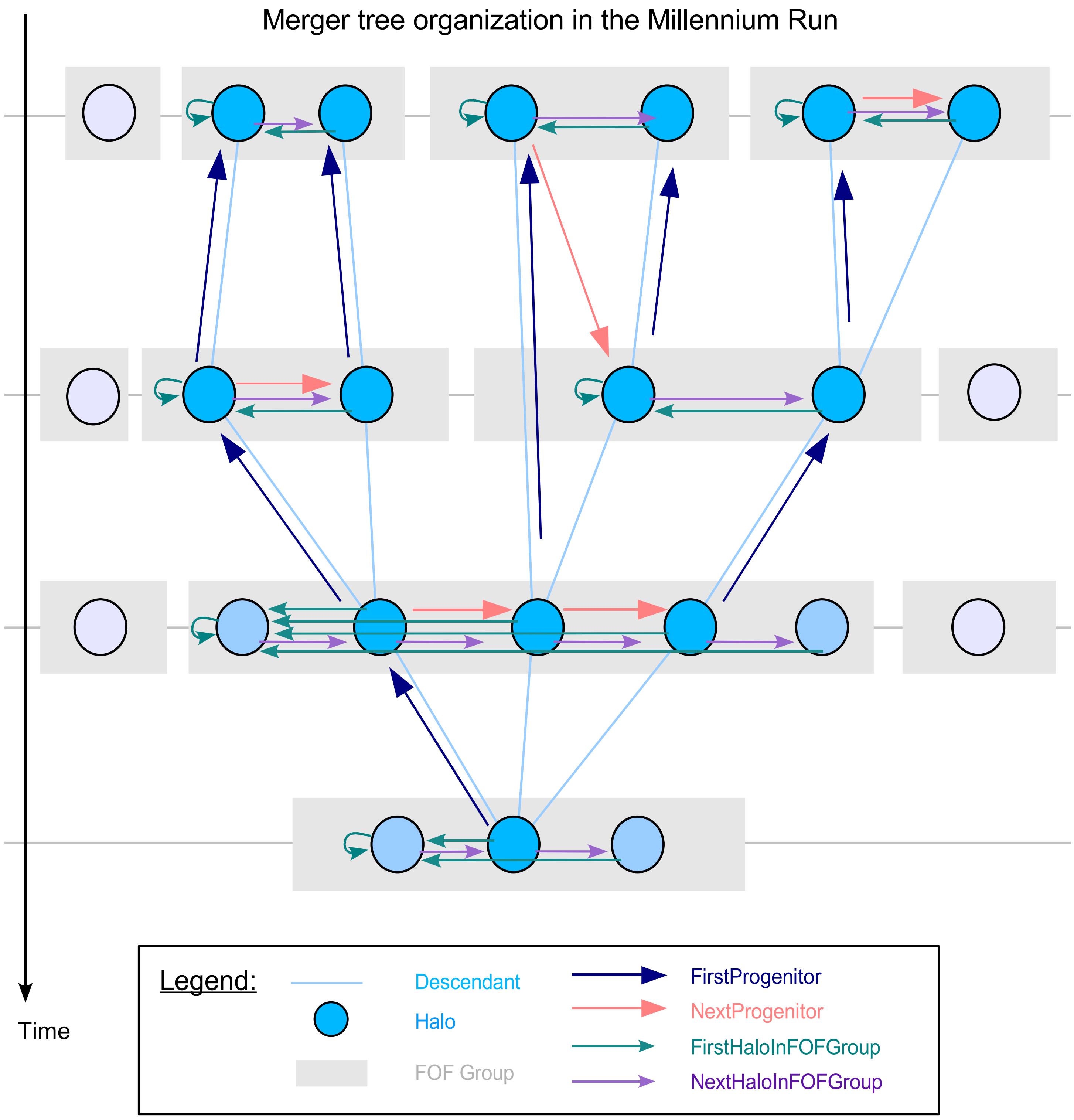

The inclusion of AGN feedback allows semi-analytic models to reproduce a multitude of observational data

K-BAND AND Bj-BAND LUMINOSITY FUNCTIONS

Croton et al. (2006)

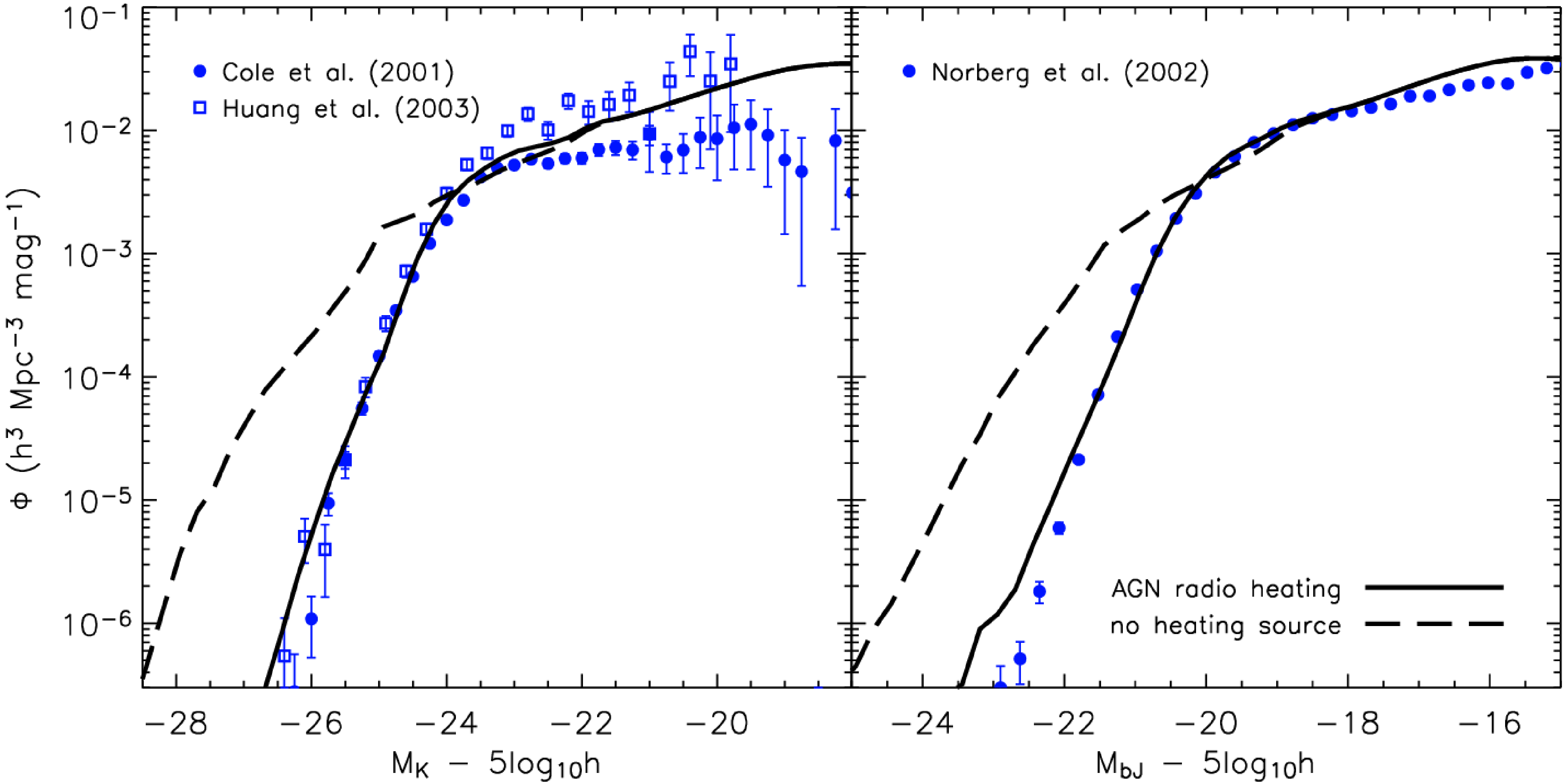

The luminosity functions split by color are well reproduced, except for faint red galaxies

LUMINOSITY FUNCTIONS SPLIT BY B-V COLOR COMPARED TO 2DFGRS

Croton et al. (2006)

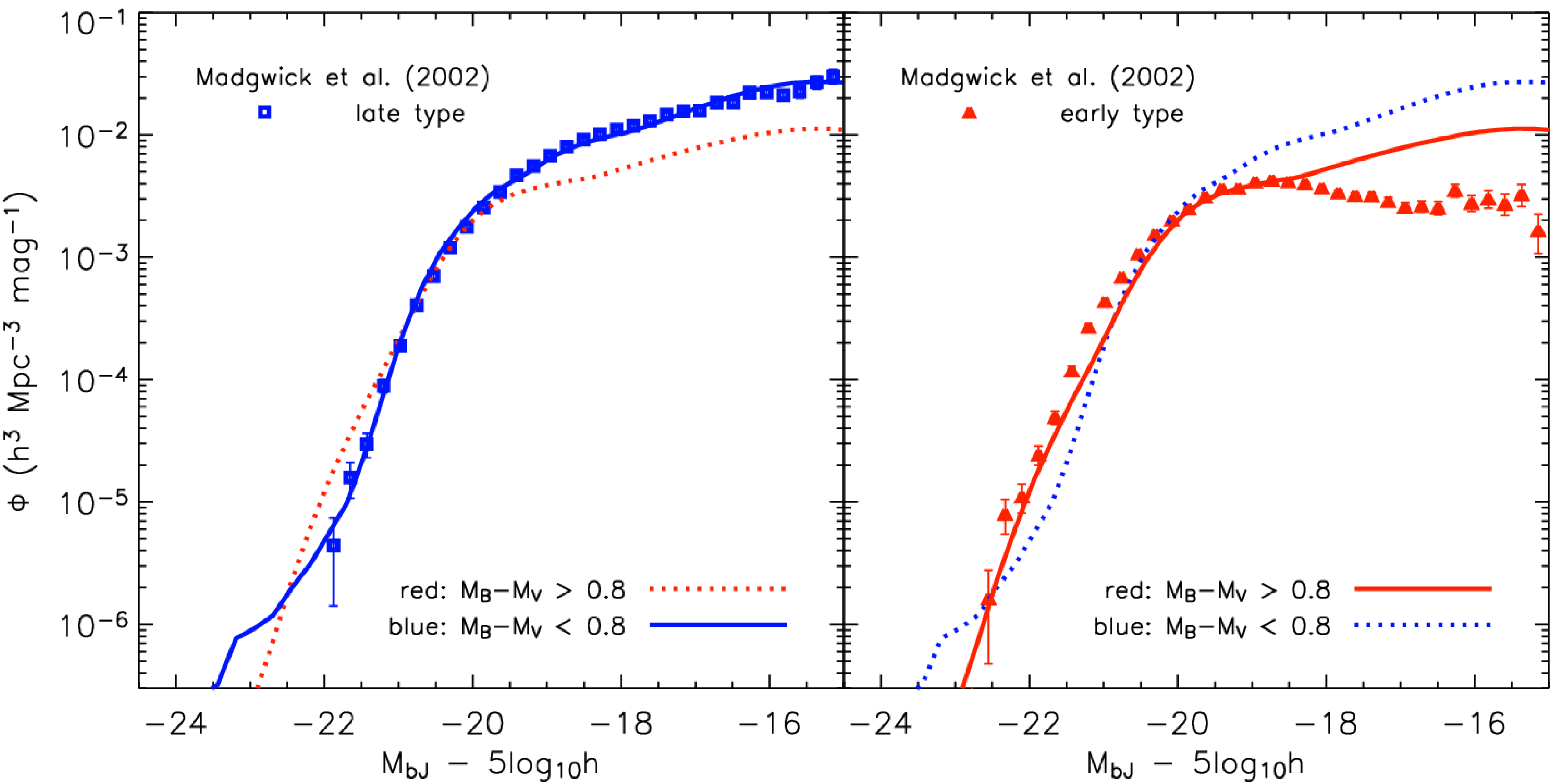

For the first time, semi-analytic models reproduce the red colours of the most luminous ellipticals

B-V COLOUR DISTRIBUTION

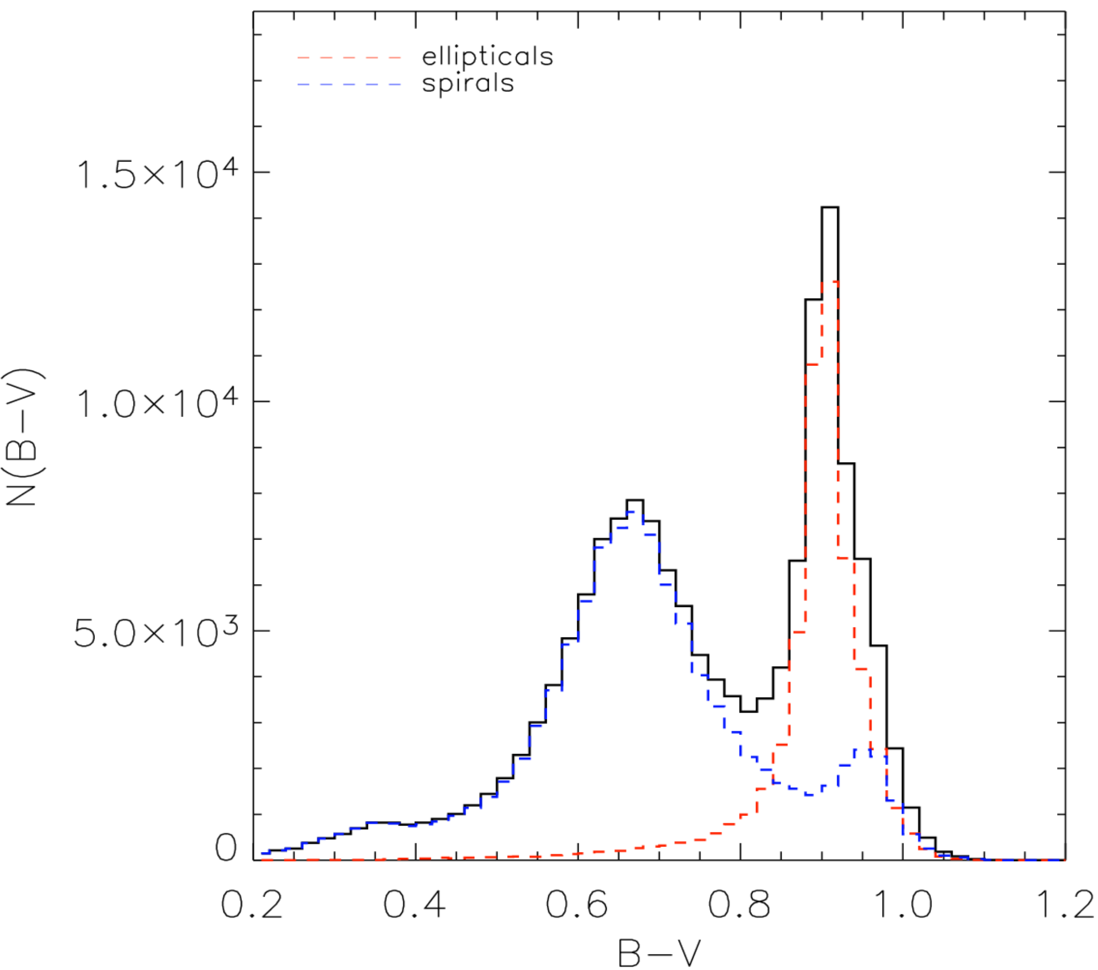

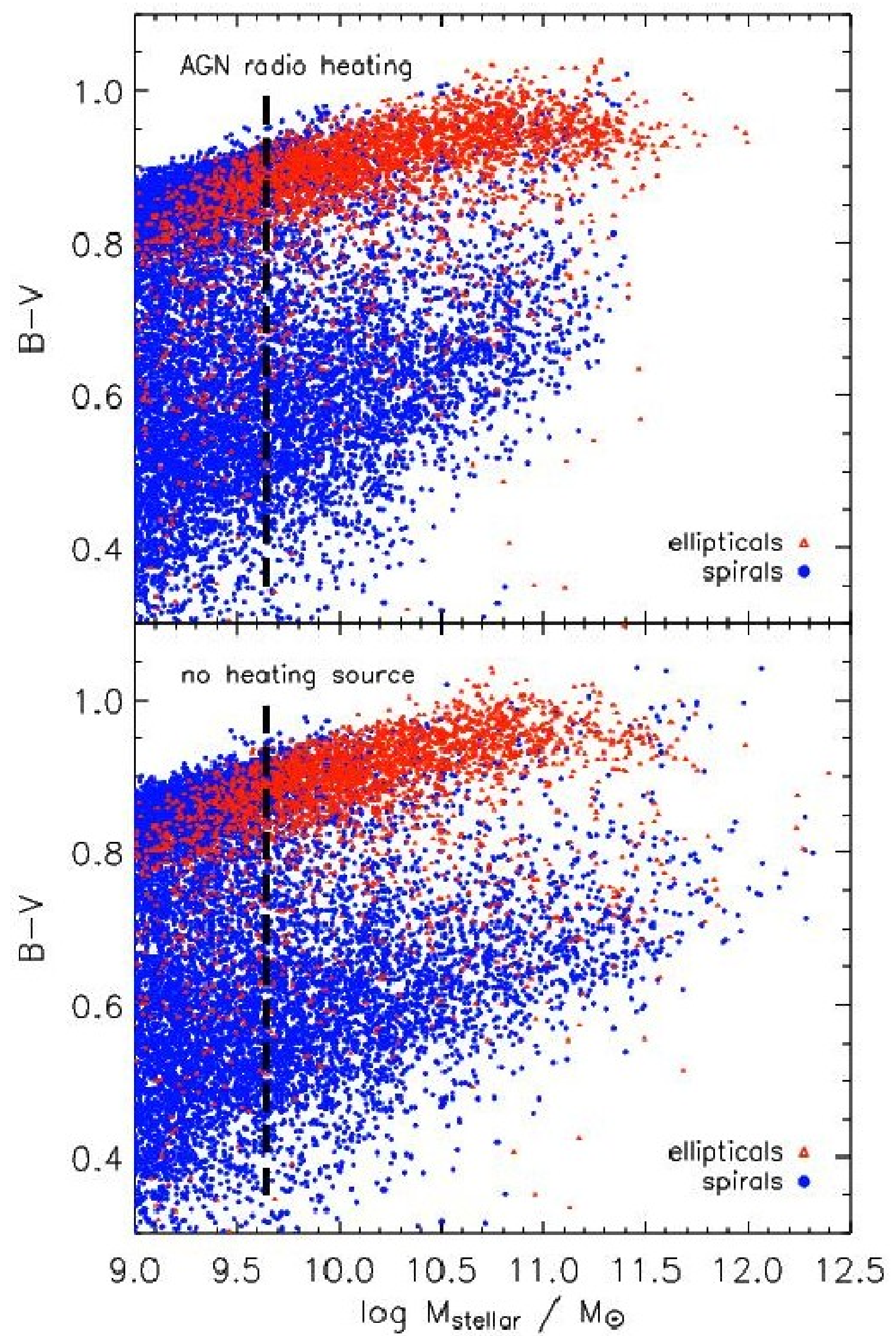

Croton et al. (2006)

Only a "radio mode" of feedback is presently included in the semi-analytic models

MODEL ASSUMPTIONS

Croton et al. (2006):

- Quasars are triggered in mergers or by disk instability (Haehnelt & Kauffmann model)

- Radio mode heating should become more efficient in large halos

$$\dot{m}'_{\rm cool} = \dot{m}_{\rm cool} - \frac{L_{\rm BH}}{\frac{1}{2} V_{\rm vir}^2}$$

$$L_{\rm BH} = 0.1\, \dot{m}_{\rm BH} c^2$$

$$\dot{m}_{\rm BH} = \kappa_{\rm AGN}\, f_{\rm hot}\, V_{\rm vir}^3\, m_{\rm BH}$$

Bower et al. (2006):

- Alternative model for radio mode: Assume that the flow will adjust itself such that heating balances cooling, whenever the Eddington luminosity of the BH of a quasistatically cooling halo is sufficiently large, i.e. when

$$L_{\rm cool} < \epsilon L_{\rm Edd}$$

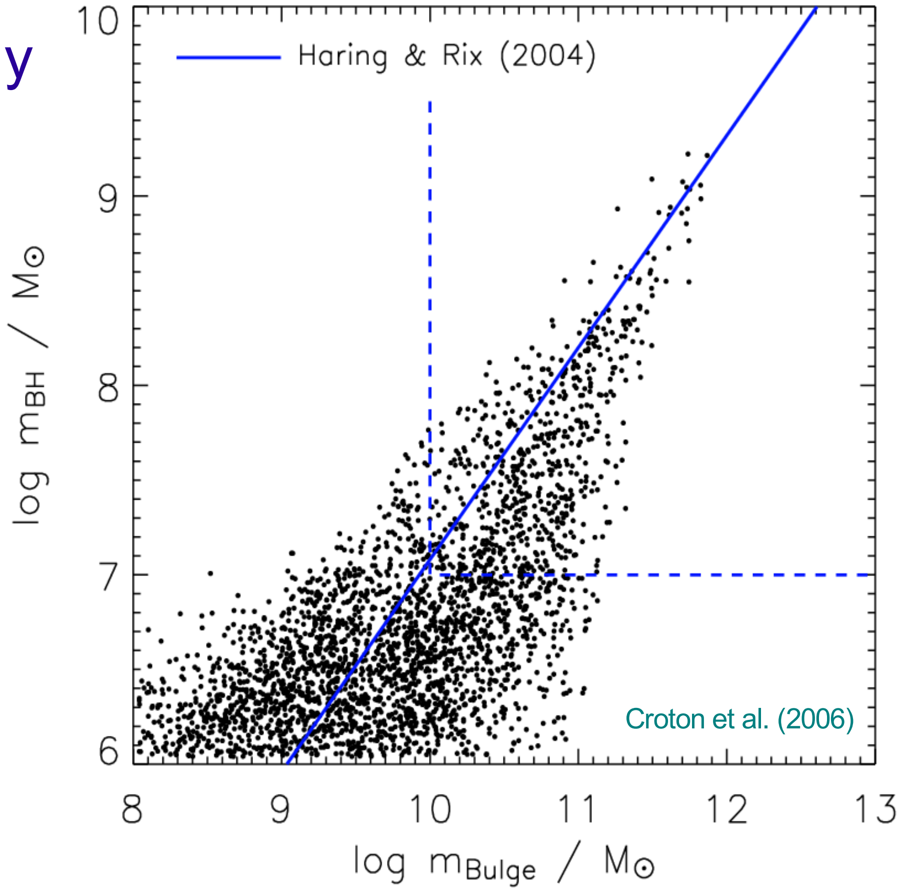

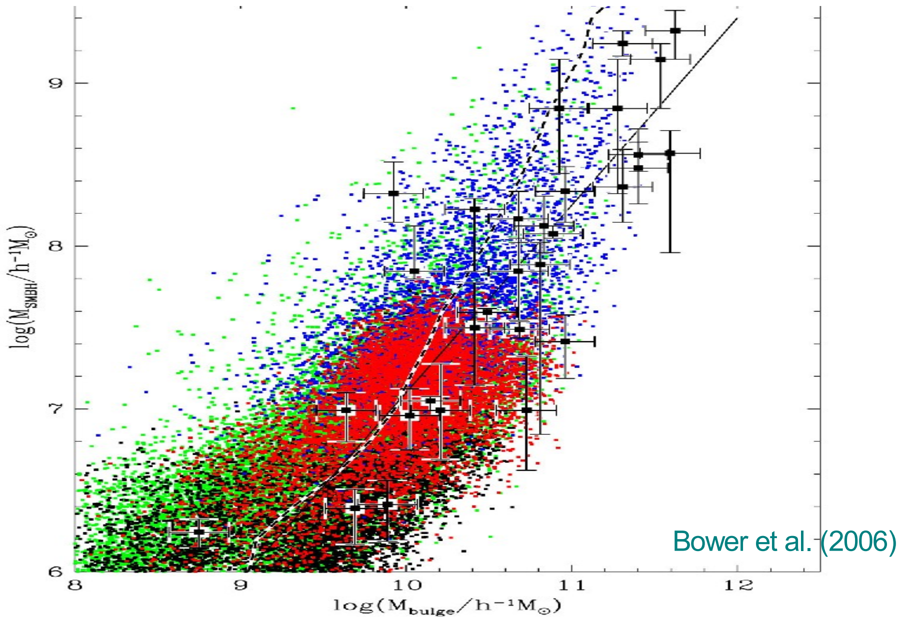

The particular assumptions made in this semi-analytic model predict an evolution in the BH-mass bulge-mass relationship

THE M_{BH} - M_{Bulge} RELATIONSHIP AT DIFFERENT TIMES

Croton (2006)

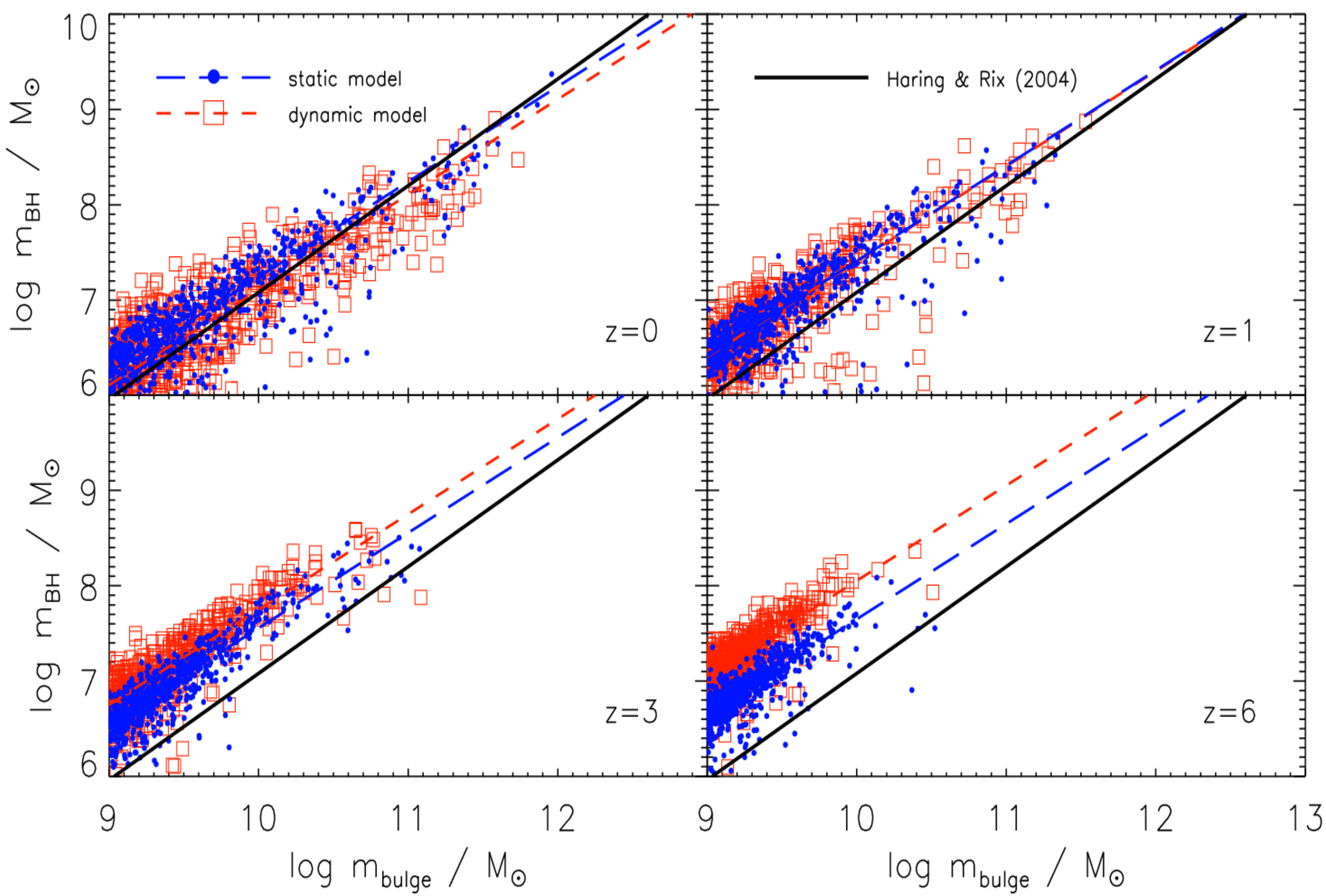

In this model, the bulge grows both from the merger-induced starburst and the associated disk disruption.

The latter channel becomes more important at low redshift, leading to evolution in the M_{BH}-M_{bulge} relation.

→ Allows interesting comparisons to the results of **Robertson et al. (2006)** based on hydro simulations, who find a very weak evolution in this relation.

History of elliptical galaxies

The formation time of halos depends strongly on mass and implies a hierarchical formation of objects

AVERAGE FORMATION TIME OF HALOS AS A FUNTION OF HALO MASS

How can it be that the most massive ellipticals are also the oldest and reddest?

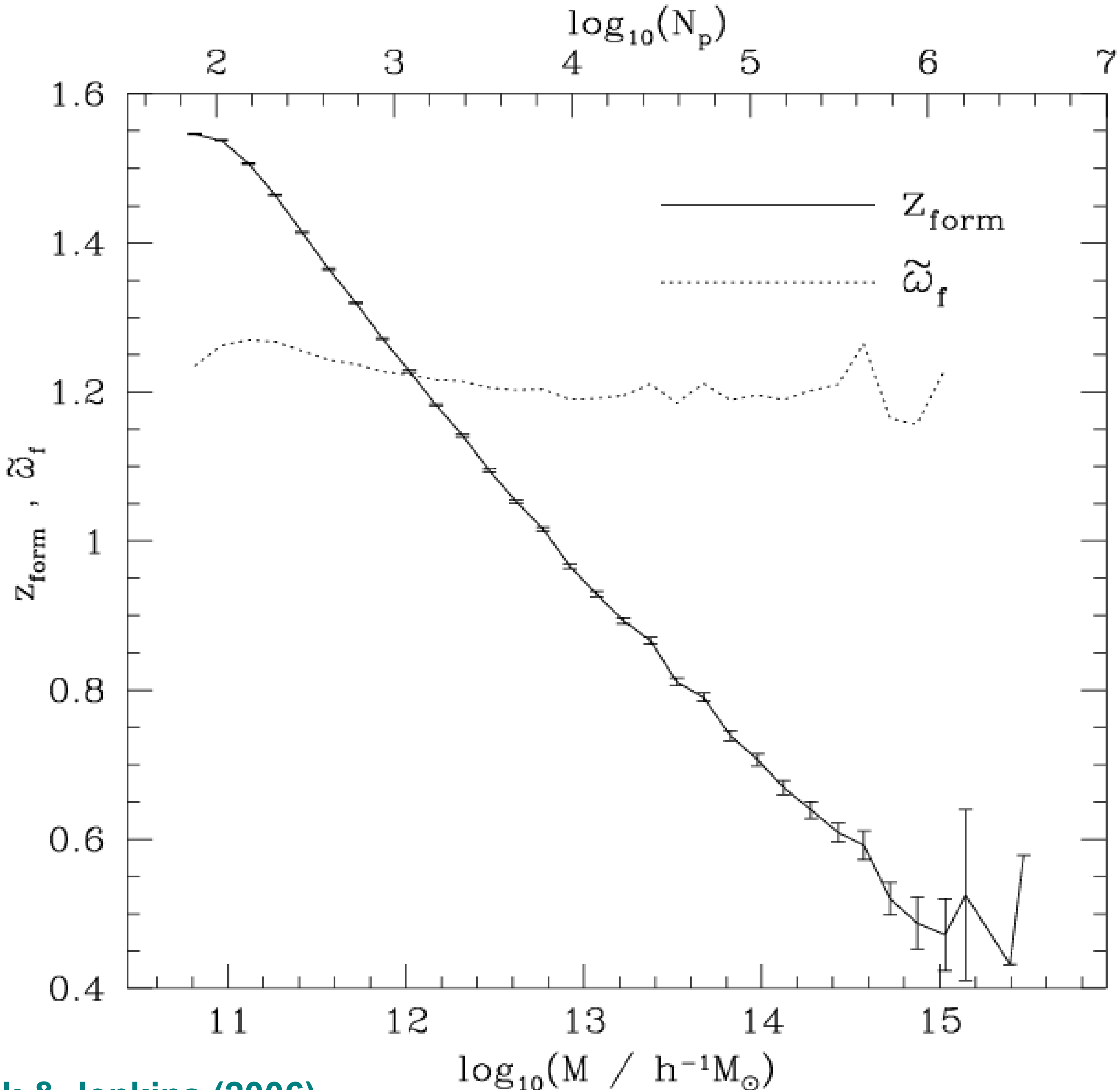

Harker, Cole, Helly, Frenk & Jenkins (2006)

More massive elliptical galaxies form their stars on average earlier

STAR FORMATION HISTORIES OF ELLIPTICALS

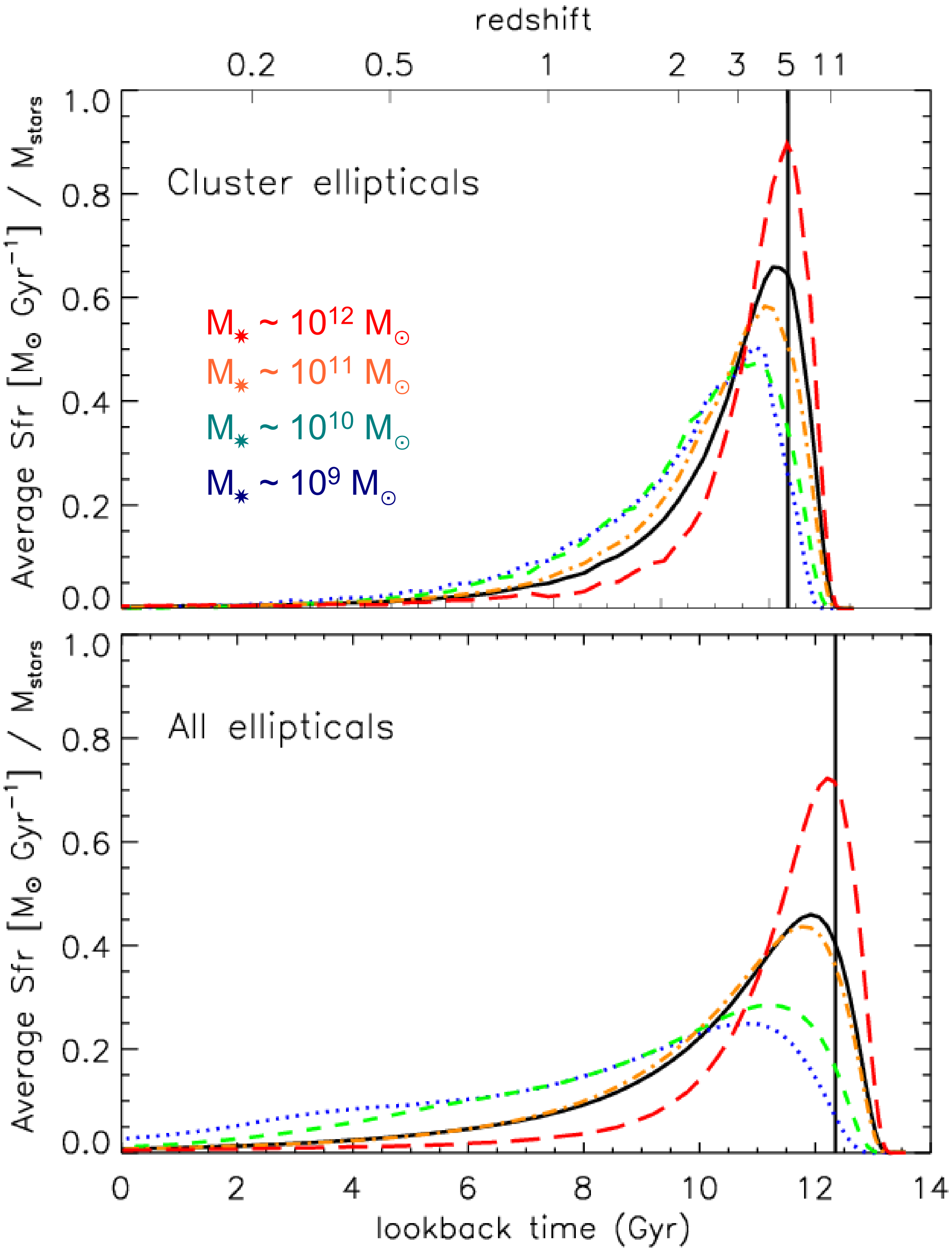

de Lucia, Springel, White, Croton & Kauffmann (2006)

The formation and assembly times differ substantially for elliptical galaxies, and show opposite trends with stellar mass

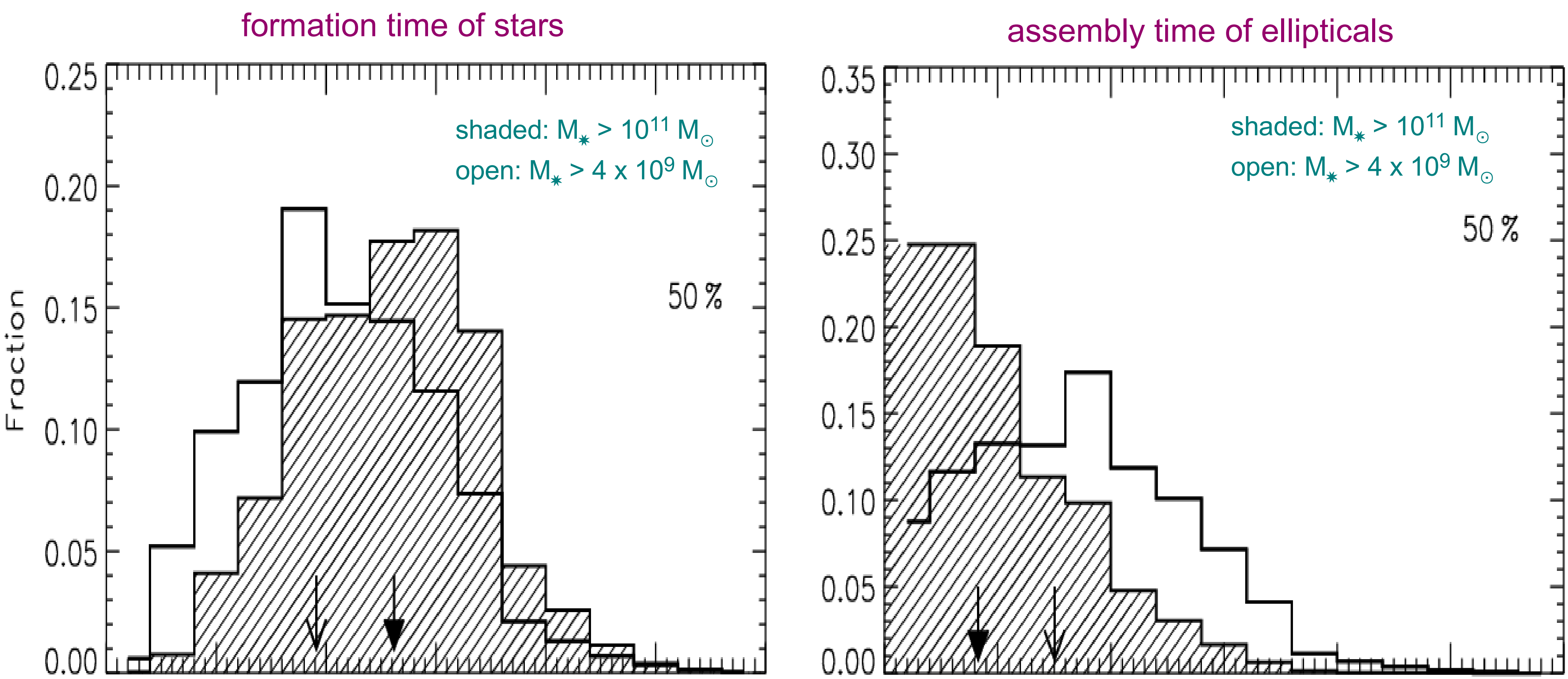

de Lucia et al. (2006)

The most massive ellipticals have the oldest, reddest and most metal rich stellar populations

THE **ANTI-HIERARCHICAL** FORMATION OF ELLIPTICALS

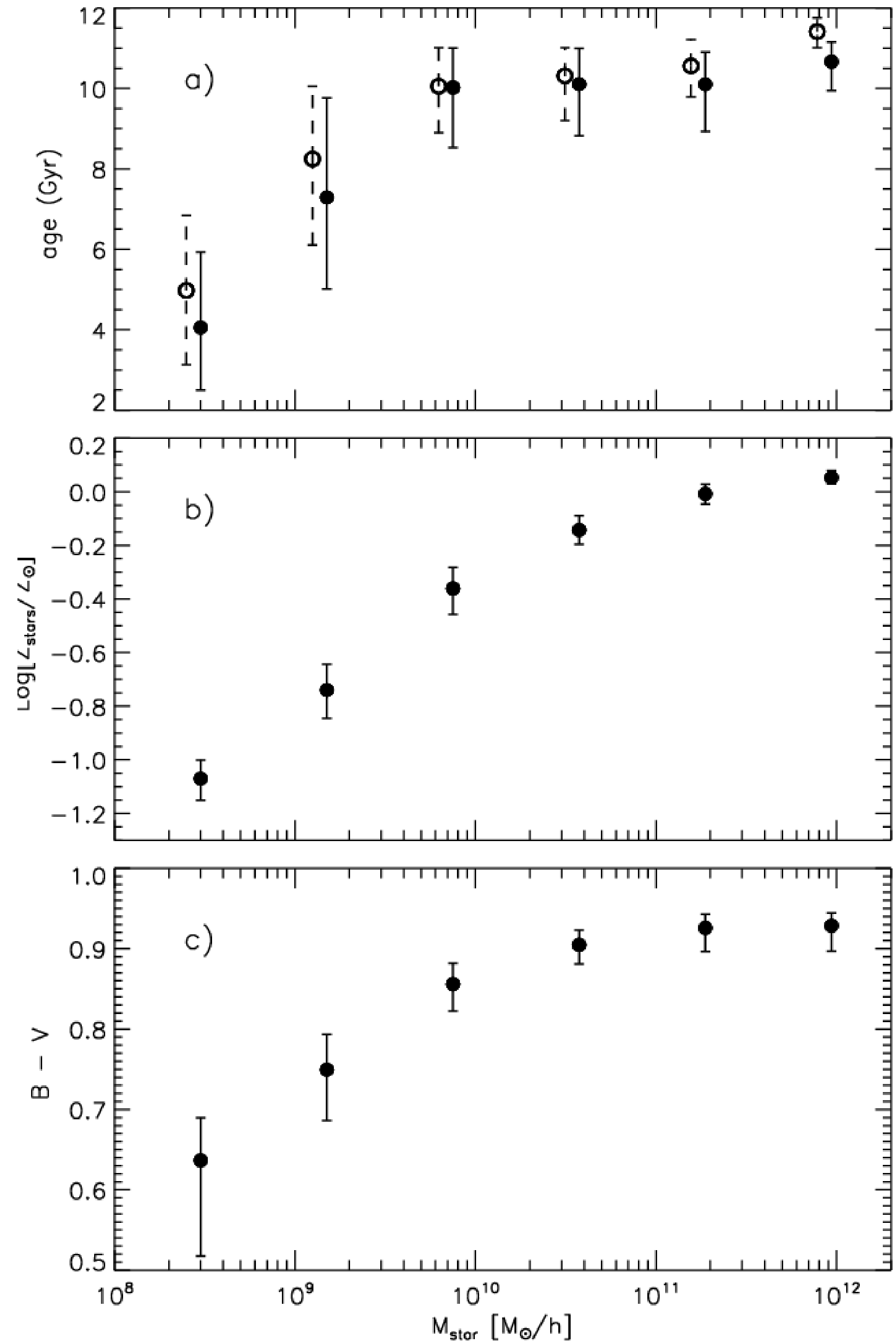

de Lucia et al. (2006)

More massive ellipticals experience a larger number of mergers

THE EFFECTIVE NUMBER OF PROGENITOR SYSTEMS

$$N_{\rm eff} = \frac{M_{\rm final}}{2\,\langle M_{\star,{\rm form}}\rangle}$$

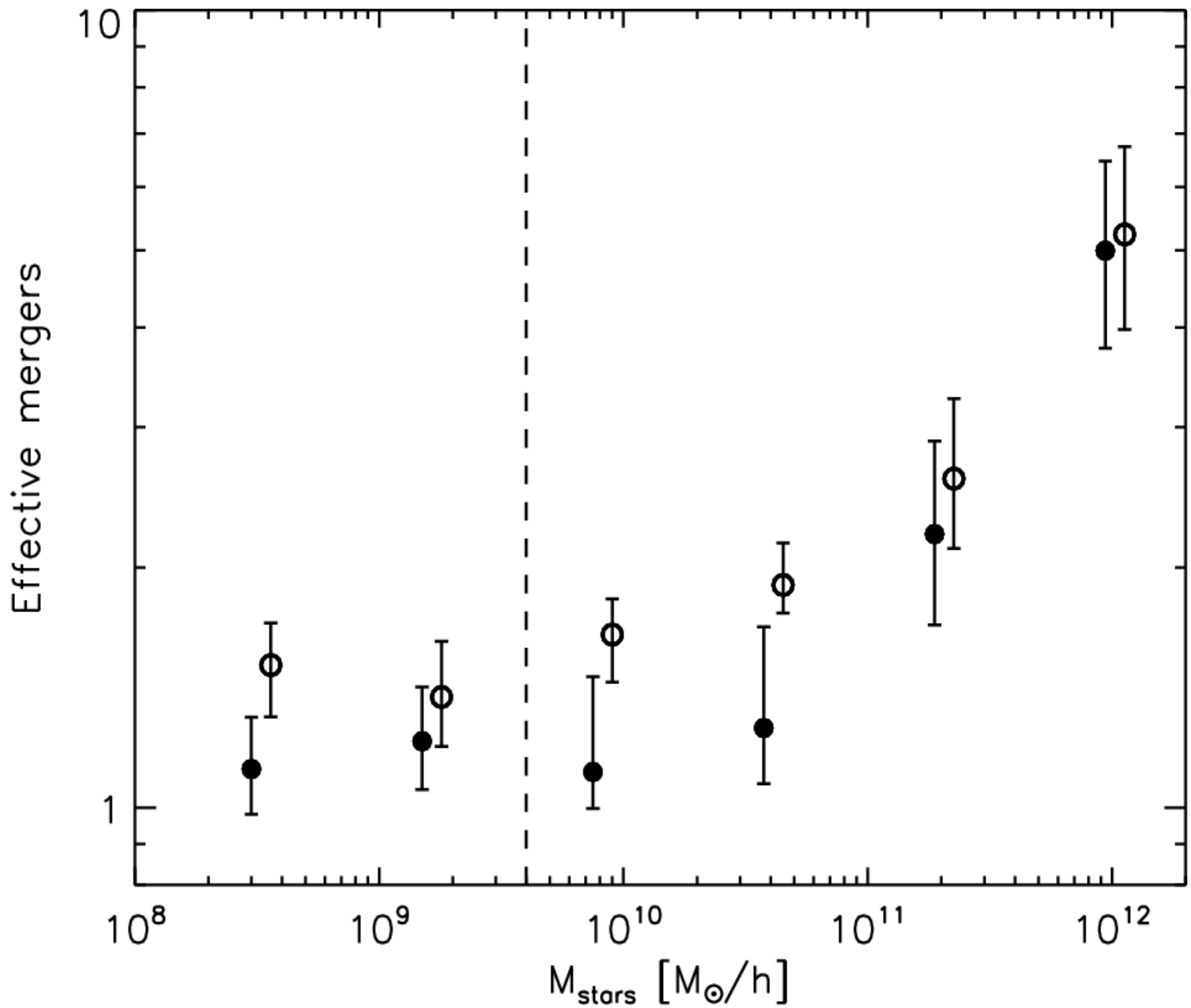

The success of the semi-analytic model has its origin in the inclusion of AGN feedback

AGE VS STELLAR-MASS RELATIONSHIP FOR DIFFERENT FEEDBACK MODELS

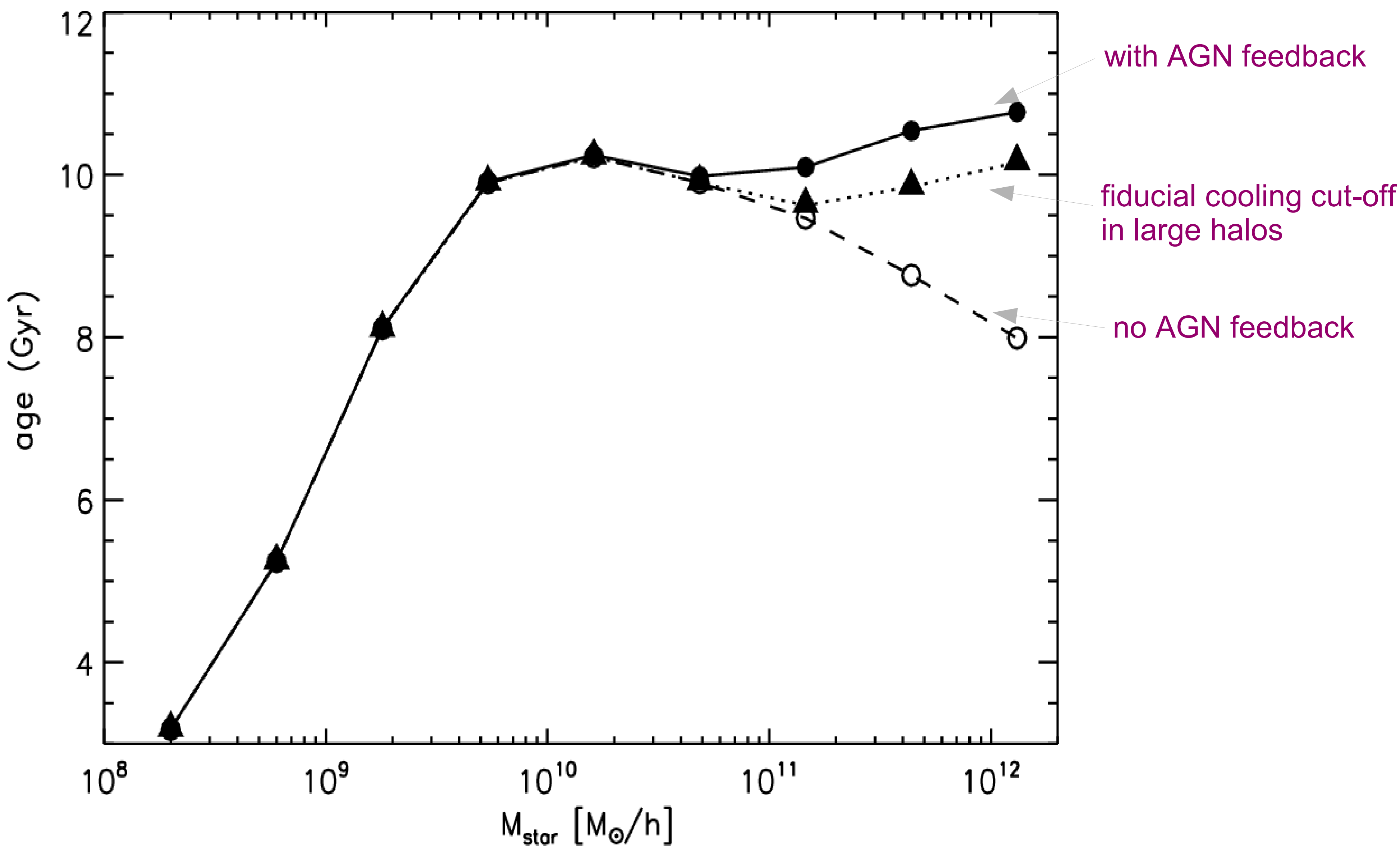

de Lucia et al. (2006)

Version control systems

Version control systems allow a convenient tracking of changes in code projects, or general text files

MAIN ADVANTAGES OF USING A VERSION CONTROL SYSTEM

Examples:

- **RCS**
- **CVS**
- **SUBVERSION**

- Keep track of any changes in a code (never accidentally loose work)
- Have a log-file about the changes
- Ability to go back to any previous versions, identified either by version number, date, etc.
- Quickly find changes between different versions
- Administer branches/releases of codes

Concurrent version control systems like CVS or SUBVERSION simplify collaboration on joint code projects

PRINCIPLE FEATURES OF CONCURRENT VERSION CONTROL SYSTEMS

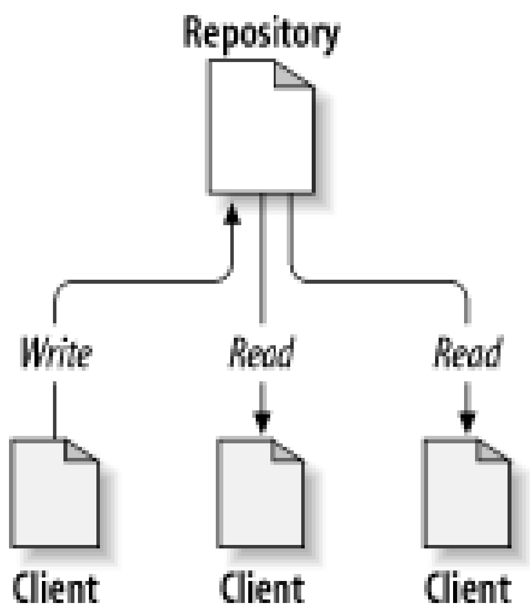

- Have a central library of the code that can be accessed conveniently from any computer
- Allow different users to change the code, and keep a log about who changed what
- Prevent that people accidentally overwrite the changes made by other people
- Inform about changes/updates made by other people in the code
- Provide access control to read/write access to the repository

When several people work on a code at the same time, the problem of coordinate arises

THE PROBLEM TO AVOID

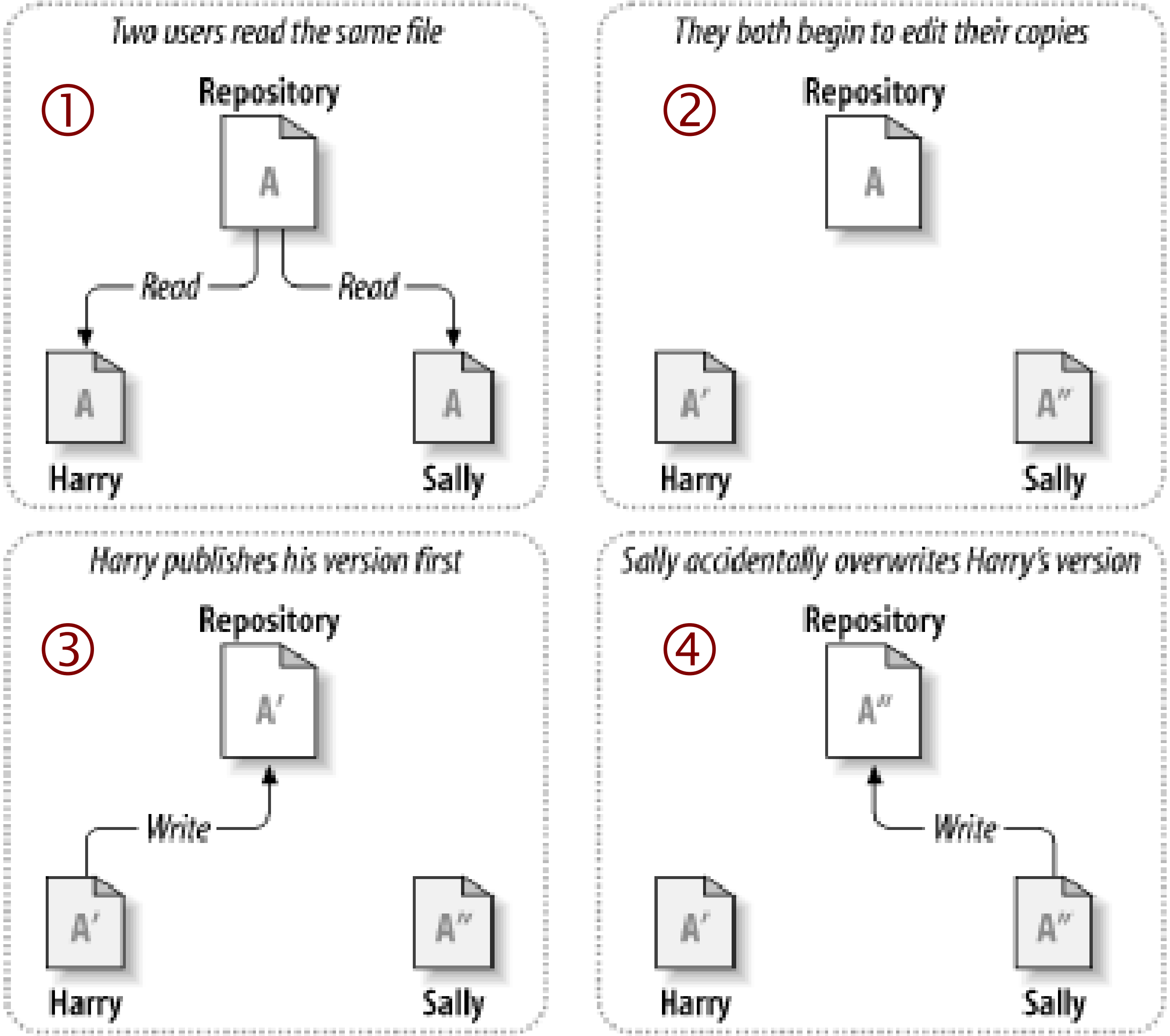

CVS and Subversion do not use file looking to avoid conflicts, but follow the copy-modify-merge paradigm

HOW CONCURRENT CHANGES ARE DEALT WITH

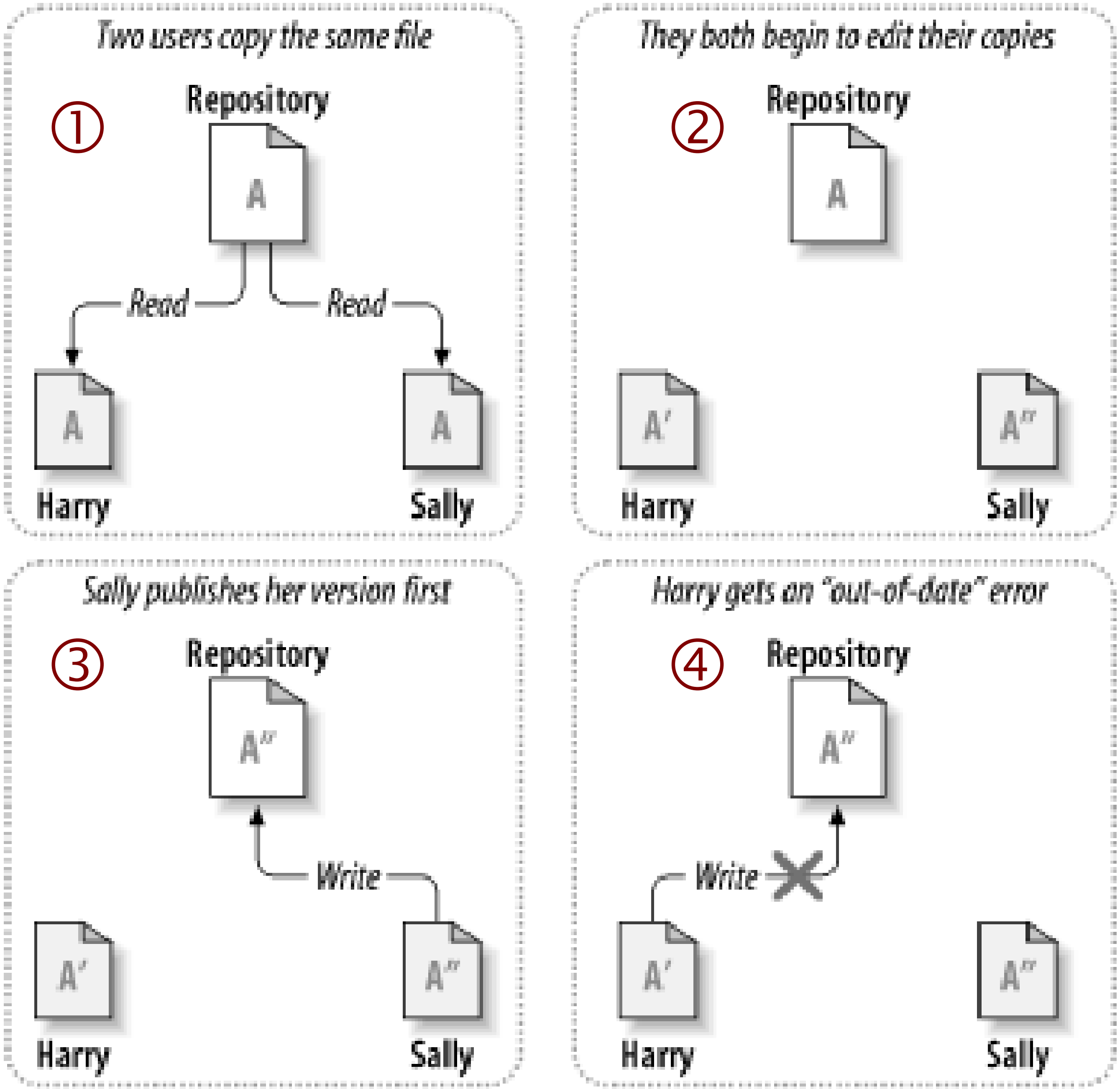

CVS and Subversion do not use file looking to avoid conflicts, but follow the copy-modify-merge paradigm

HOW CONCURRENT CHANGES ARE DEALT WITH

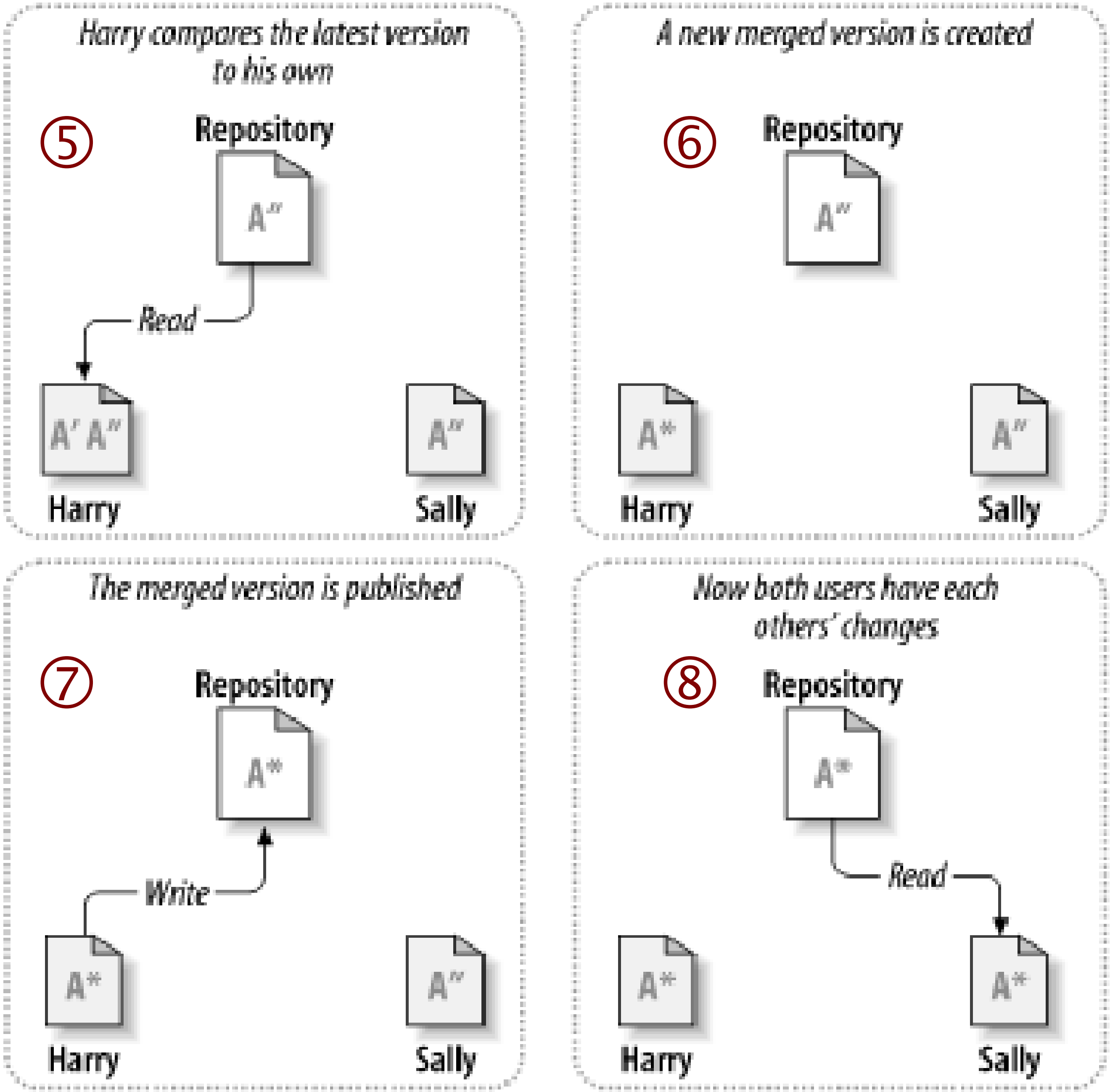

Subversion is the more modern successor CVS

ADVANTAGES OF SUBVERSION

- Directory versioning
- Atomic commits
- Simple and flexible access control at directory level
- Repository access via URL and Apache web-server
- Efficient branching and tagging
- Binary data can be versioned as well
- Better recognition and treatment of conflicts
- Works well over low-bandwith connections
- Single revision number for the whole repository

Ly-alpha forest

Since the Ly-α probes low density gas, it might in principle be affected by CR pressure injected at large-scale structure shock waves

ILLUSTRATION OF A QUASAR ABSORPTION SPECTRUM

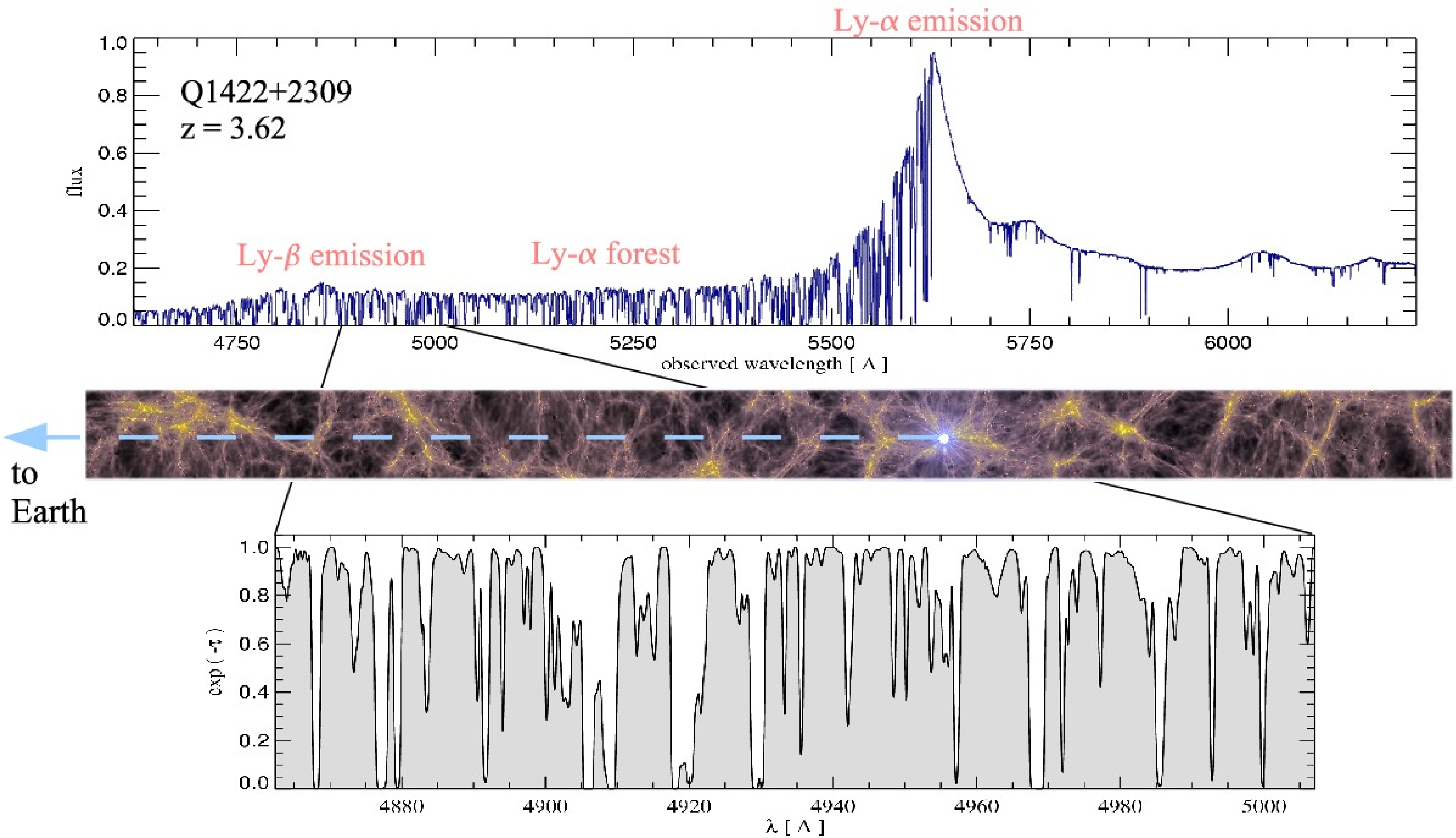

The Ly-α forest can be used to probe the power spectrum at comparatively small scales, and at intermediate redshifts

DIFFERENT PROBES OF THE MASS POWER SPECTRUM

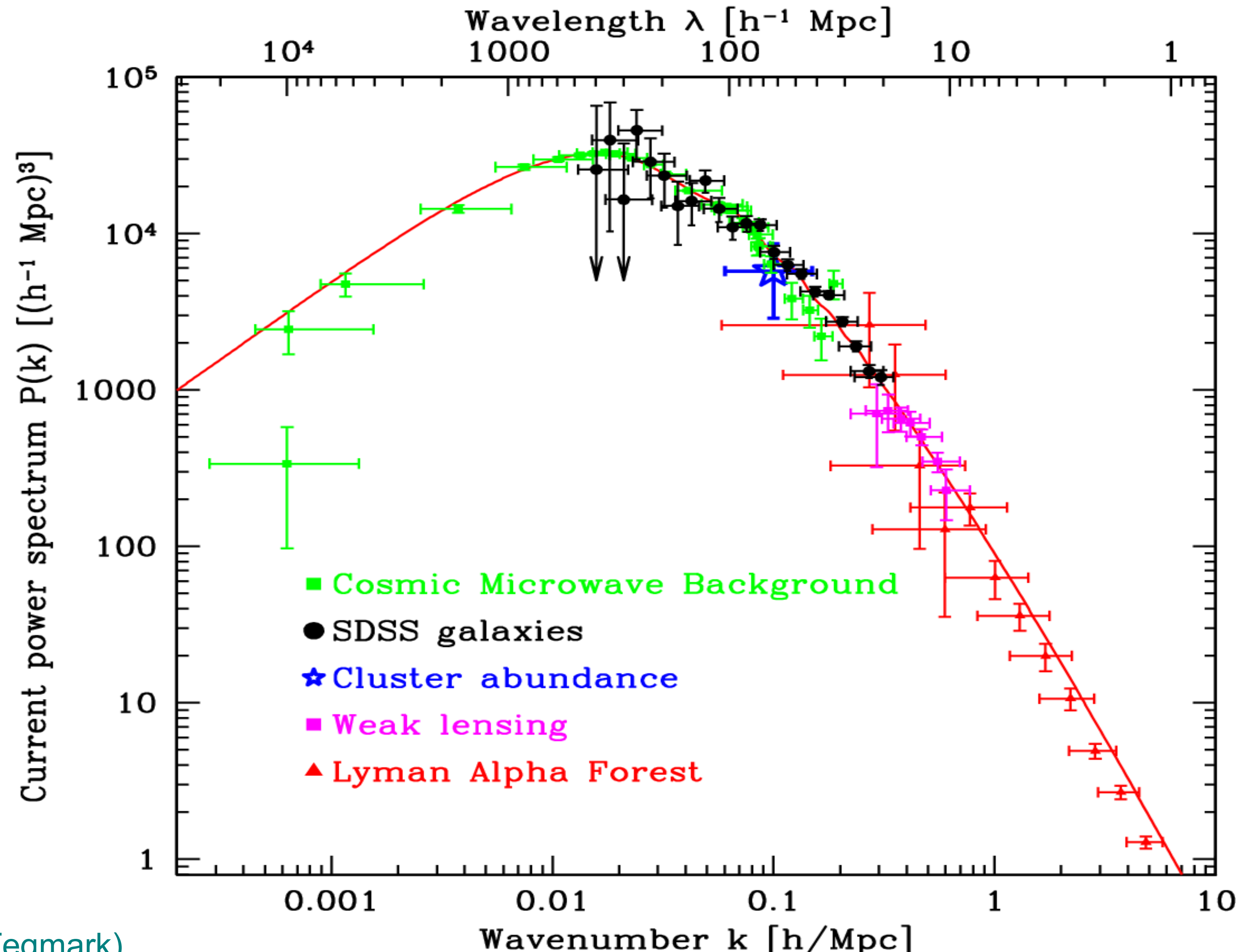

(figure from Max Tegmark)

Galactic winds that escape from galaxies are producing shocks in the IGM, dissipating their kinetic energy into heat

HOT BUBBLES IN THE IGM GENERATED BY WINDS

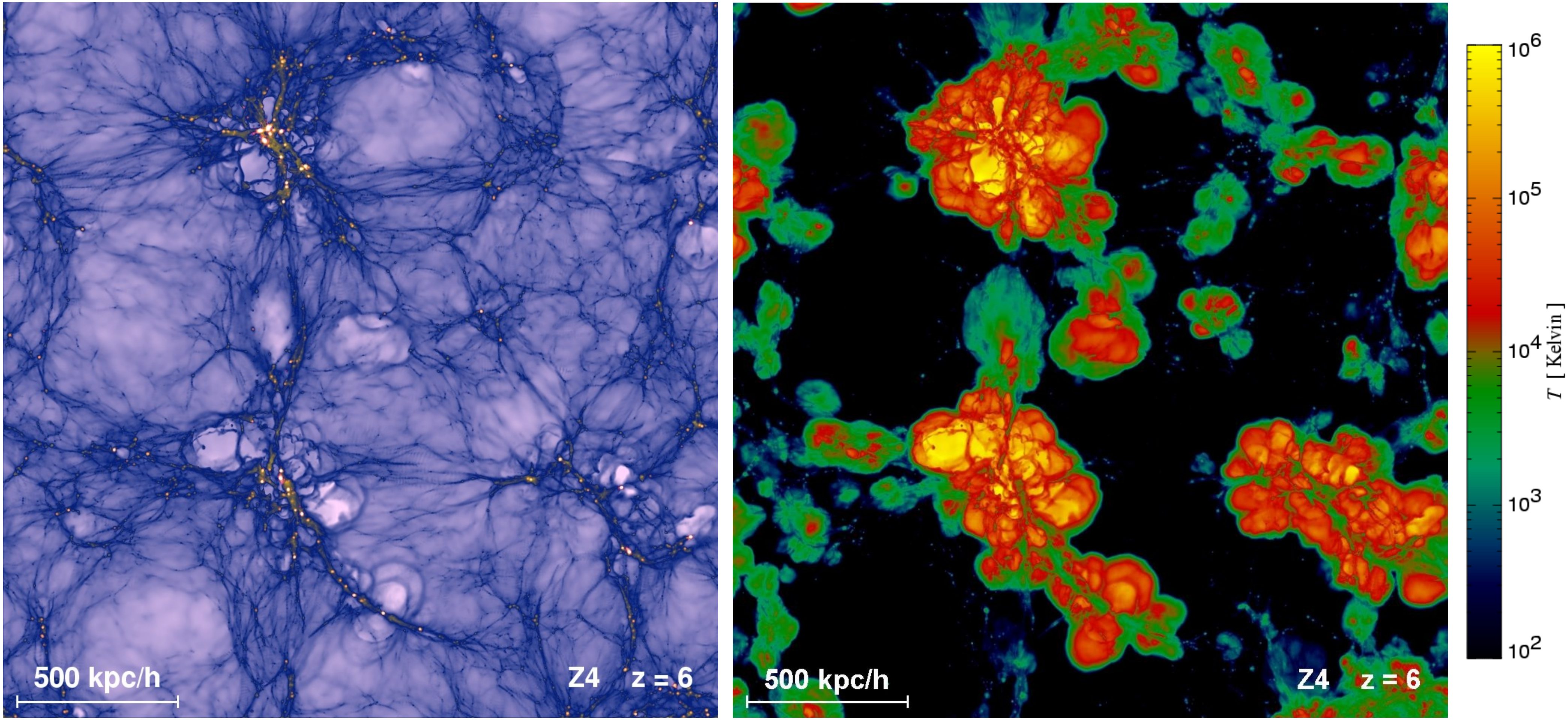

Even though galactic winds heat parts of the IGM significantly, most of the volume still follows the ordinary "equation of state"

VOLUME-WEIGHTED PHASE-SPACE DIAGRAMS

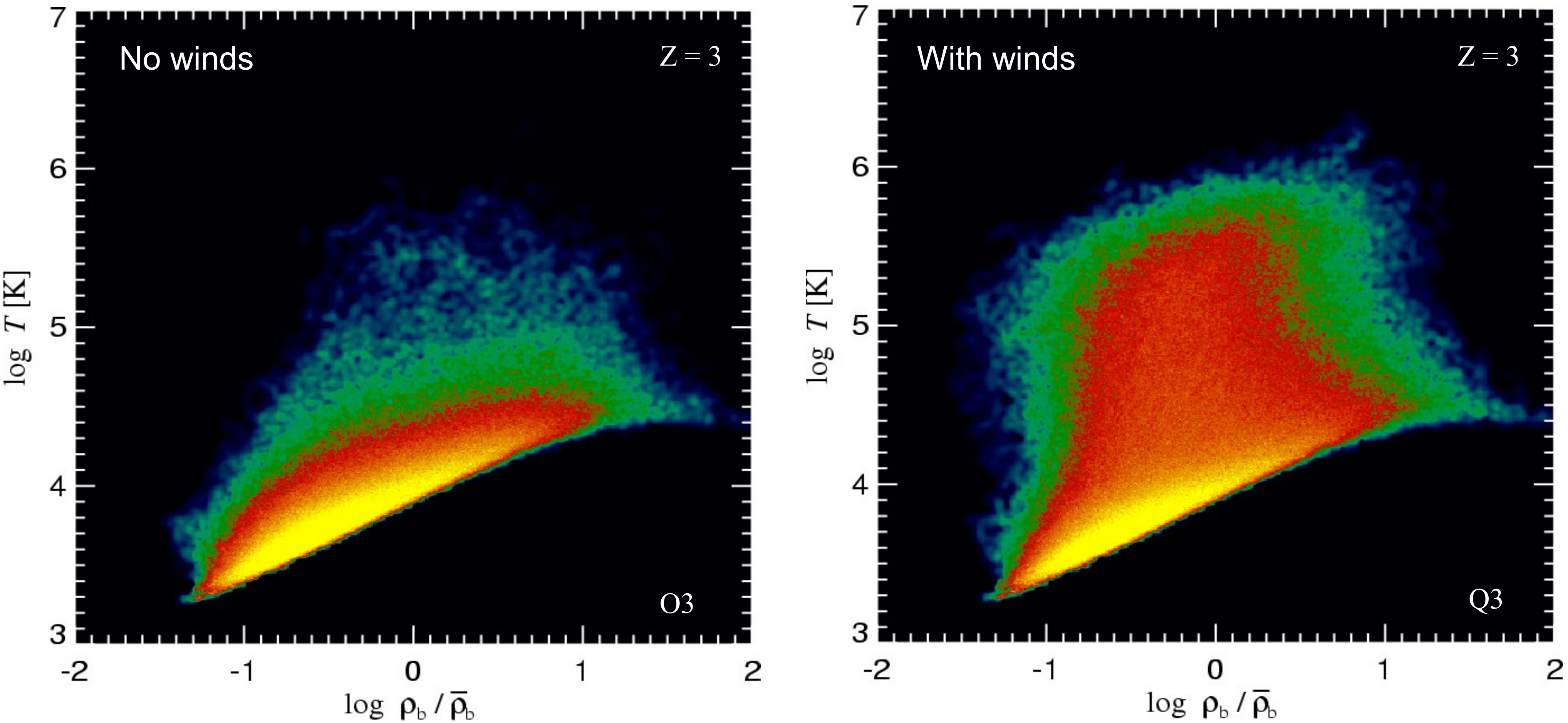

Only a small volume fraction of the IGM is heated by galatic winds

DIFFERENTIAL DISTRIBUTION OF VOLUME AS A FUNCTION OF TEMPERATURE

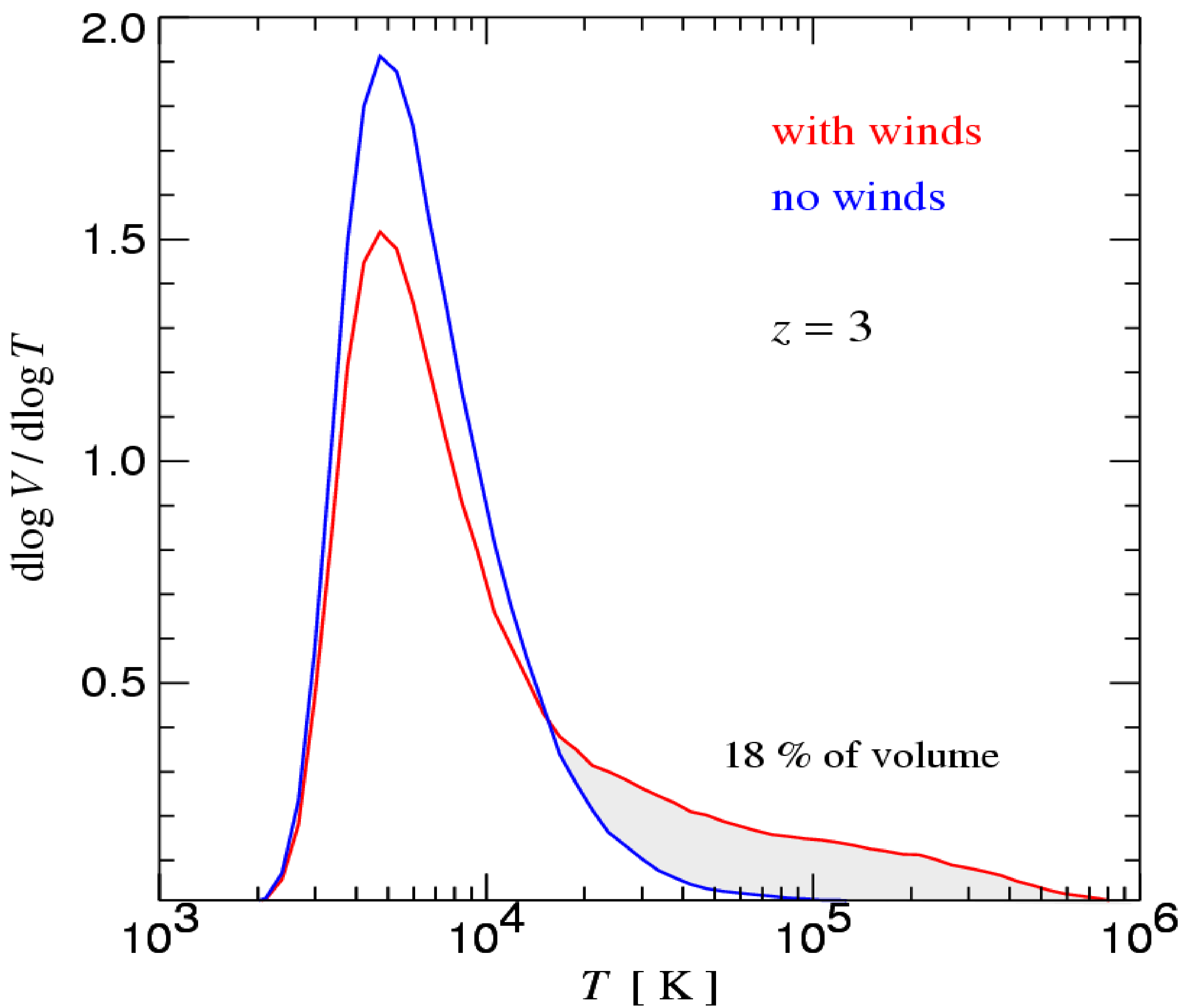

The Lyman alpha forest appears to survive nicely even for strong winds

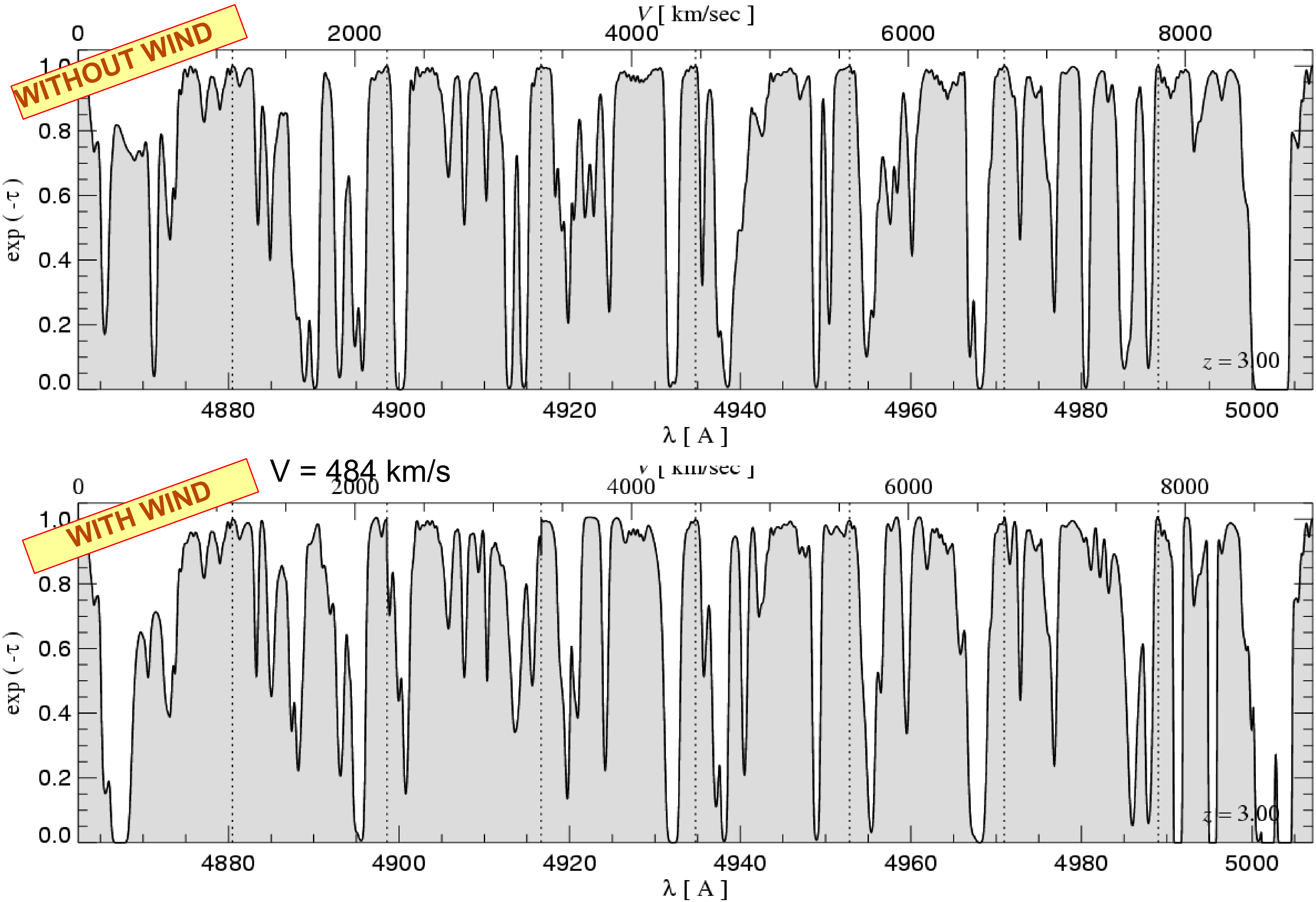

Winds induce differences in transmission

IDENTICAL
LINES OF SIGHT

Without wind:

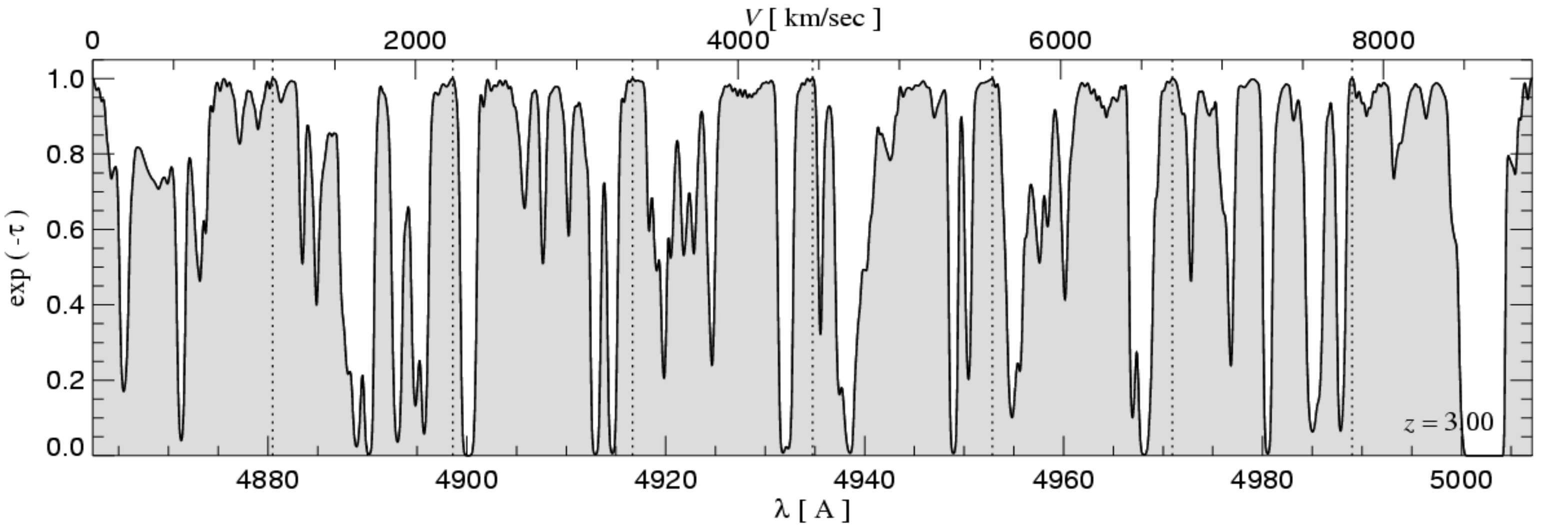

With wind:

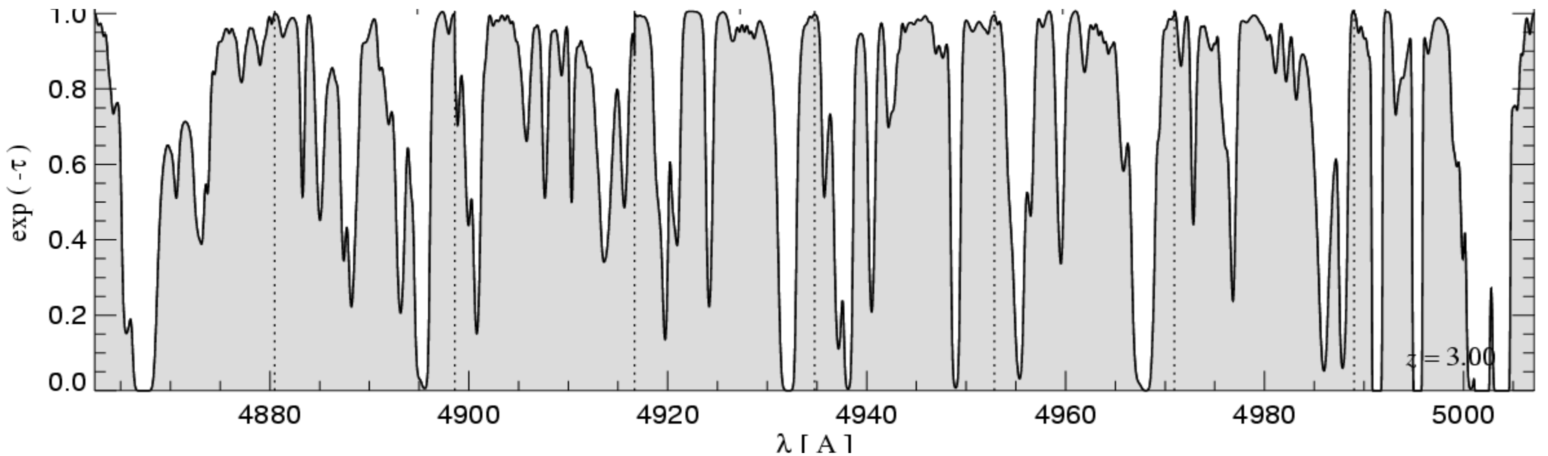

Difference in
transmission:

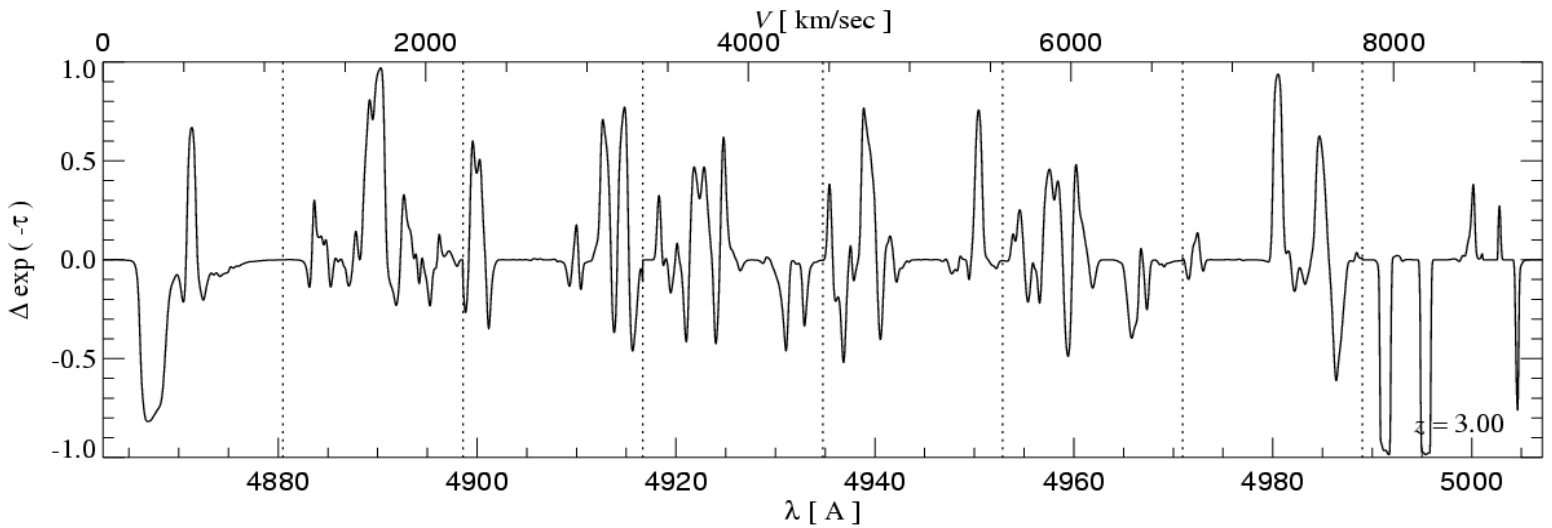

(maximum difference selection)

Difference in **velocity**:

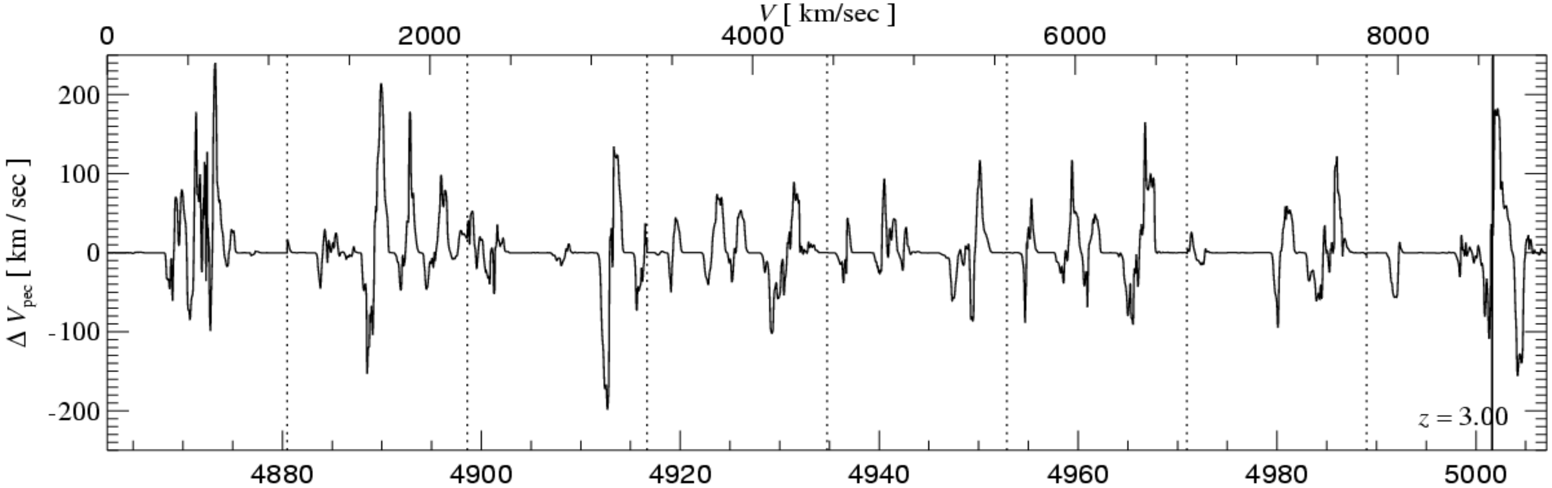

Difference in **temperature**:

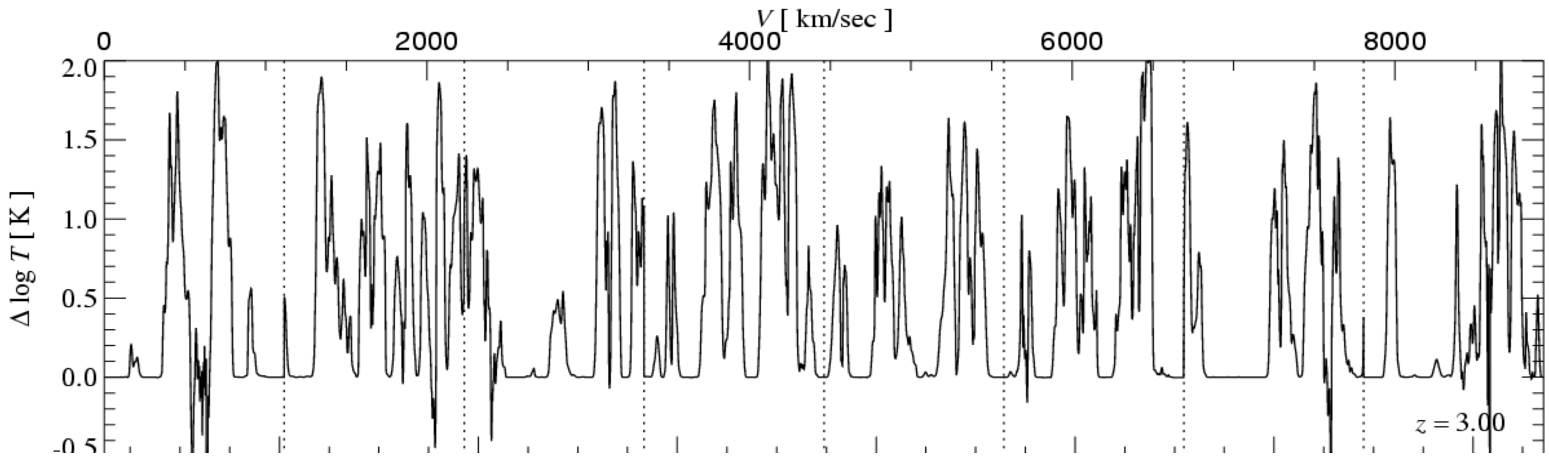

Difference in **metallicity**:

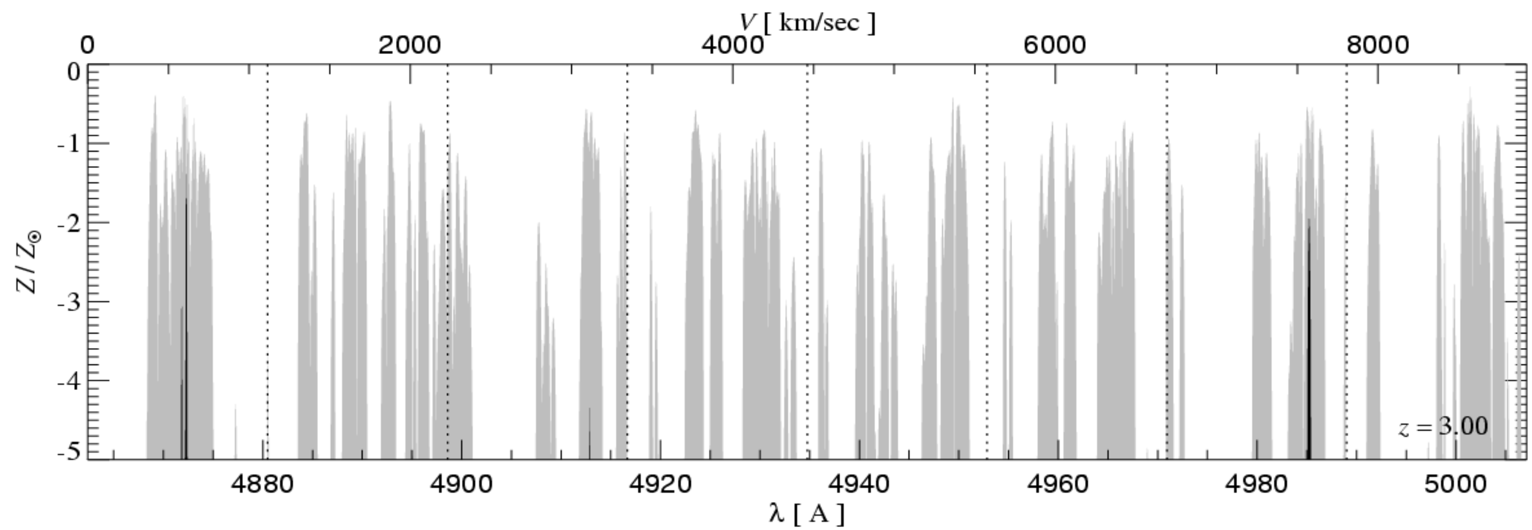

(maximum difference selection)

Random lines of sight are only mildly affected by winds

IDENTICAL RANDOM LINES OF SIGHT

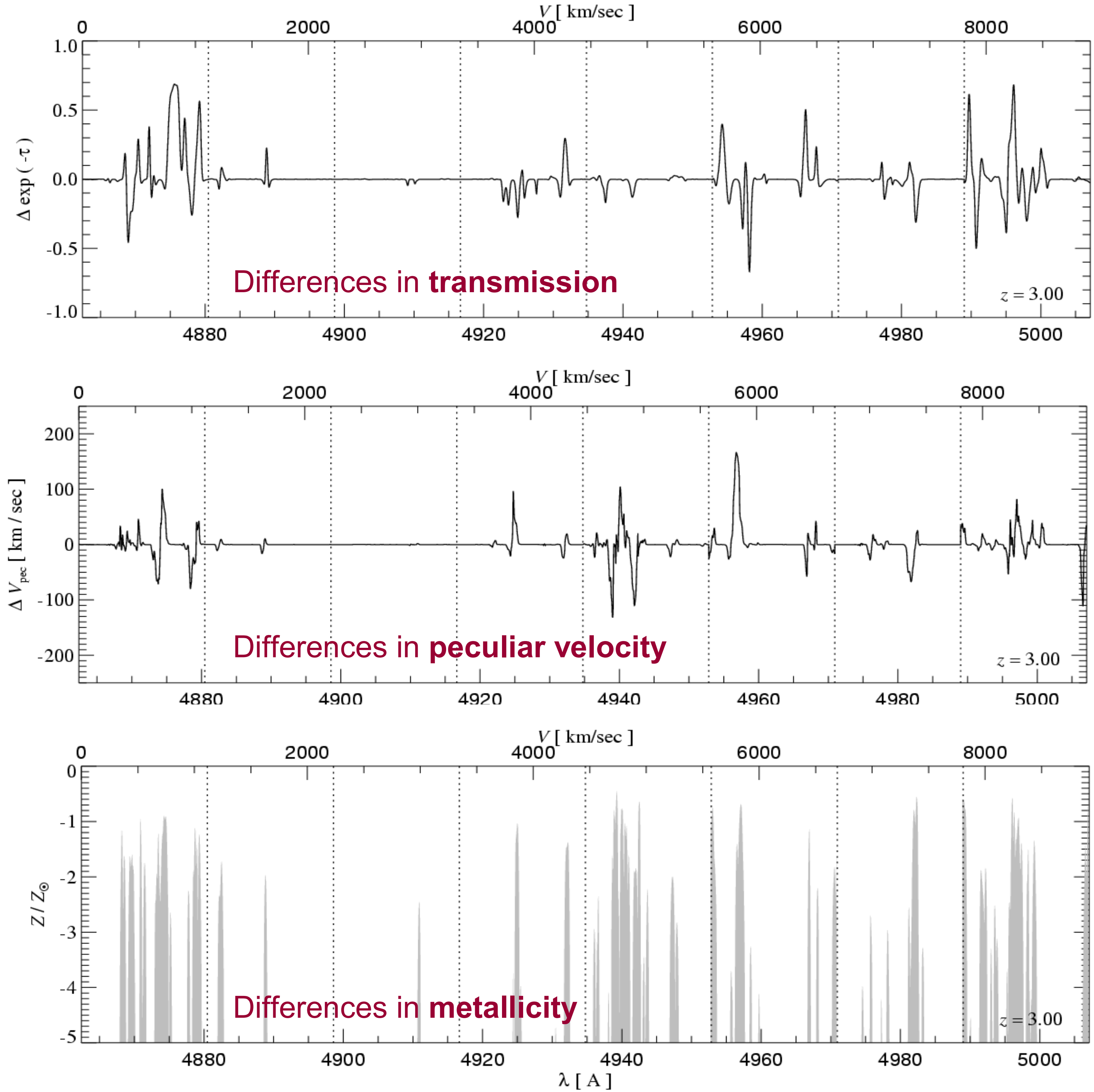

The absorption spectra can be subjected to automated line-fitting algorithms

VOIGT-PROFILE FITTING

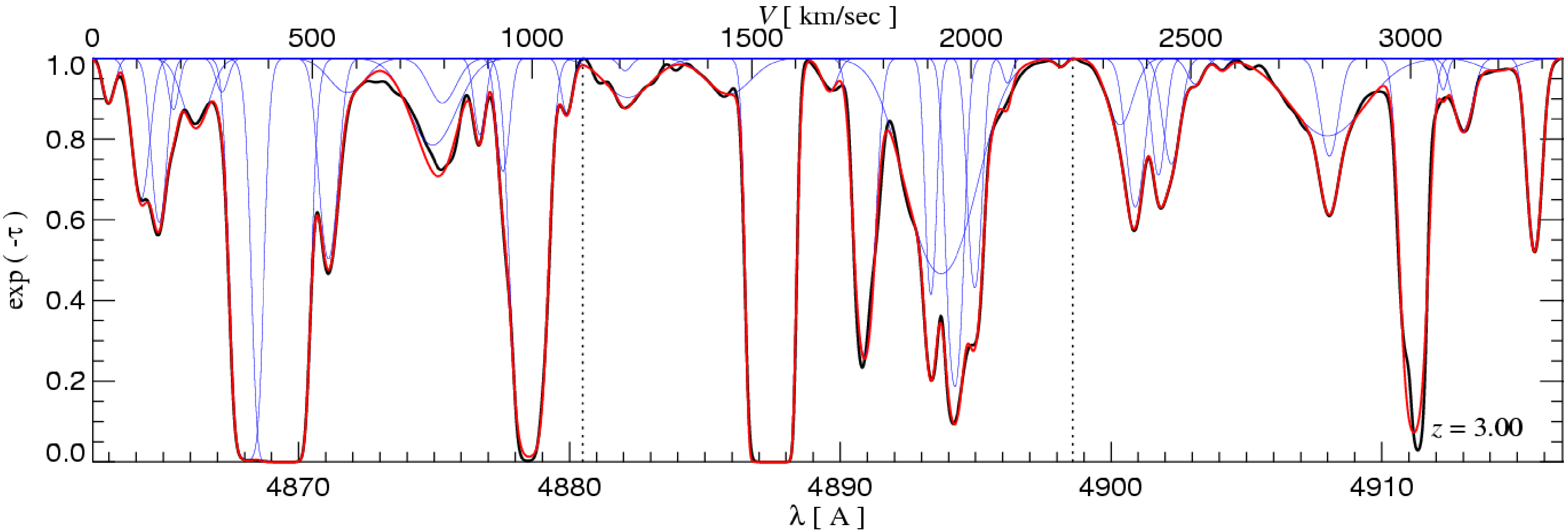

Our simulation technique provides good convergence for the *b*-parameter distribution

COMPARISON OF LINE-WIDTH DISTRIBUTIONS

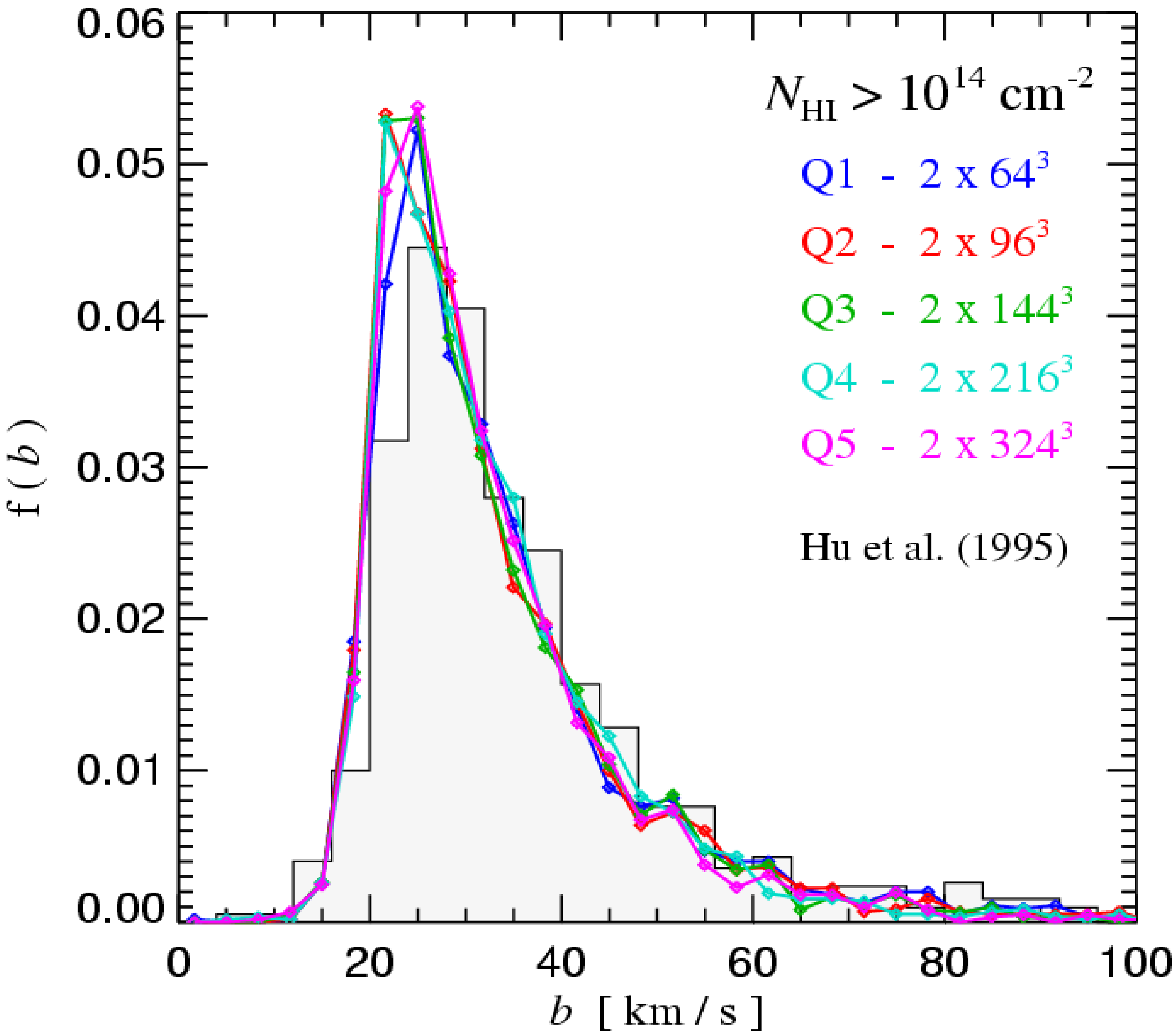

Theuns et al. (1998)

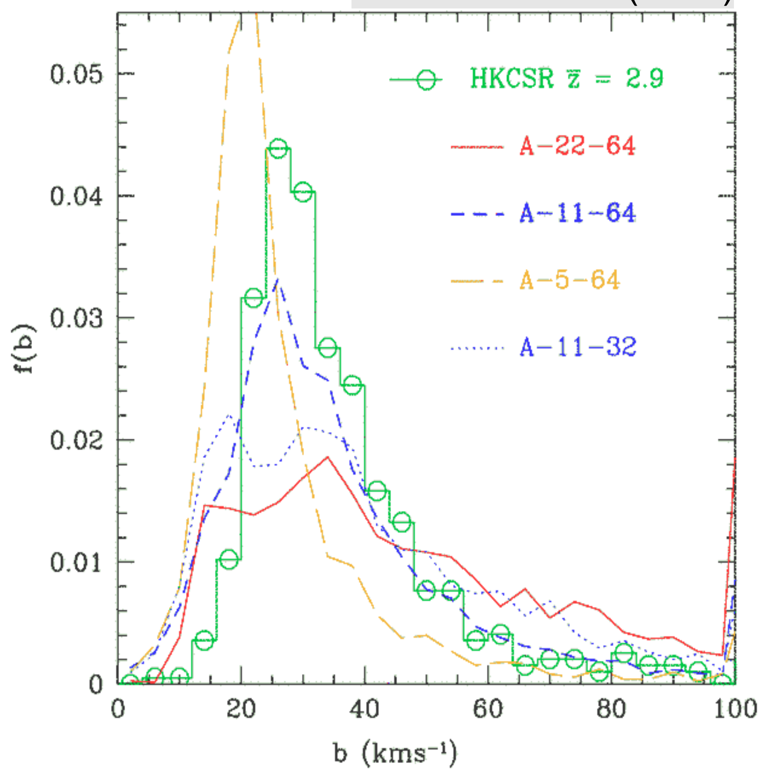

Bryan et al. (1999)

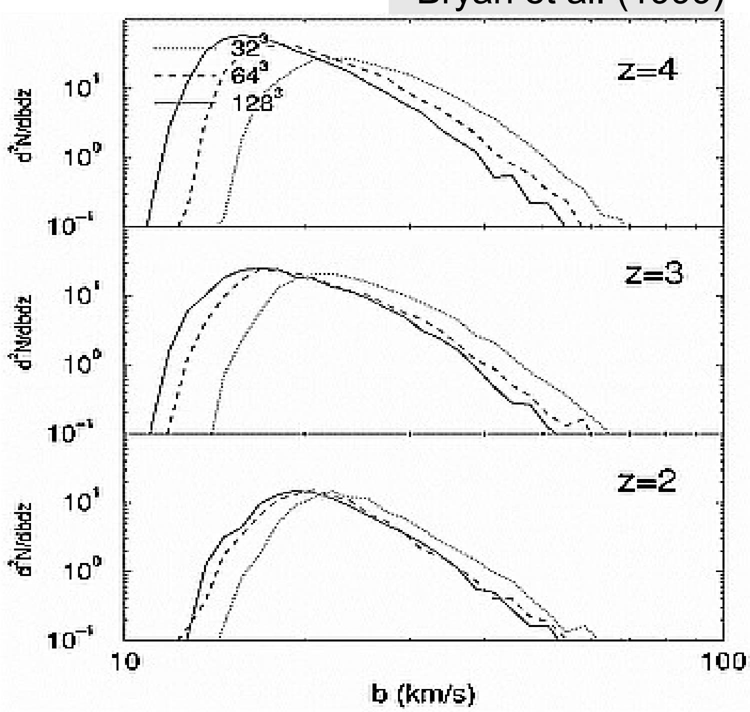

Improved numerical resolution leads to slightly narrower weak lines

COMPARISON OF LINE-WIDTH DISTRIBUTONS

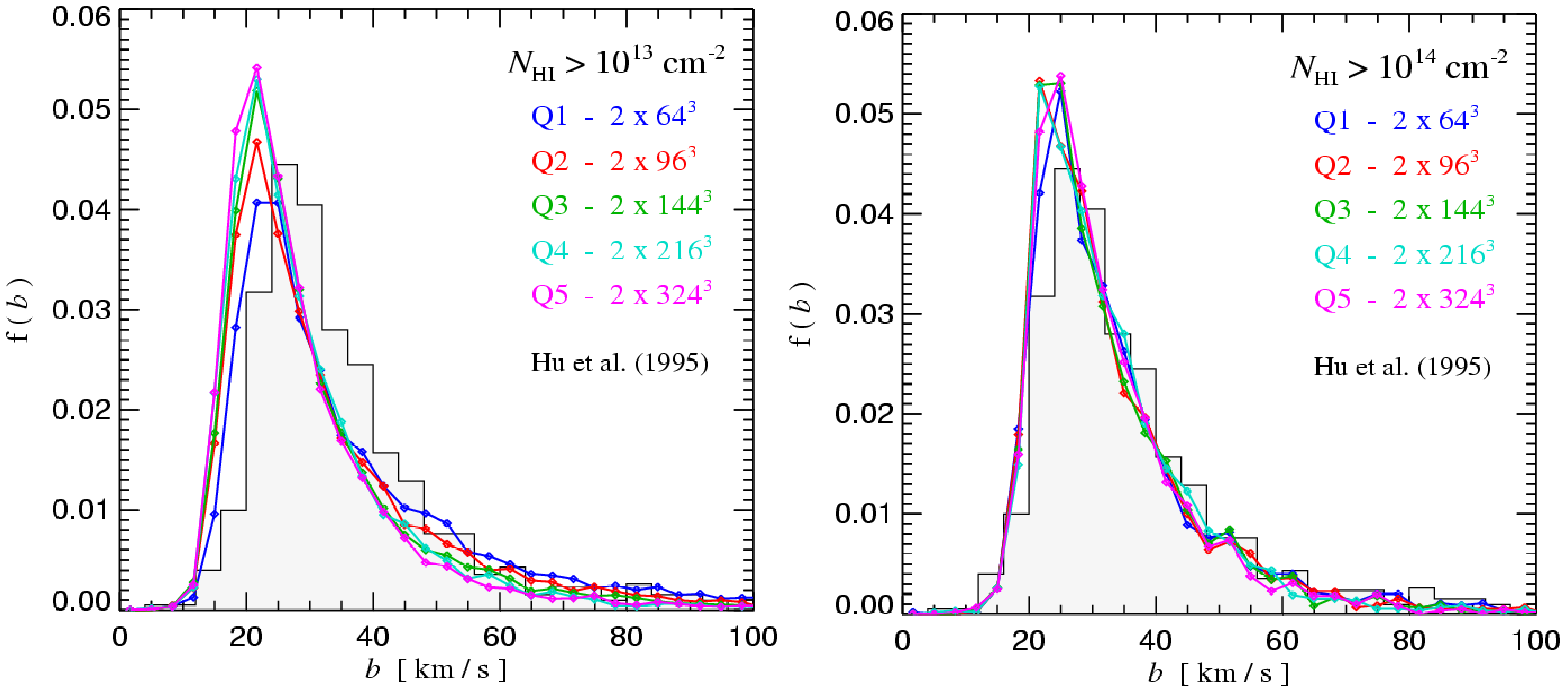

Regions of the IGM that have been influenced by galactic winds show slightly broader lines

BROADING OF LINES IN HEATED/METAL-ENRICHED REGIONS

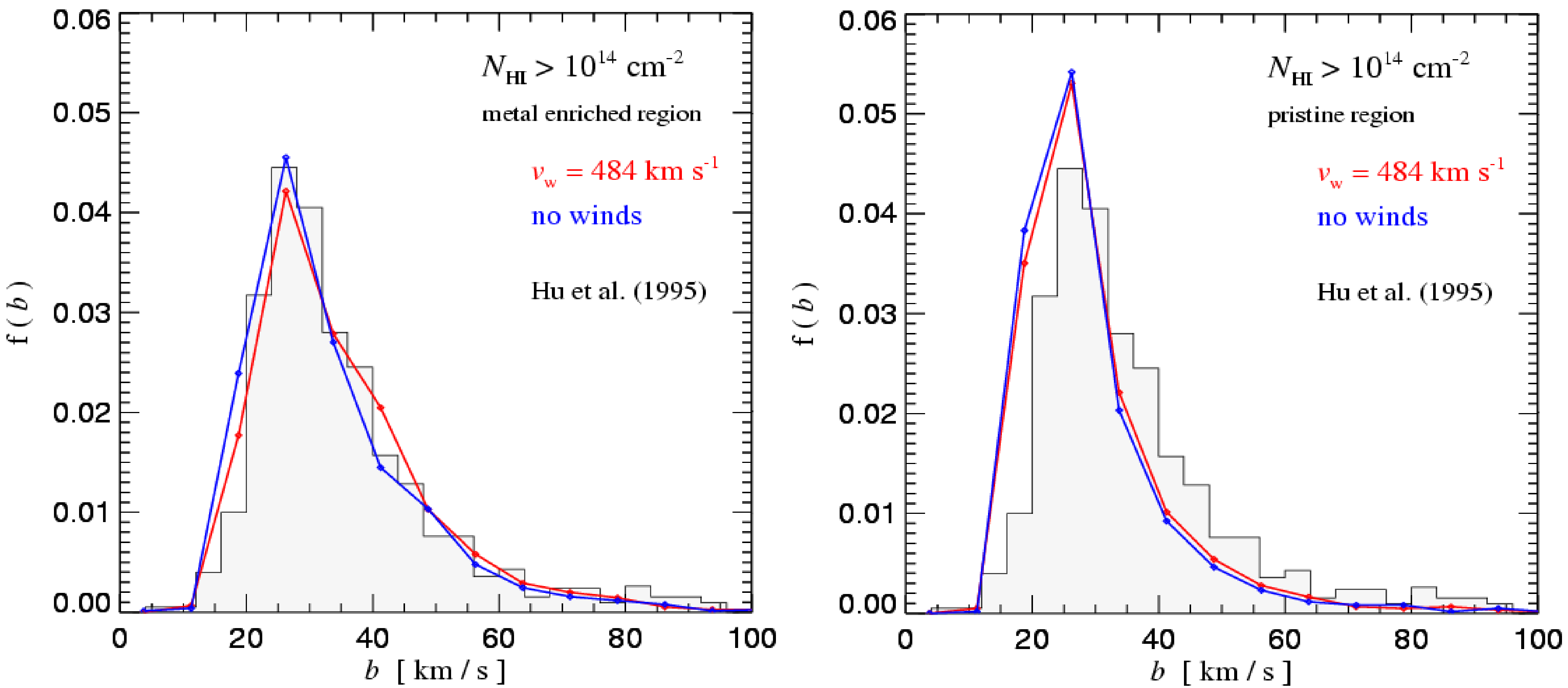

→ *Only a tiny effect !*

The column density distribution provides a good fit to data and is hardly affected by galactic winds

NUMBER DENSITY OF LINES AS A FUNCTION OF COLUMN DENSITY

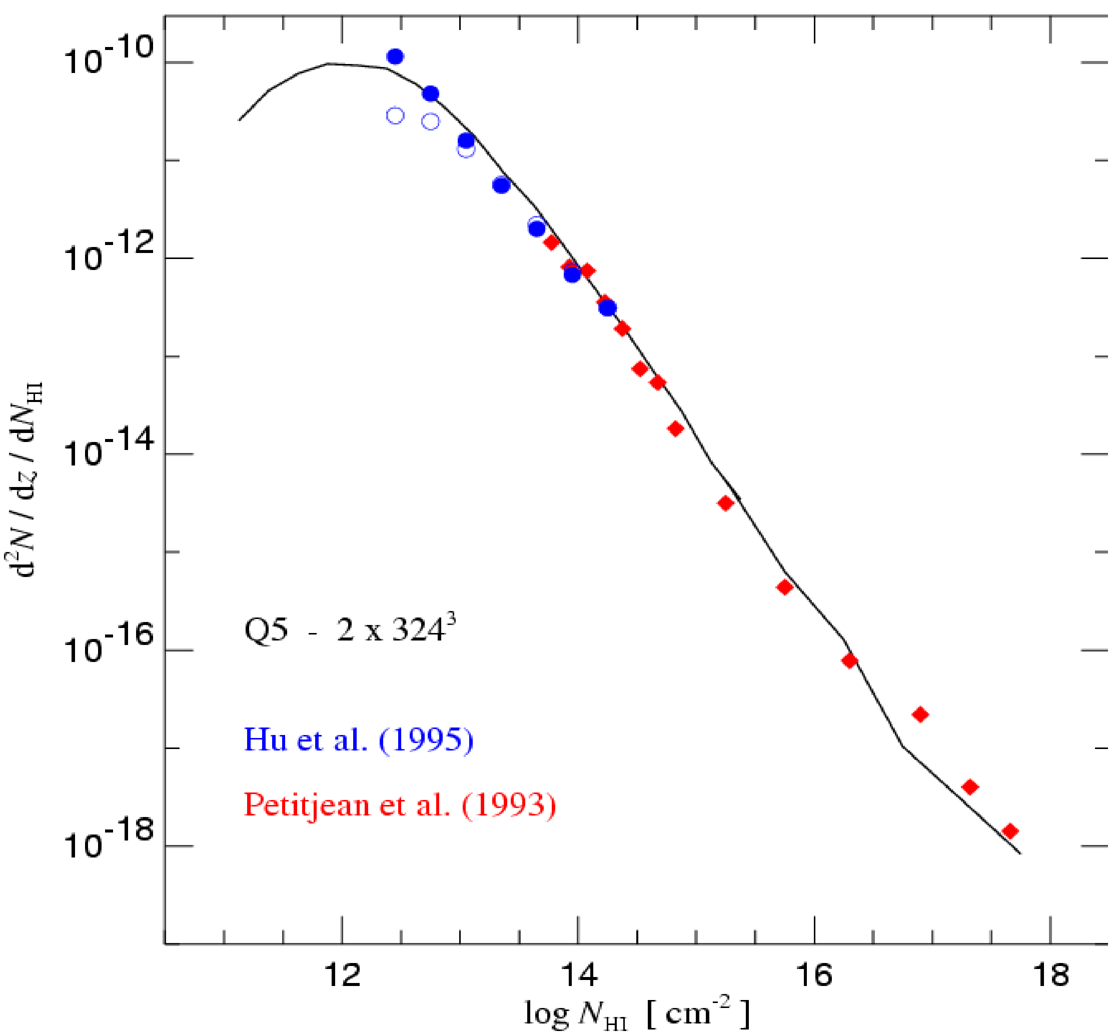

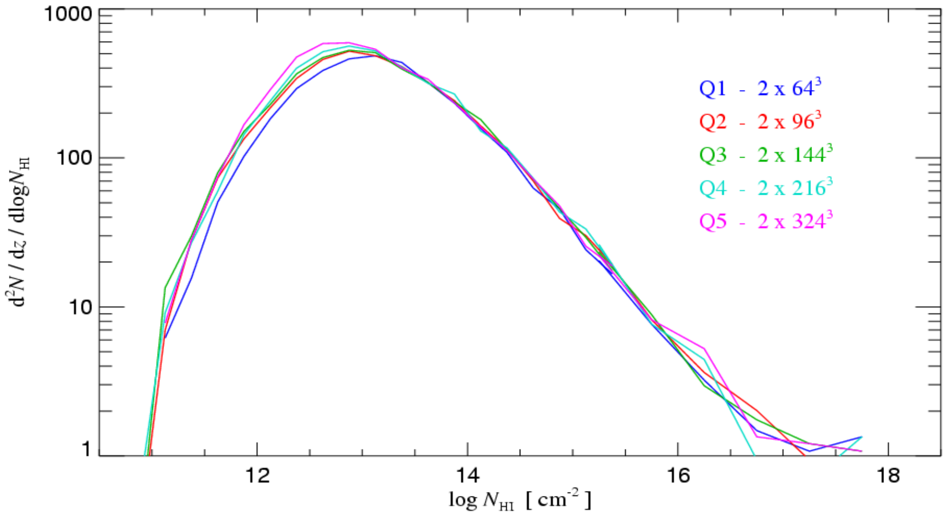

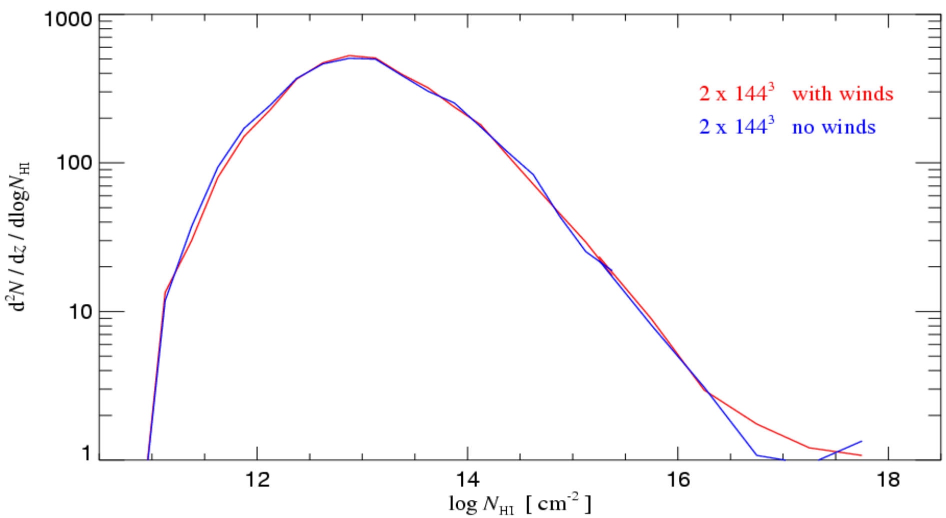

Feedback has been predicted to have a major impact on lines with $N_{HI} \sim 10^{16}$ cm $^{-2}$ (e.g. Theuns, Mo & Schaye 2001) → Not the case in our models

The amount of small-scale power measured in the flux power spectrum is slightly reduced by galactic winds

COMPARISON OF FLUX POWER SPECTRA WITH AND WITHOUT WINDS

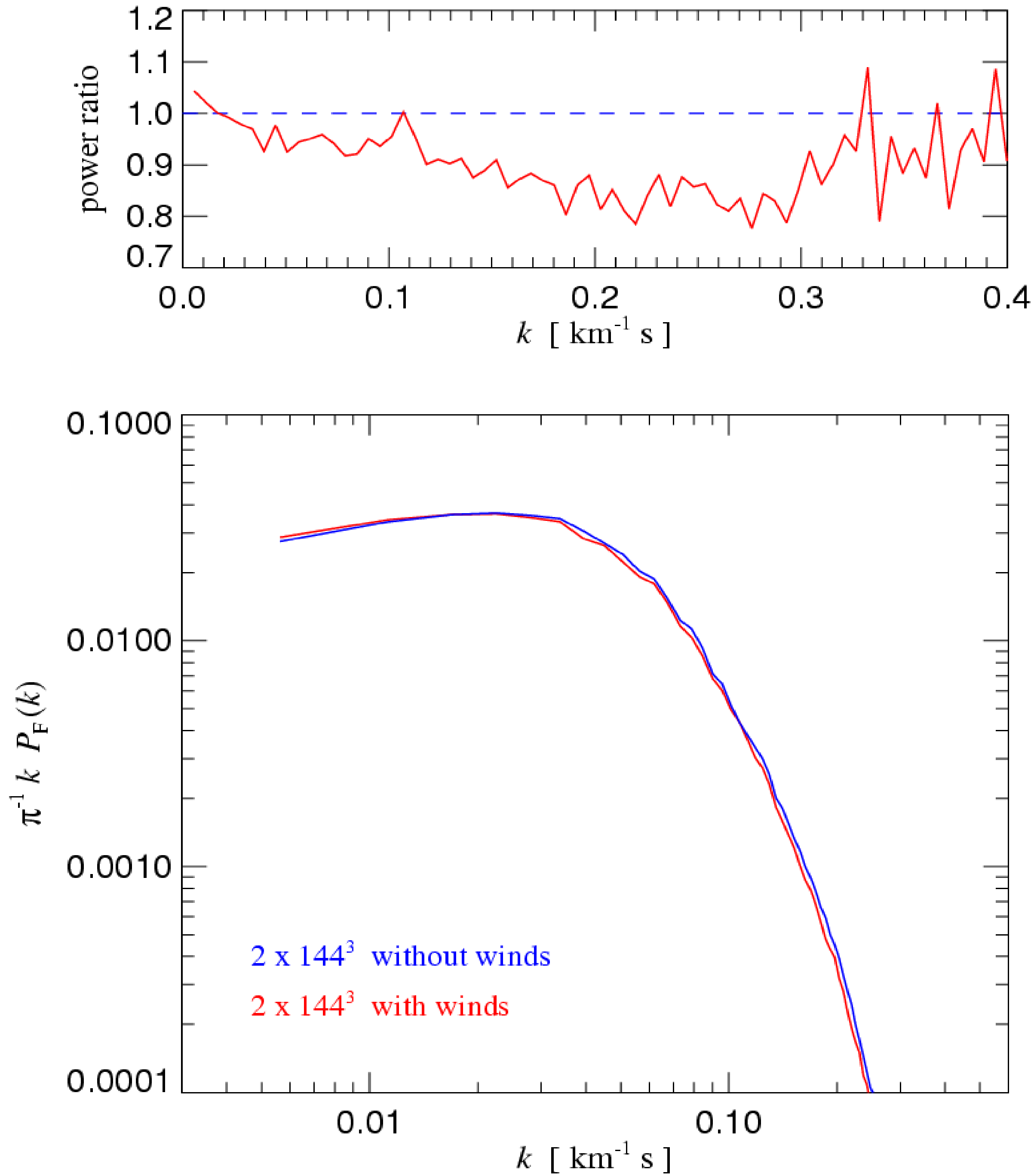

The flux power spectrum is very well converged, except for our lowest resolution simulations

RESOLUTION STUDY FOR THE FLUX POWER SPECTRUM

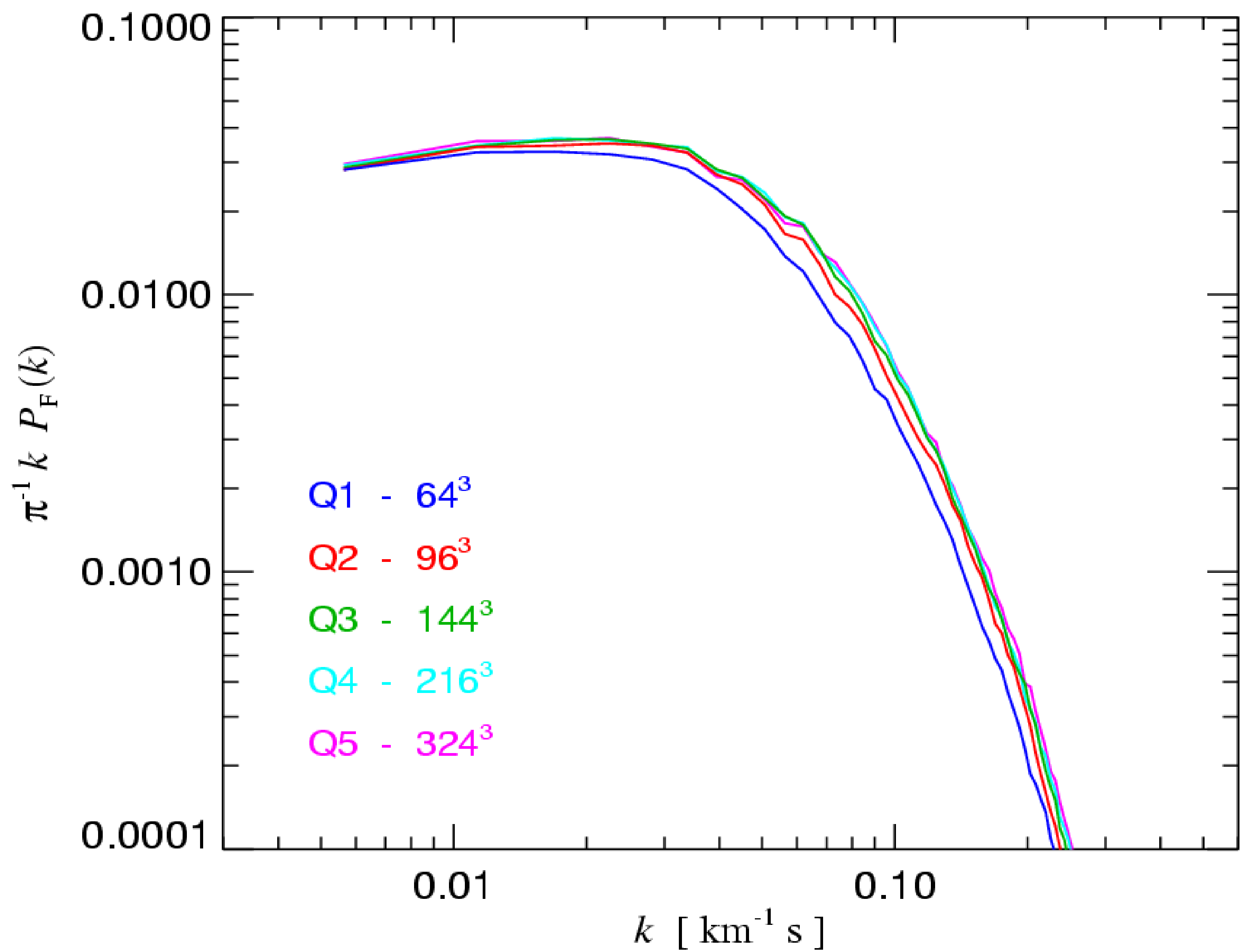

The flux power spectrum matches observational data well, but depending on the correction for meta-line regions, there may be slightly too much small-scale power

FLUX POWER SPECTRUM COMPARED TO OBSERVATIONAL DATA

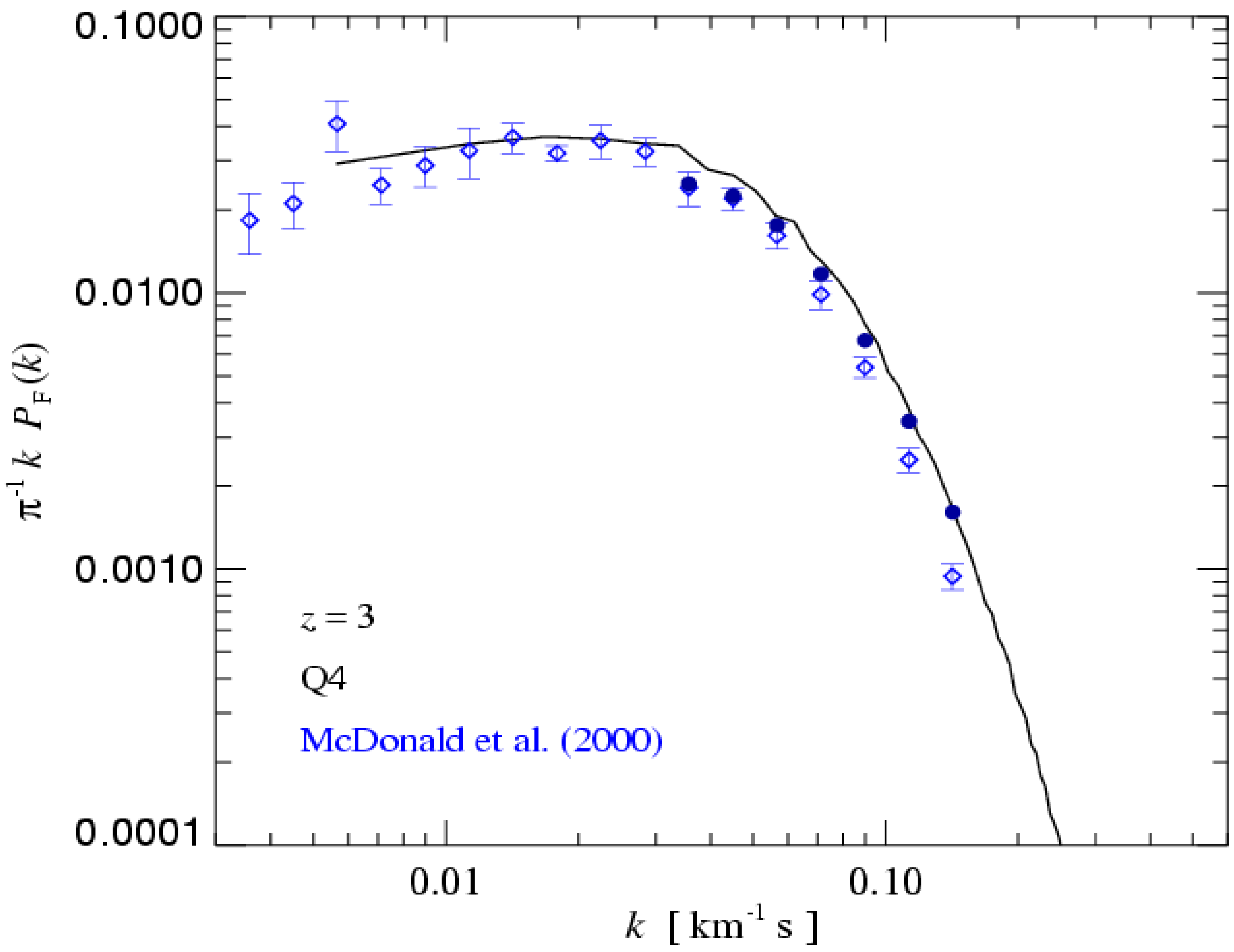

The one-point function of the flux is insensitive to resolution, and to the presence of galactic winds

PROBABILITY DISTRIBUTION OF TRANSMITTED FLUX

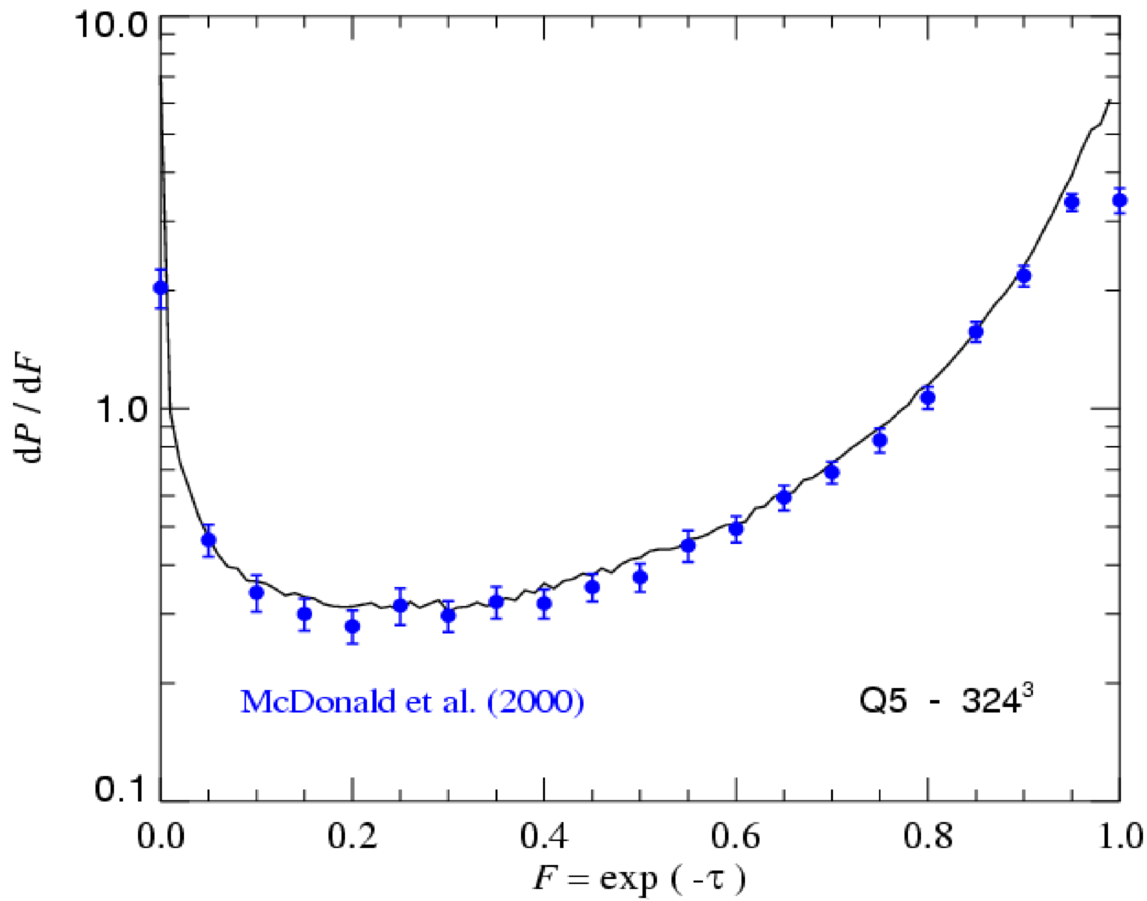

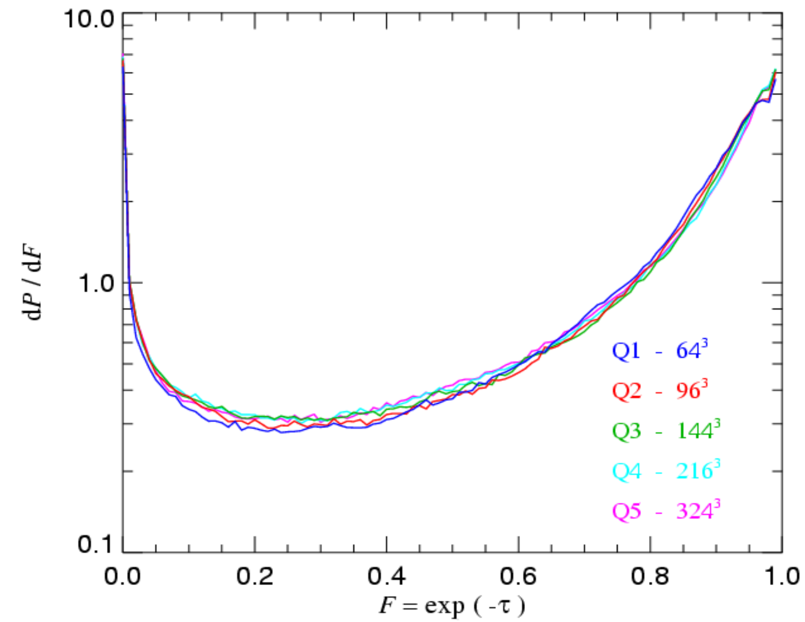

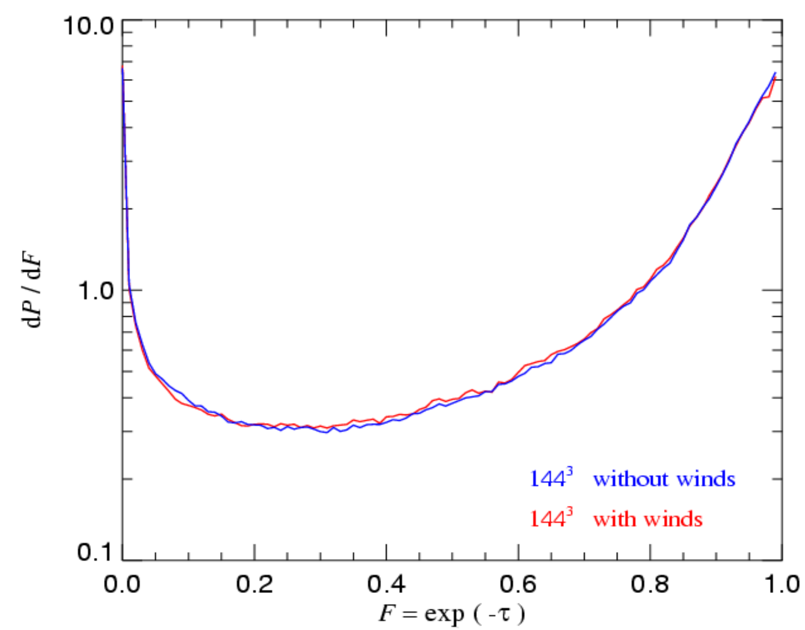

Comparison of observed and simulated flux power spectra allows a measurement of the matter power spectrum

MATTER POWER SPECTRUM OF THE LUQAS SAMPLE

Viel, Haehnelt, Springel (2004)

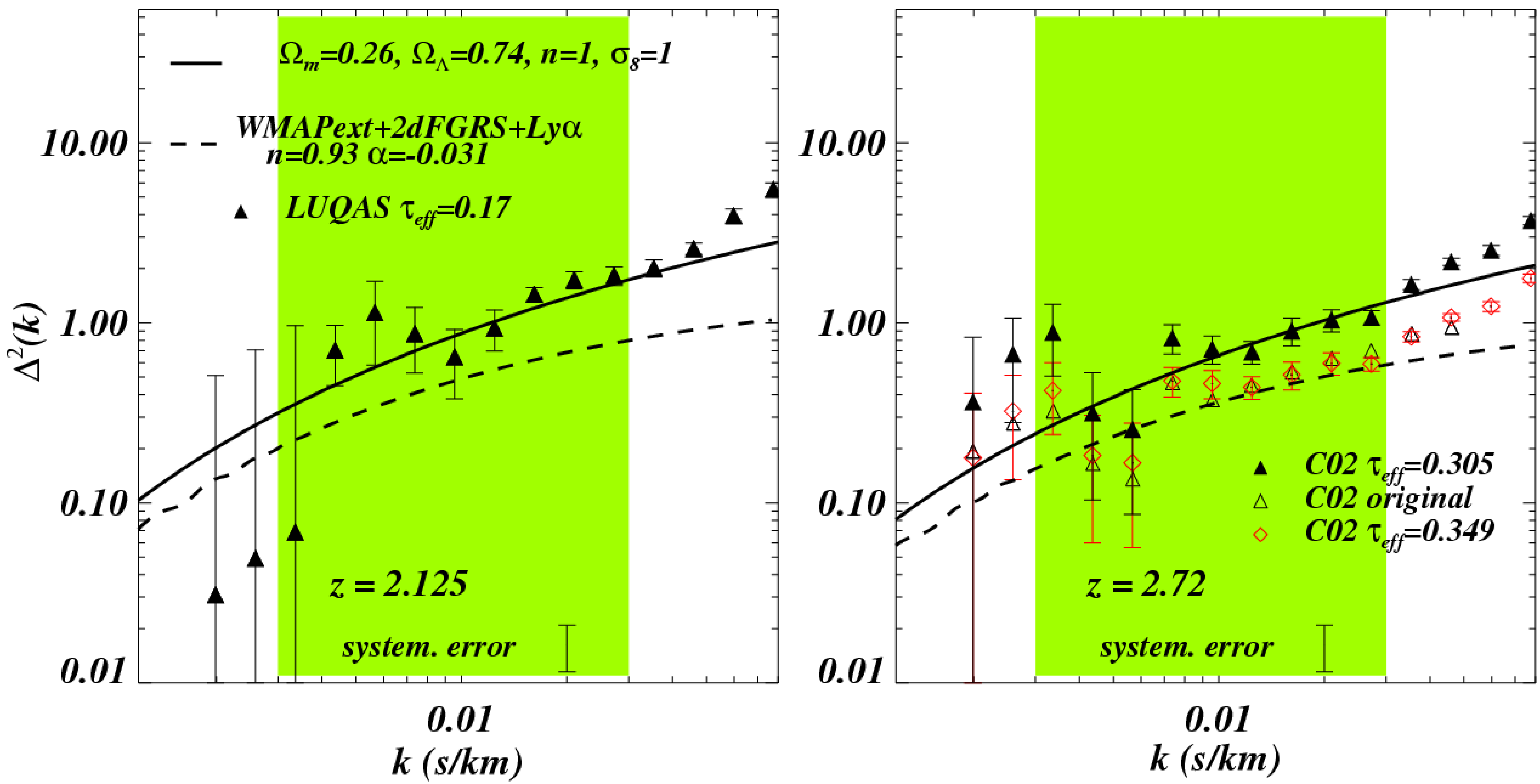

Estimated cosmological parameters depend on continuum fitting and the assumed effective optical depth

COSMOLOGICAL PARAMETERS AS A FUNCTION OF EFFECTIVE OPTICAL DEPTH

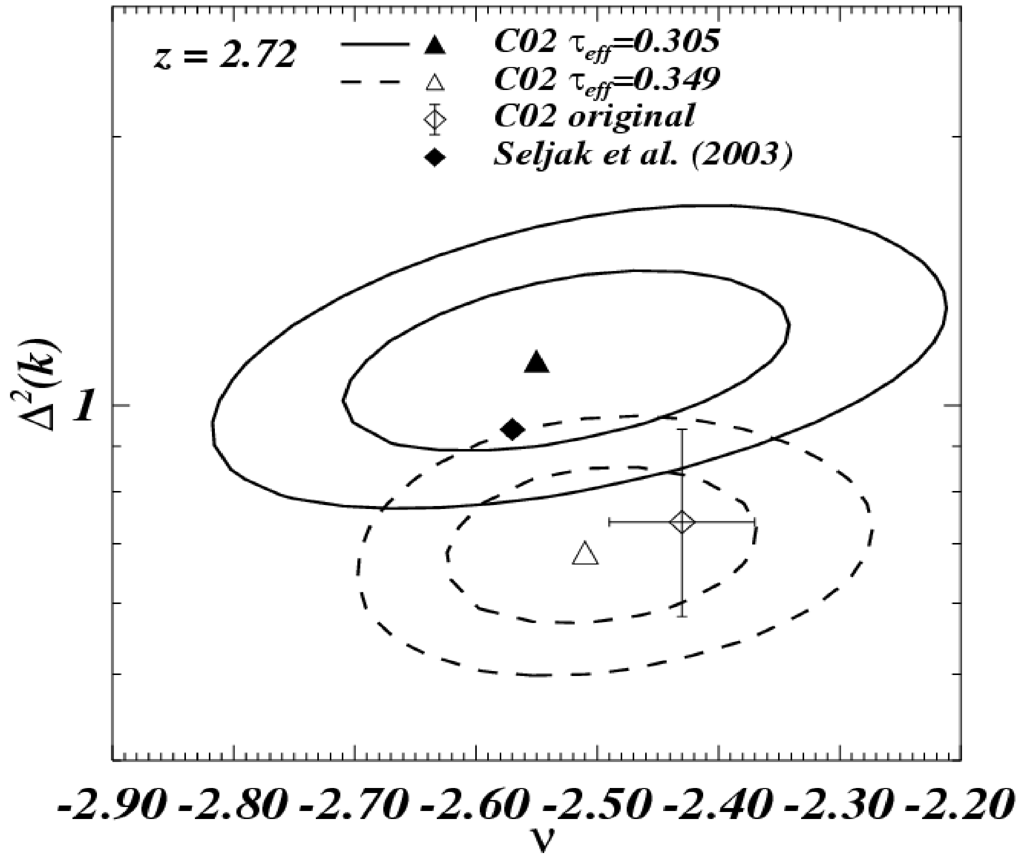

Viel, Haehnelt, Springel (2004)

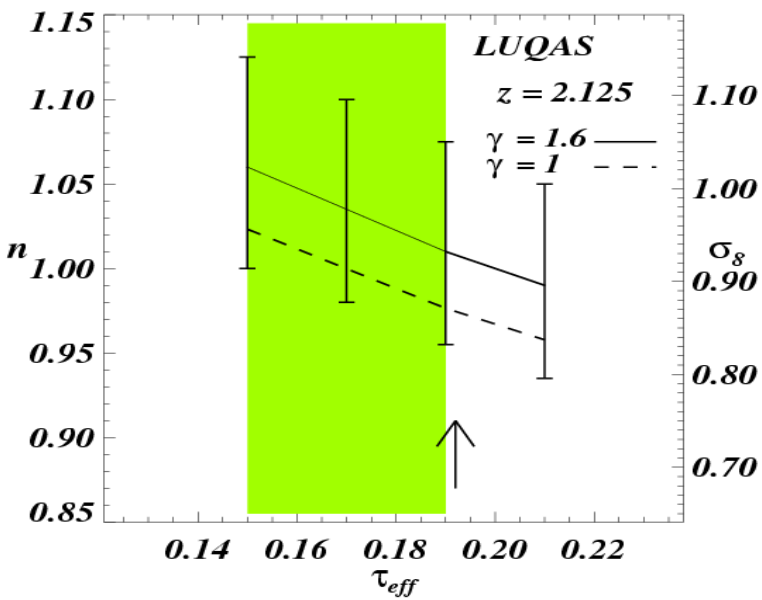

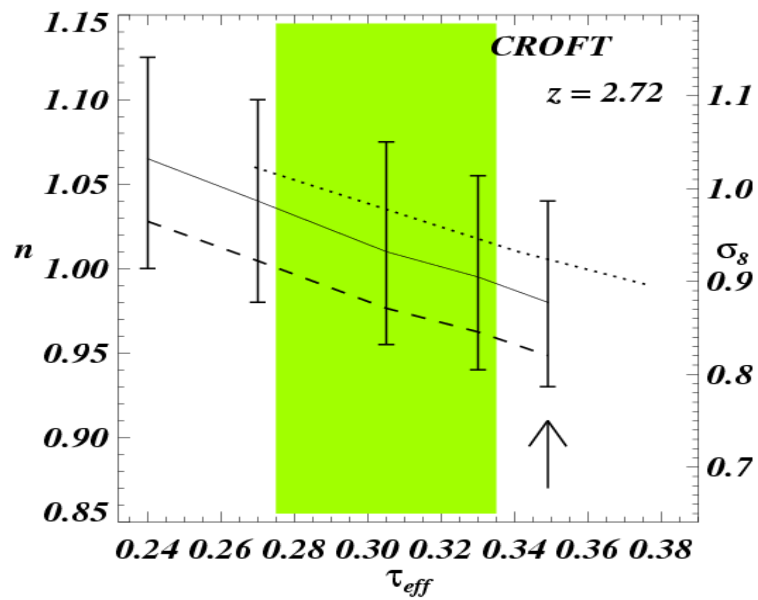

Lyman-alpha forest clustering studies contrain the amplitude and slope of the power spectrum on the scales probed by the forest

LIKELIHOOD CONTOURS OF DIFFERENT LYMAN-ALPHA DATA SETS AND WMAP(3)

Viel, Haehnelt & Lewis (2006)

astro-ph/0604310

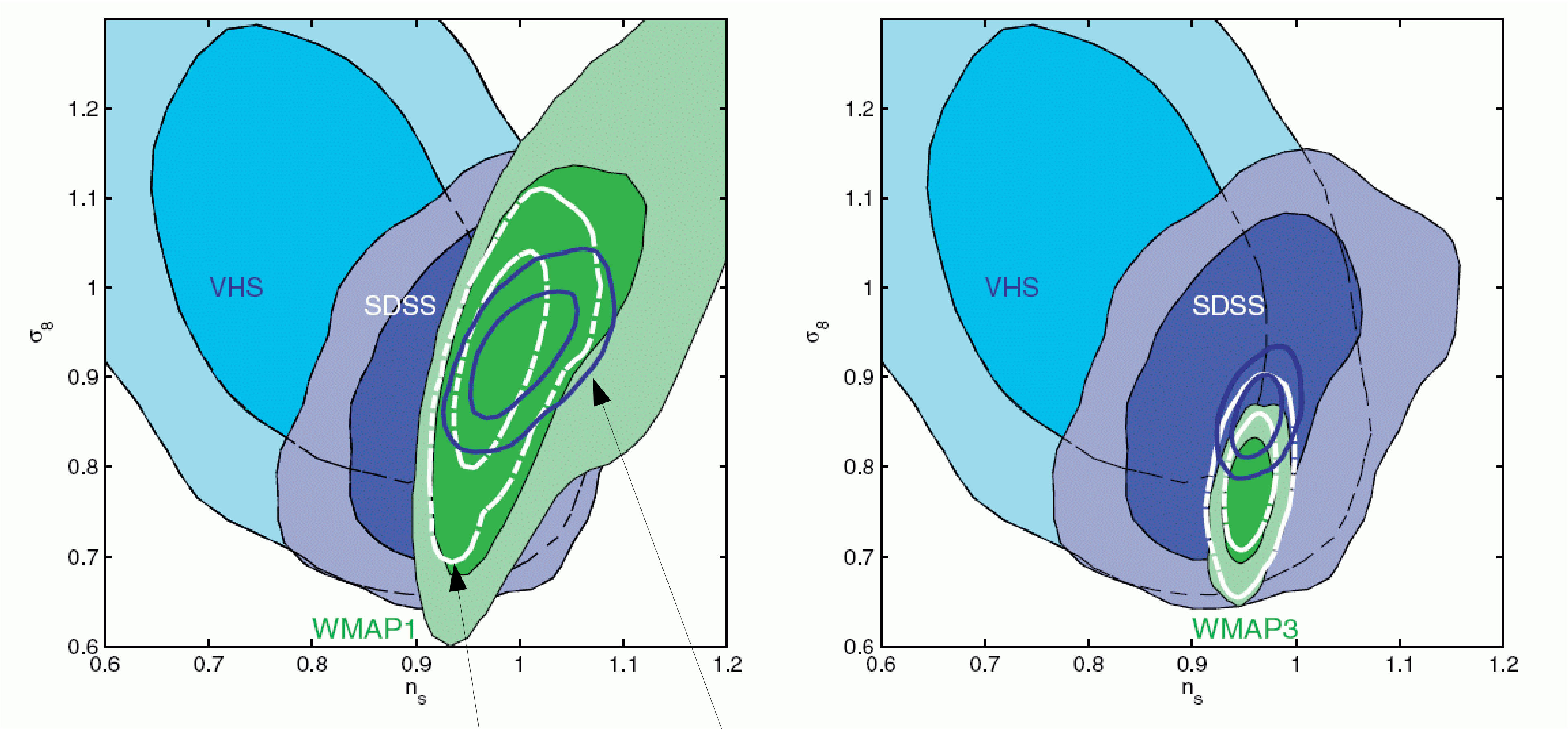

VHS+WMAP1
(VHS is based on
LUQAS+Croft spectra)

SDSS+WMAP1
(Mc Donald analysis)

A joint likelihood analysis of Lyman-alpha forest and WMAP3 pushes sigma8 to a value about 2sigma higher

LIKELIHOOD CONTOURS OF DIFFERENT LYMAN-ALPHA DATA SETS AND WMAP(3)

Viel, Haehnelt & Lewis (2006)
astro-ph/0604310

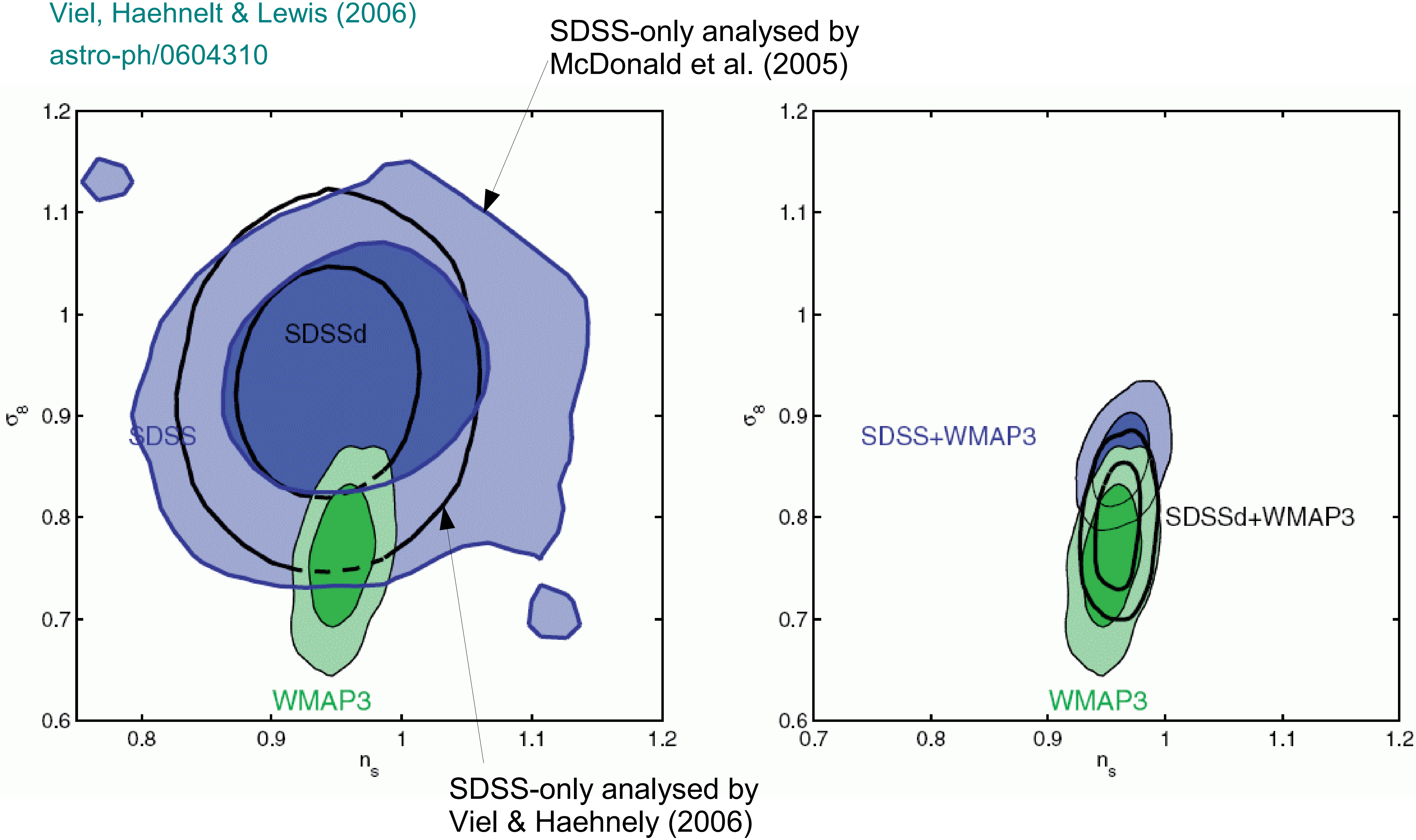

Massive neutrinos act as hot dark matter admixture and reduce the clustering amplitude on small scales

RATIO OF THE POWER SPECTRUM IN THE CASE WITH NEUTRINOS TO THE CASE WITHOUT

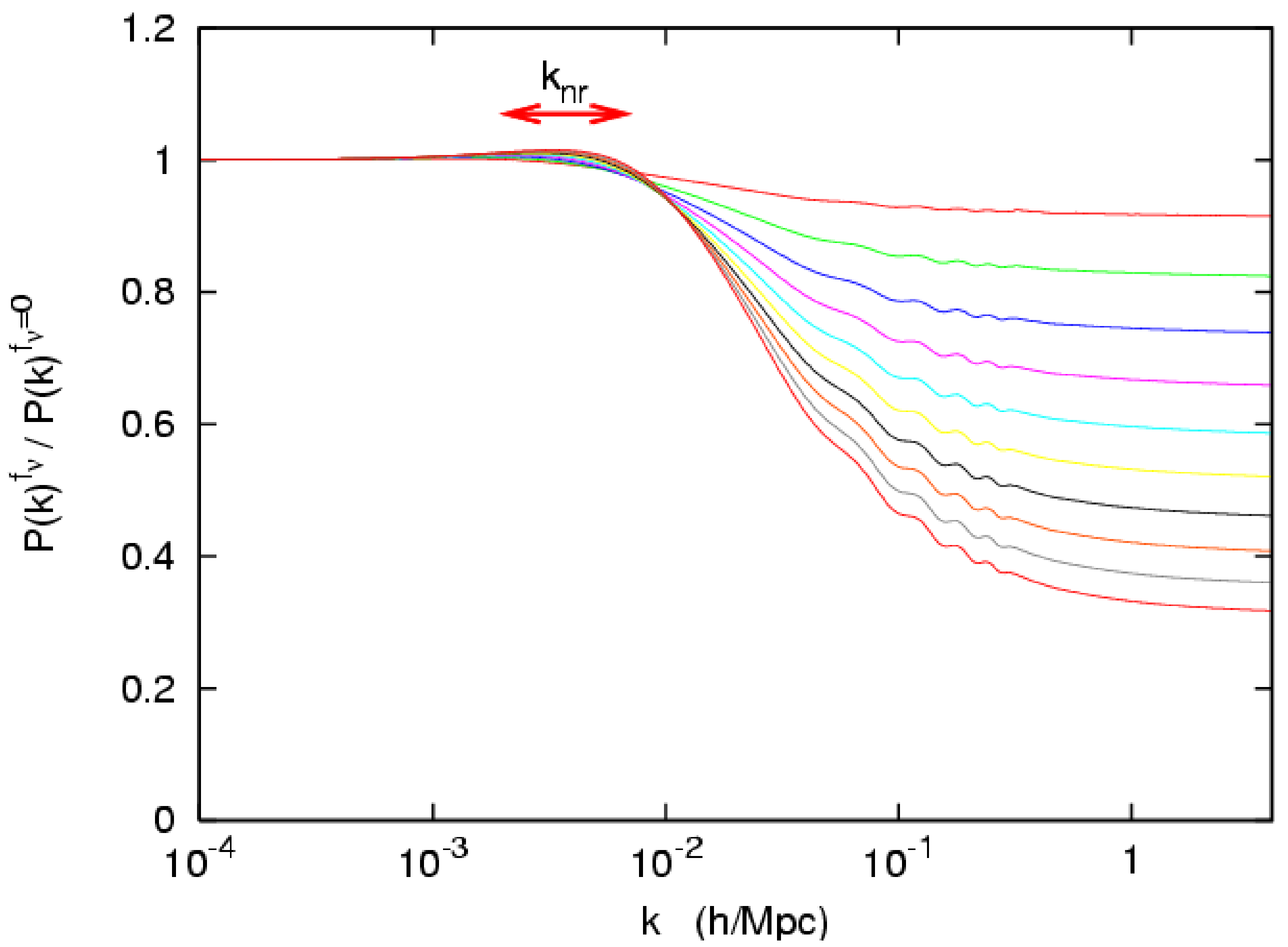

Based on the tension between WMAP3 and Ly-alpha, Seljak et al. have inferred a powerful limit on the sum of the neutrino masses

POSSIBLE NEUTRINO MASSES AS A FUNCTION OF THE SUM OF THE MASSES

Seljak, Slosar & McDonald (2006)

astro-ph/0604335

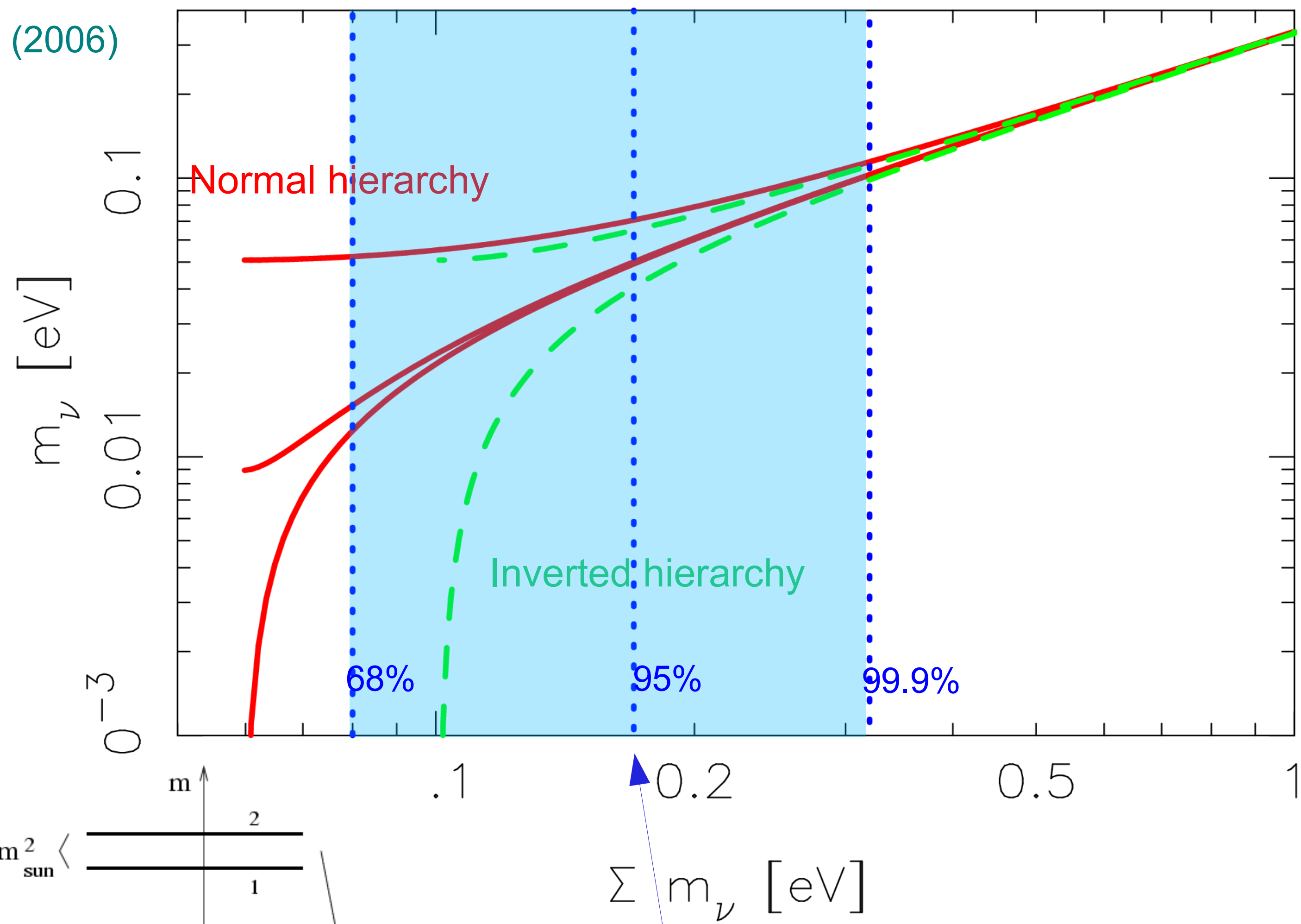

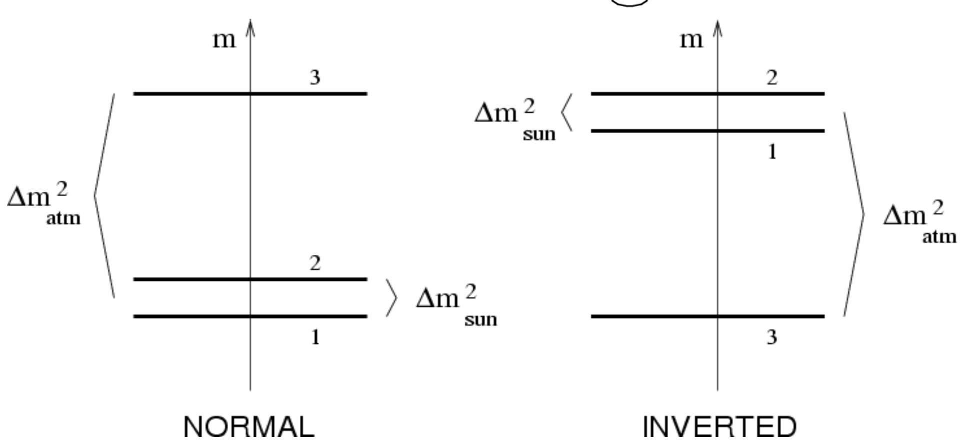

Limit by **Seljak, Slosar & McDonald (2006):**

$$\sum m_\nu \leq 0.17\,\mathrm{eV} \quad (95\%)$$

Metal enrichment of the intergalactic medium

Projected metallcity maps reveal a highly non-uniform enrichment pattern

PROJECTED MEAN GAS METALLICITY

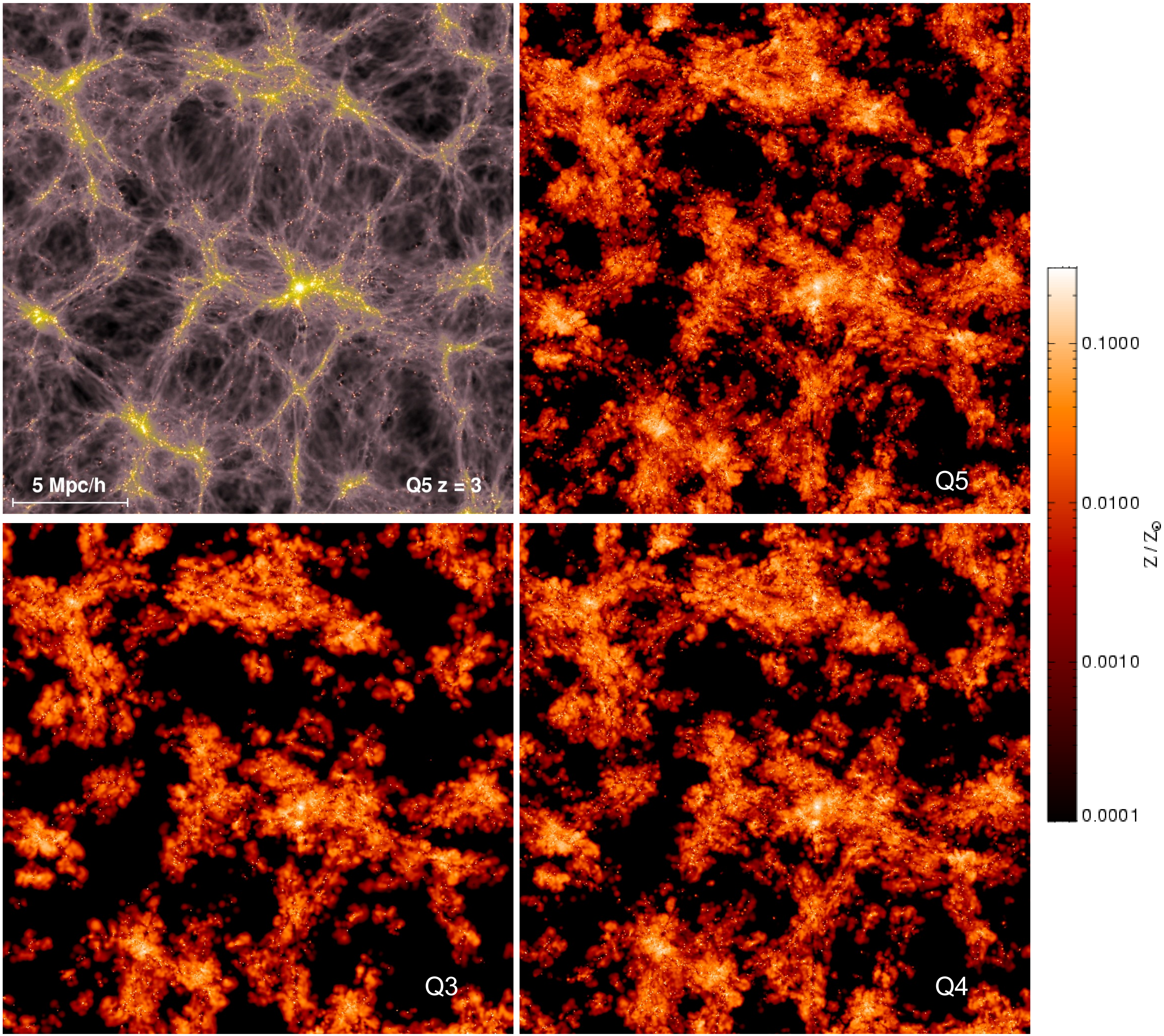

Metal enrichment by winds establishes a bimodal metallicity-density distribution

METAL ABUNDANCE AS A FUNCTION OF GAS OVERDENSITY

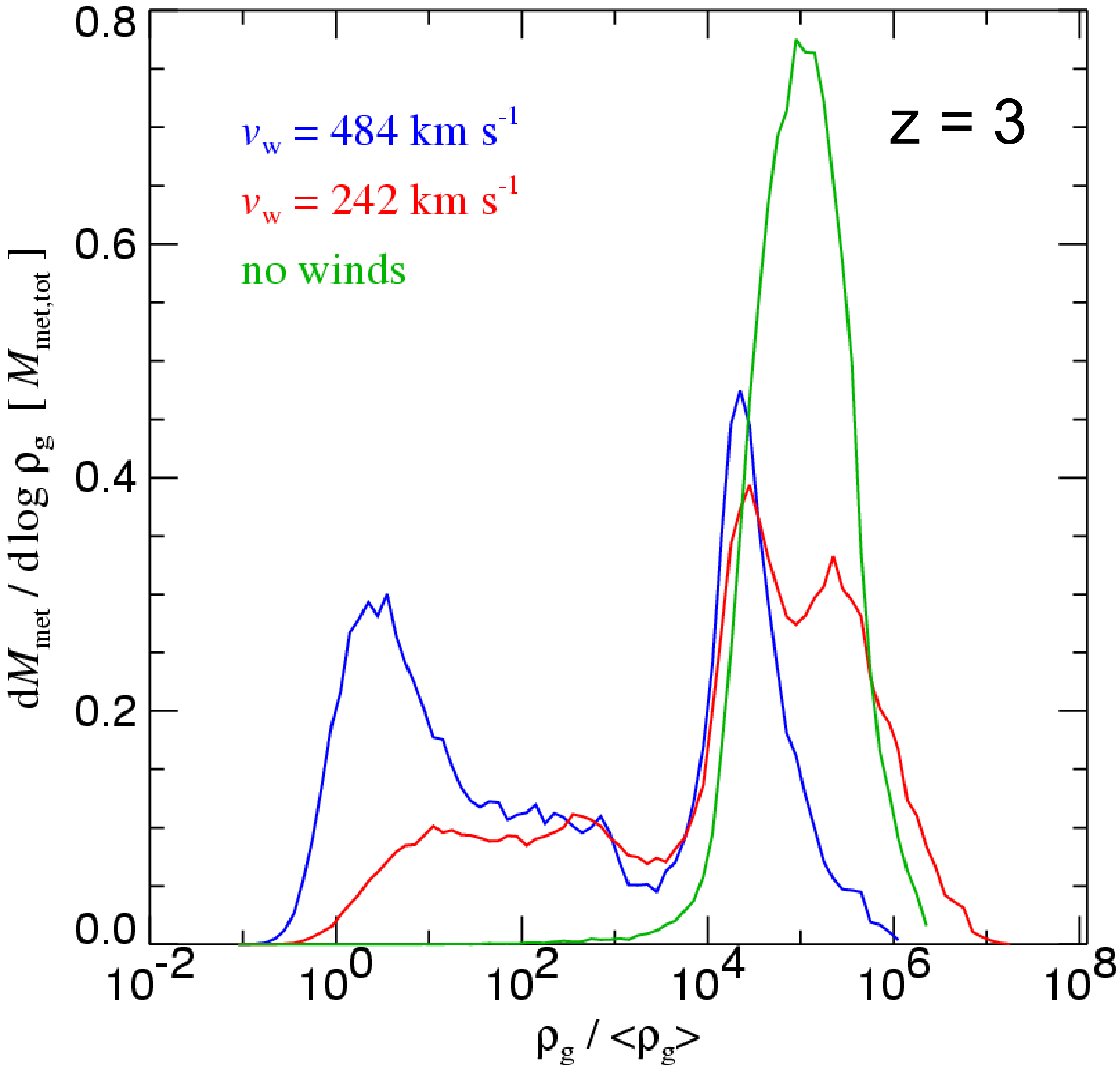

The transport of metals by winds appears to be well resolved by our simulation technique, but full convergence requires high resolution

METAL ABUNDANCE VERSUS GAS OVERDENSITY AT DIFFERENT RESOLUTIONS

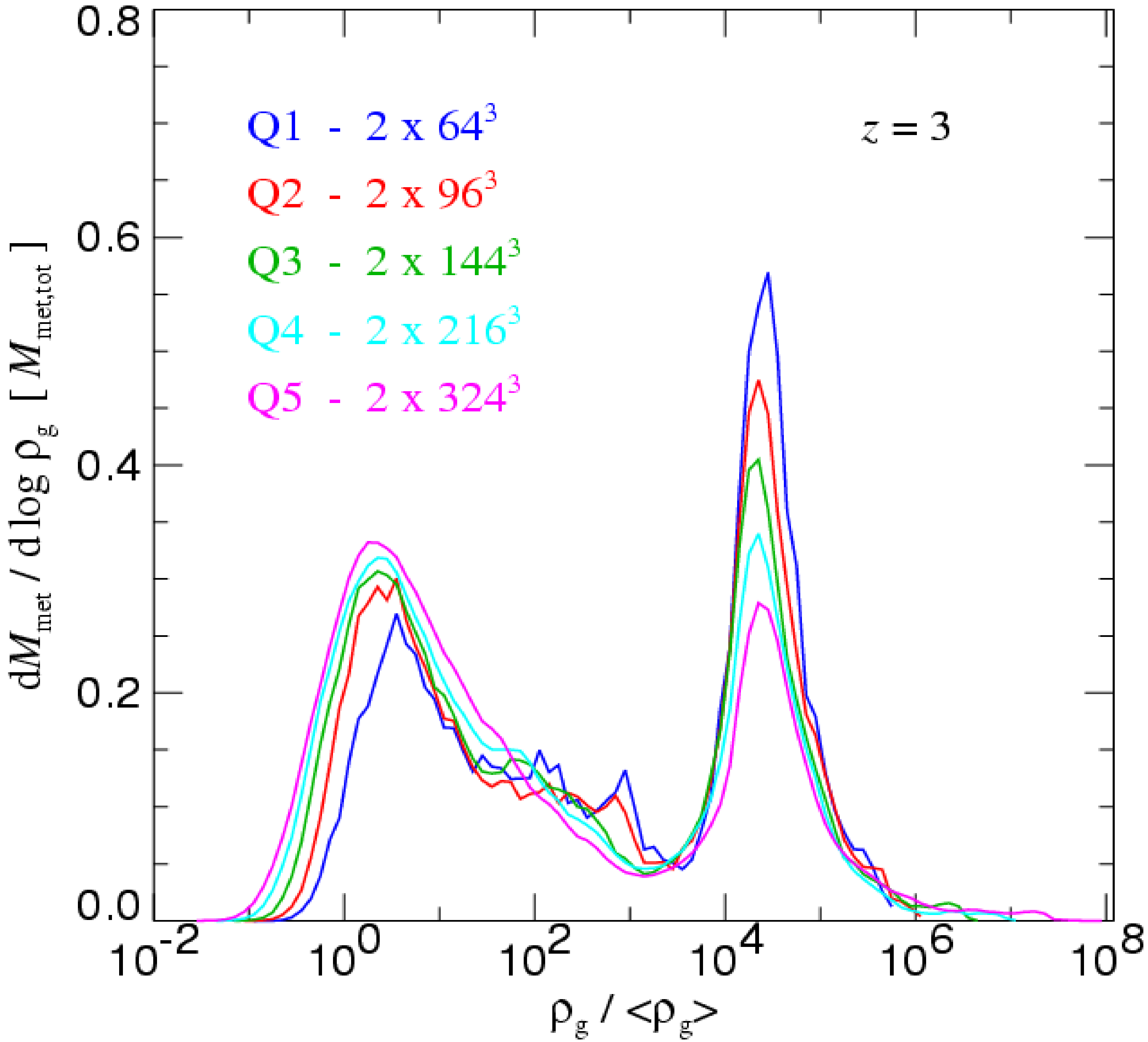

Galactic winds may enrich a sizable fraction of the total volume, while without them the IGM remains completely pristine

POLUTED VOLUME FRACTION

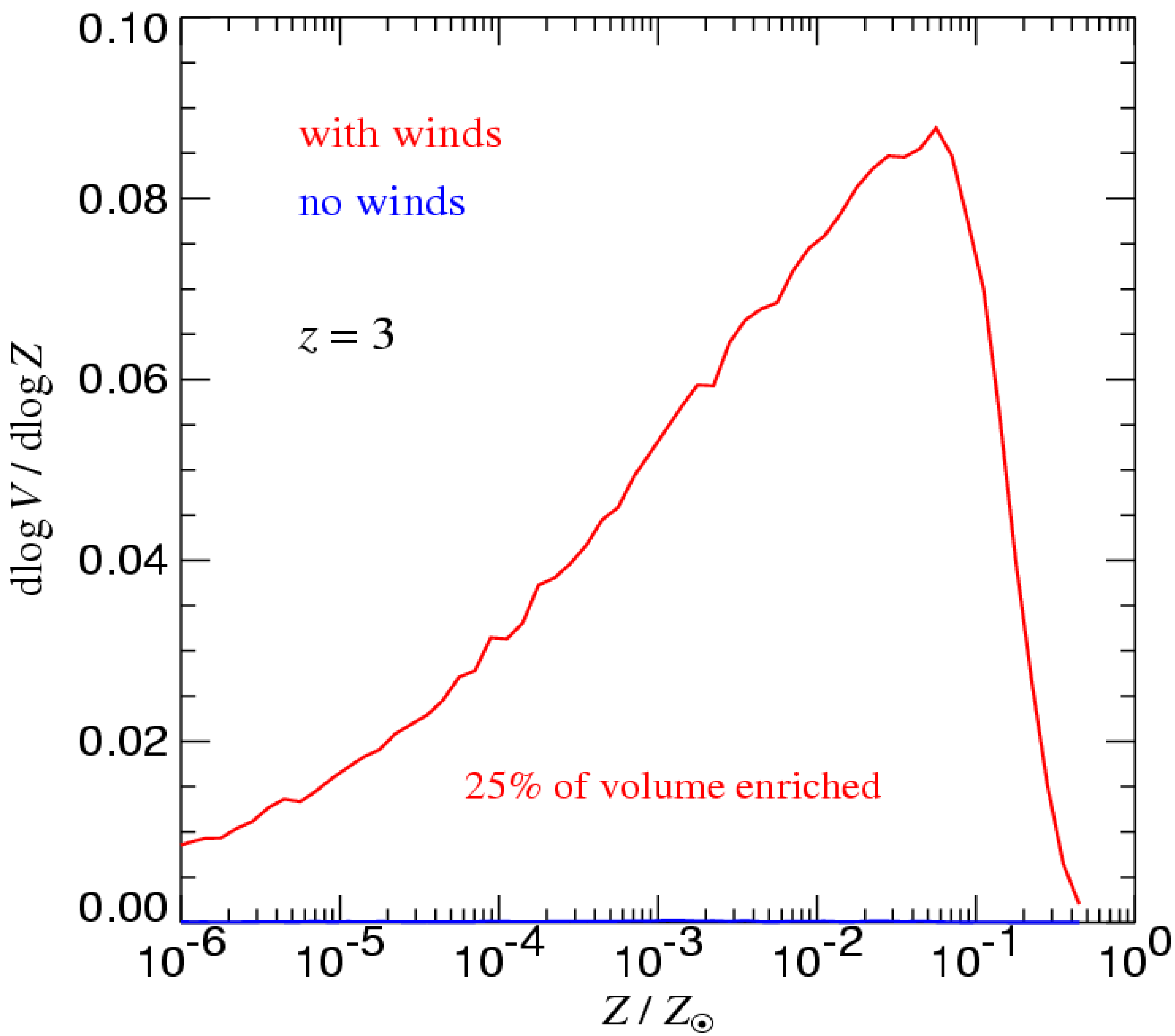

Gnedin (1998): “...that the dominant mechanism for transporting heavy elements from protogalaxies into the intergalactic medium (IGM) is the merger mechanism as discovered by Gnedin & Ostriker. Direct ejection of the interstellar gas by supernovae plays only a minor role in transporting metals into the IGM.ƒ

Similarly, it is challenging to obtain a numerically converged result for the volume fraction heated by galactic winds

DIFFERENTIAL VOLUME DISTRIBUTION AS A FUNCTION OF TEMPERATURE

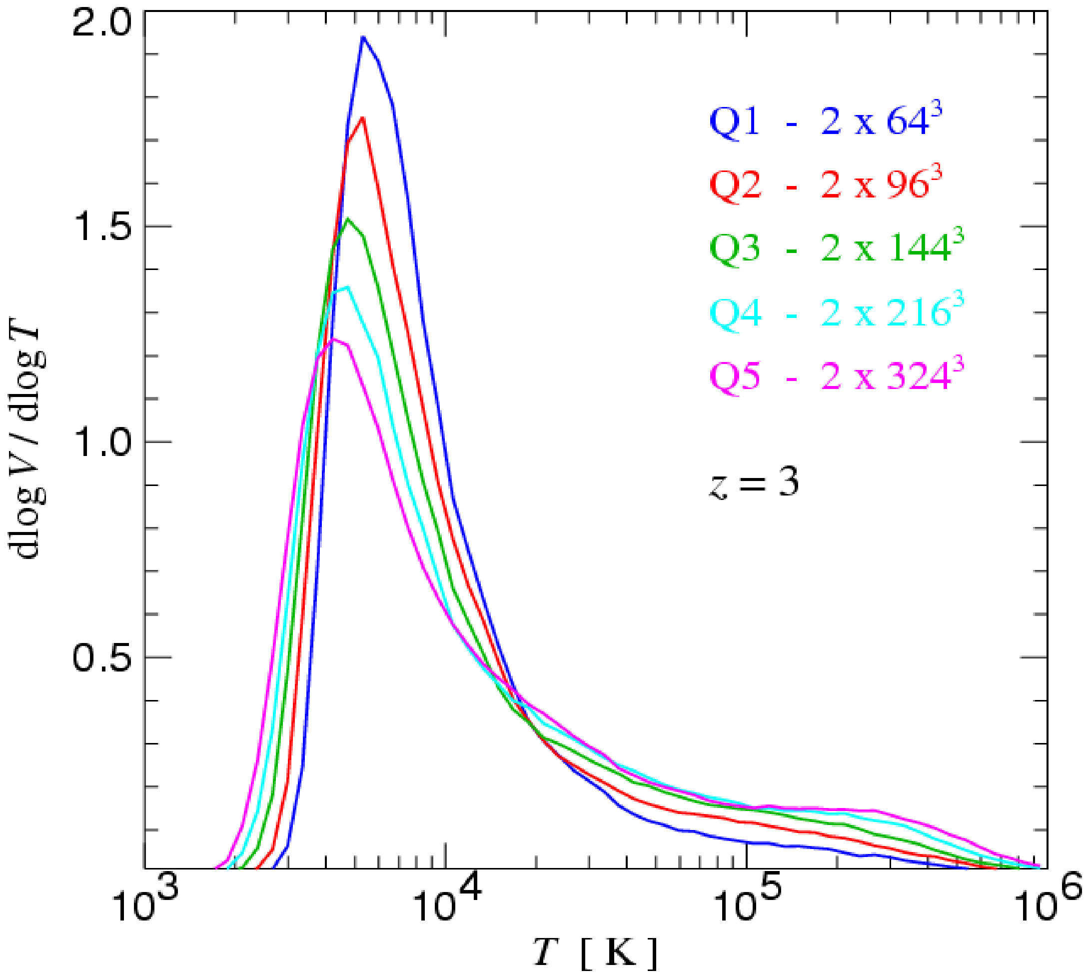

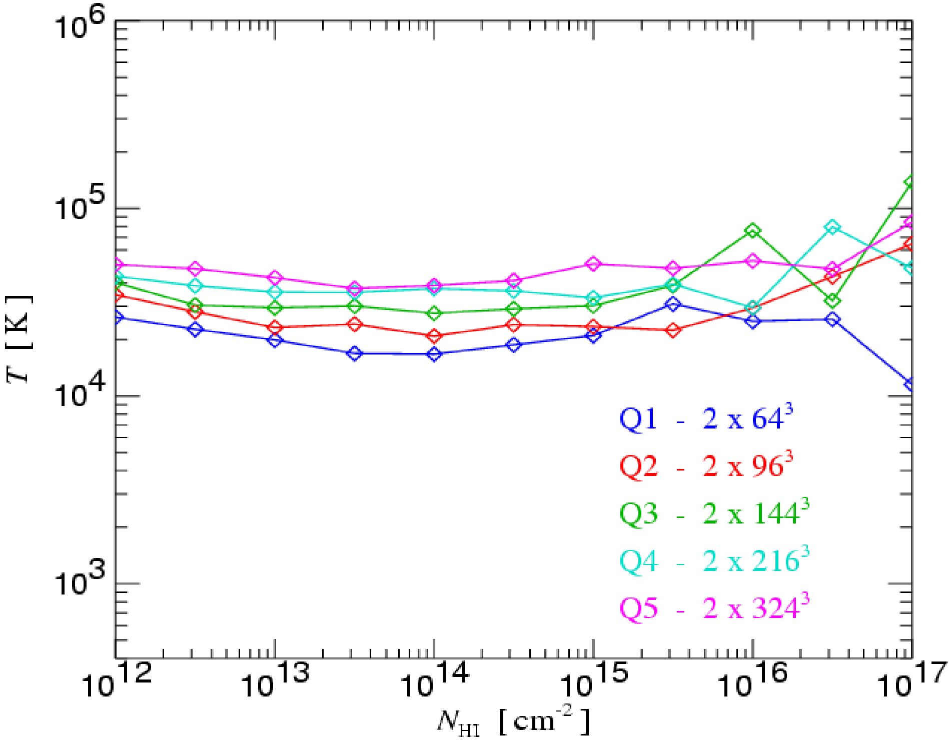

Winds can enrich the low-density IGM to levels suggested by obervations of the Lyman-α forest

MEAN NEUTRAL-WEIGHTED METALLICITY AS A FUNCTION OF OVERDENSITY

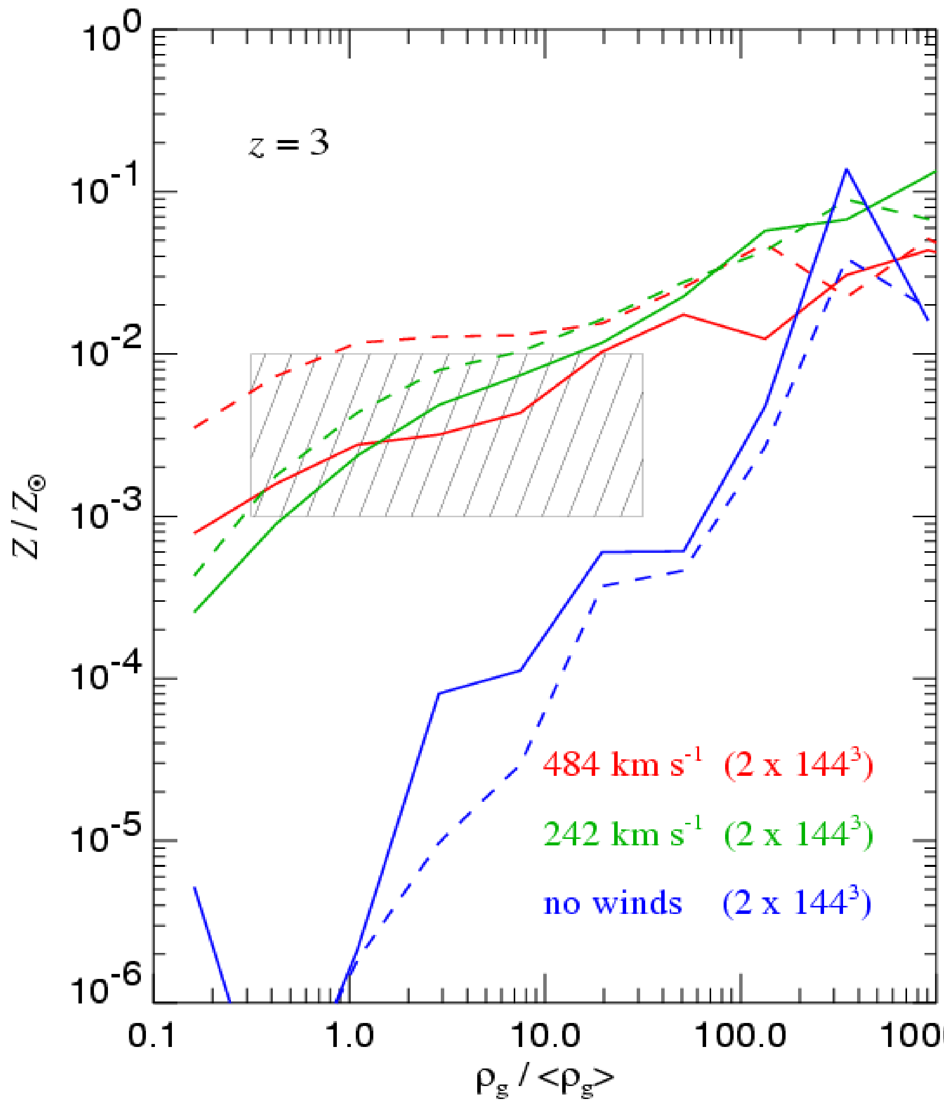

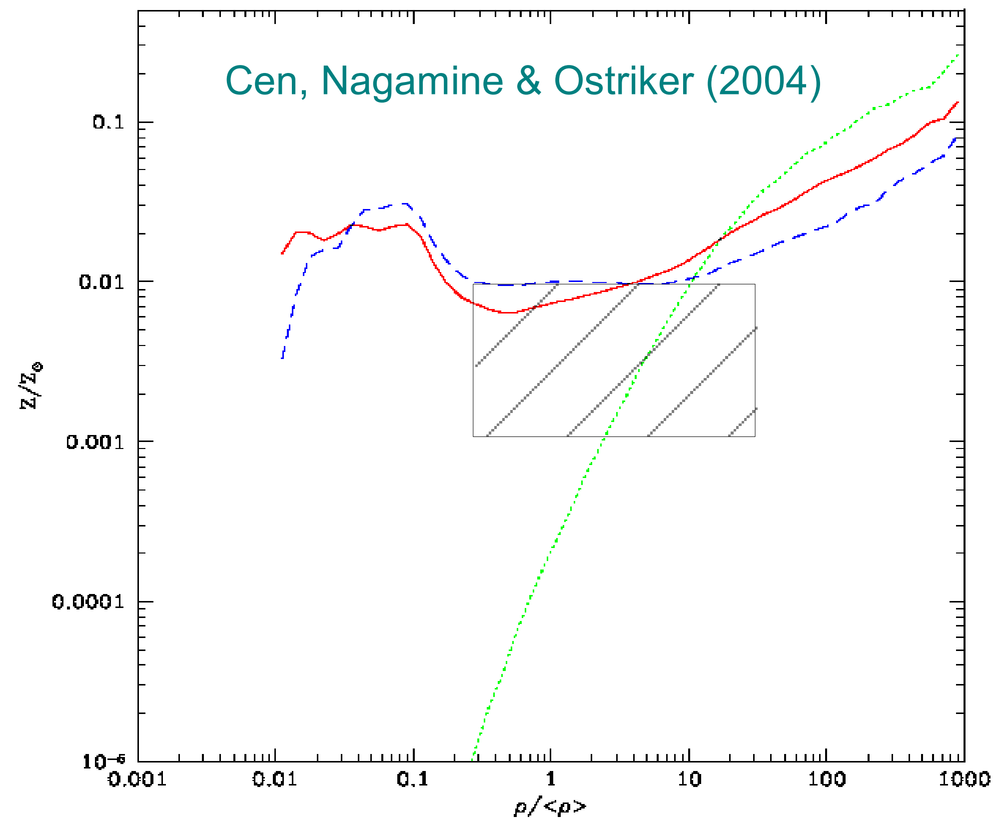

The enriched gas shows too little C-IV absorption

COMPARISON OF CARBON ABSORPTION IN SIMULATIONS AND OBSERVATIONS

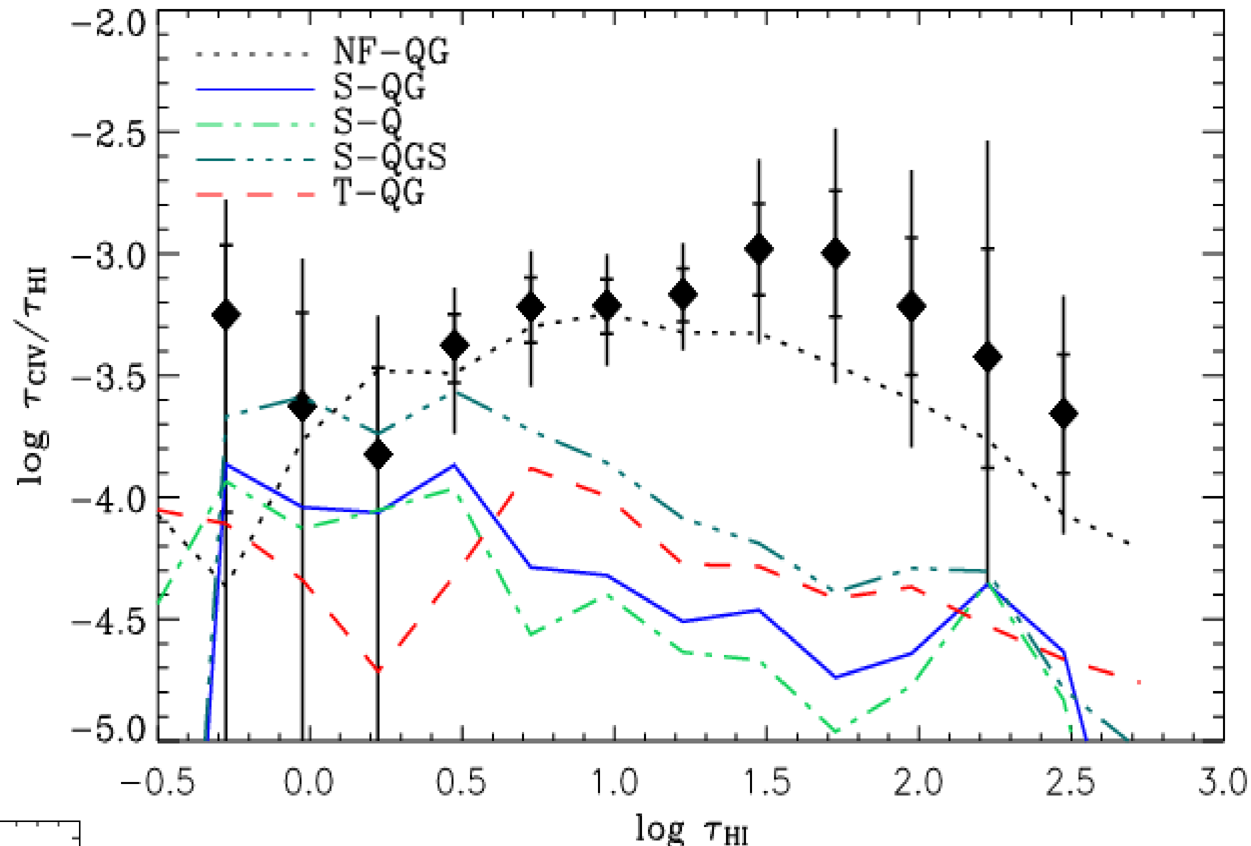

Aguirre, Schaye, Hernquist, Kay, Springel, Theuns (2005)

hot particles set to $2x10^4$ K

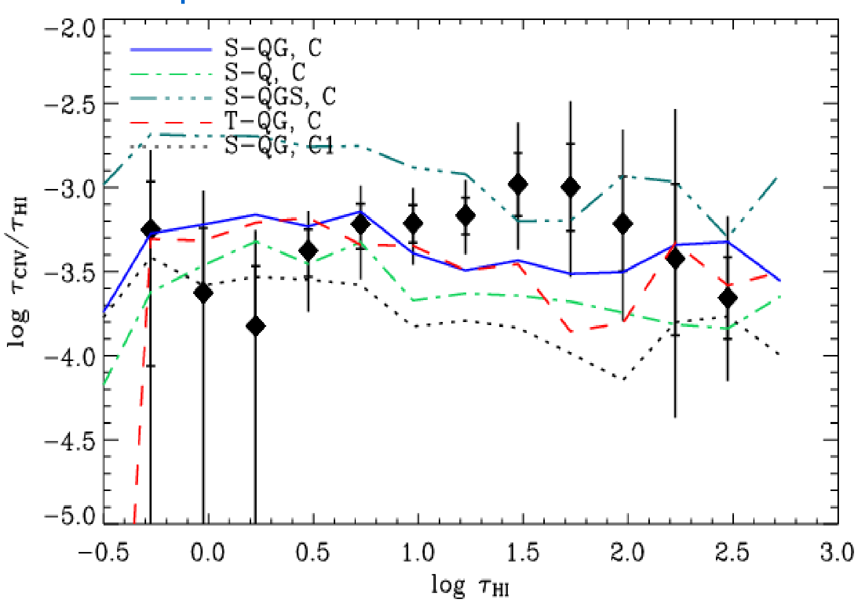

→ The enriched gas is too hot

The enriched gas shows defficient CIII / CIV ratios

COMPARISON OF CARBON ABSORPTION IN SIMULATIONS AND OBSERVATIONS

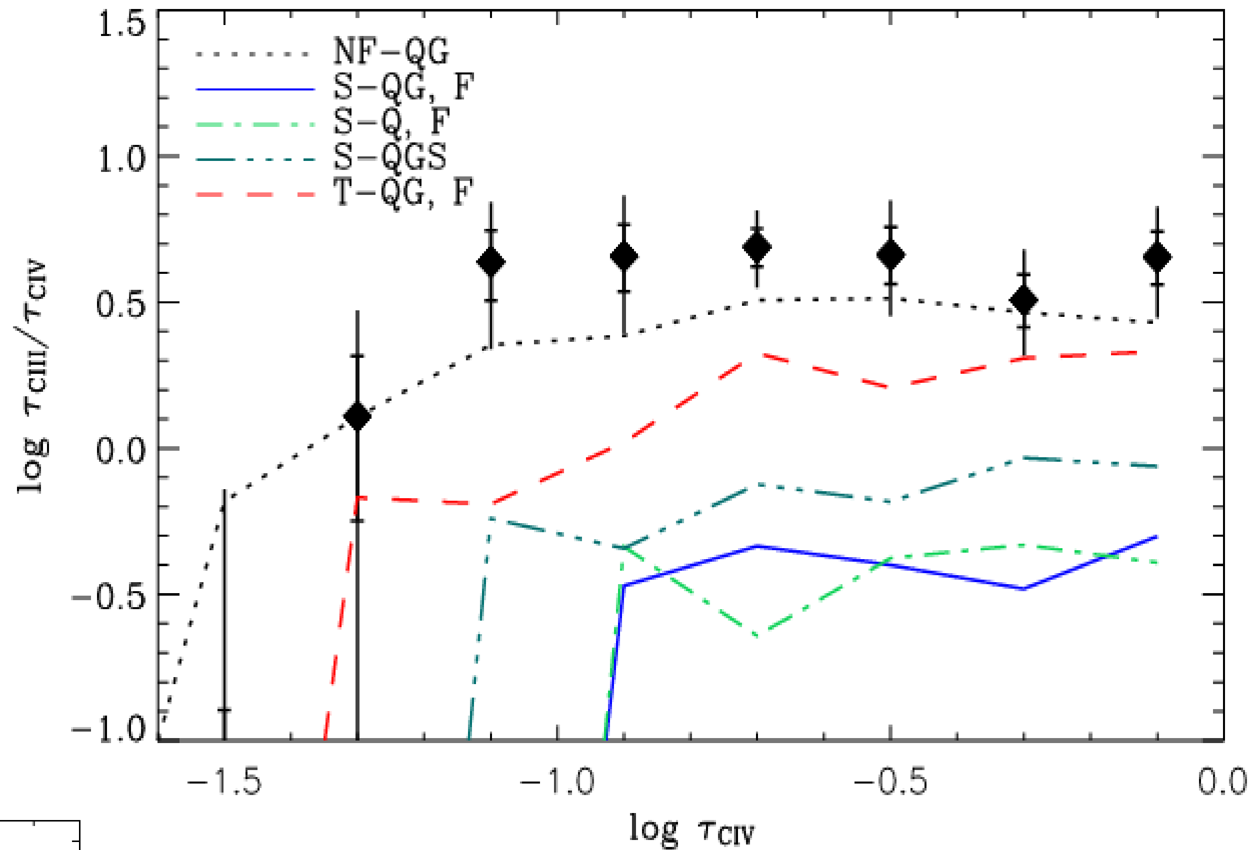

hot particles set to 2×10^4 K

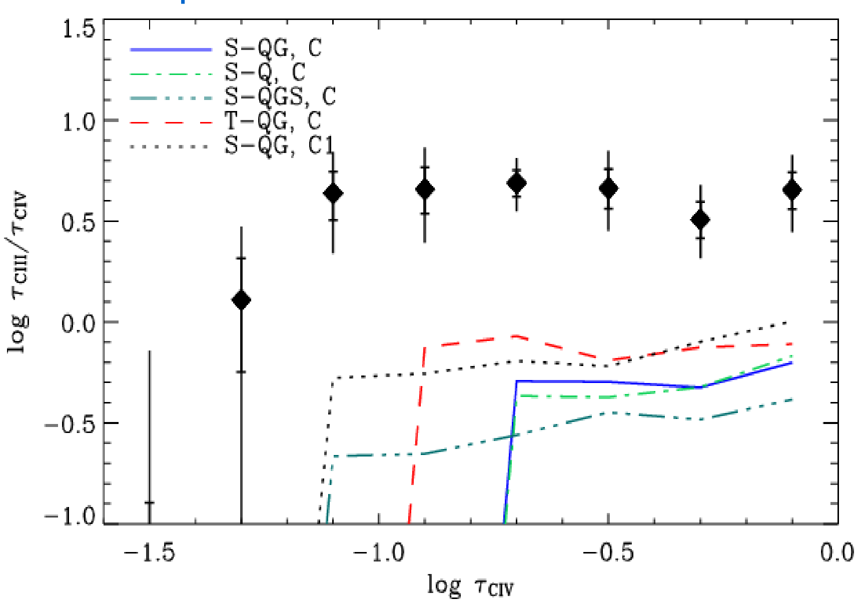

Aguirre, Schaye, Hernquist, Kay, Springel, Theuns (2005)

→ The enriched gas has too low density

Changes in the abundance of objects due to the revised WMAP3 cosmology

The evolution of the halo mass function is arguably the most fundamental tracer of nonlinear structure growth

HALO MASS FUNCTION OF THE MILLENNIUM COSMOLOGY

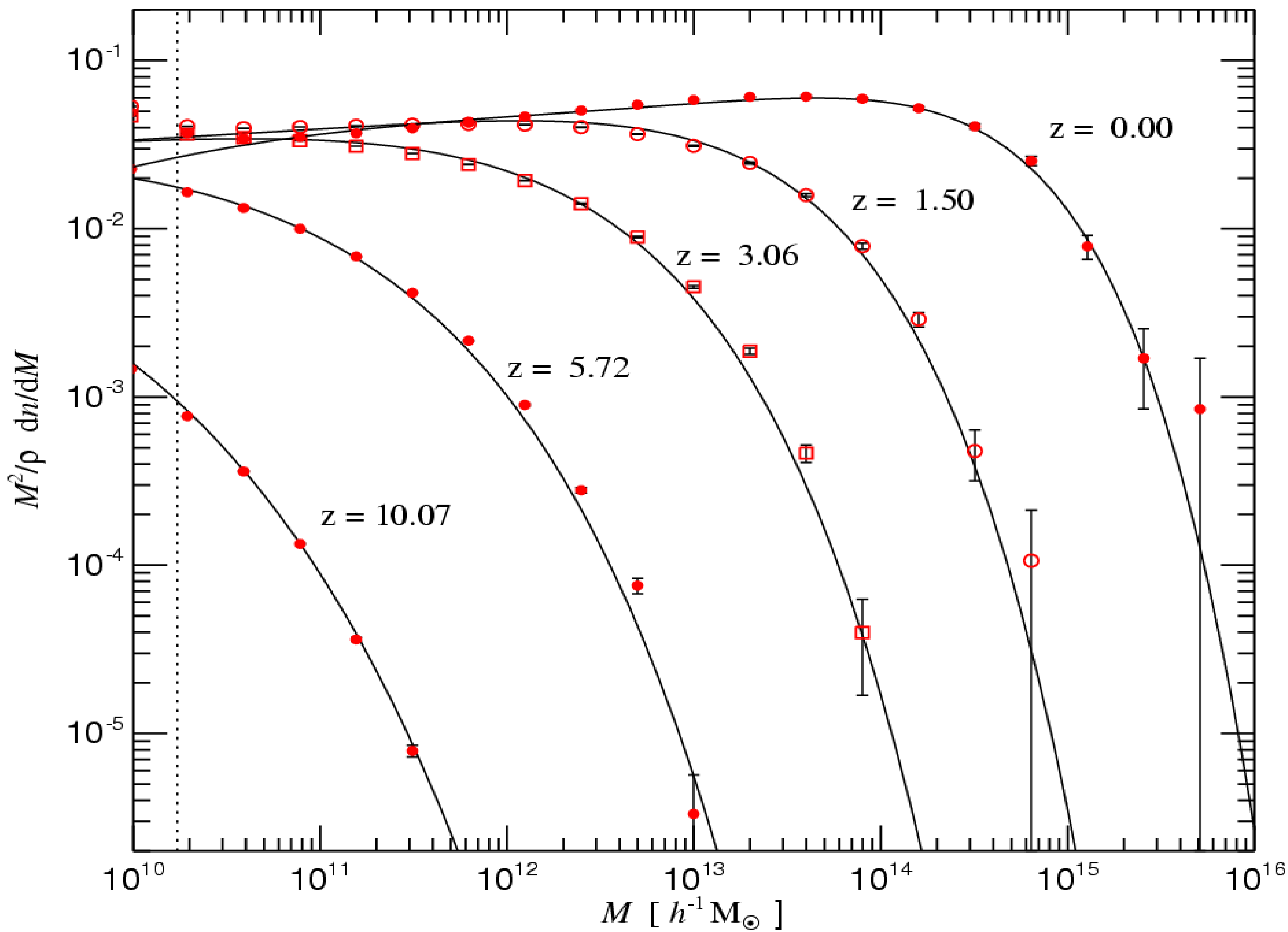

The Sheth & Tormen mass function provides a significantly better description than Press & Schechter

MASS MULTIPLICITY FUNCTION

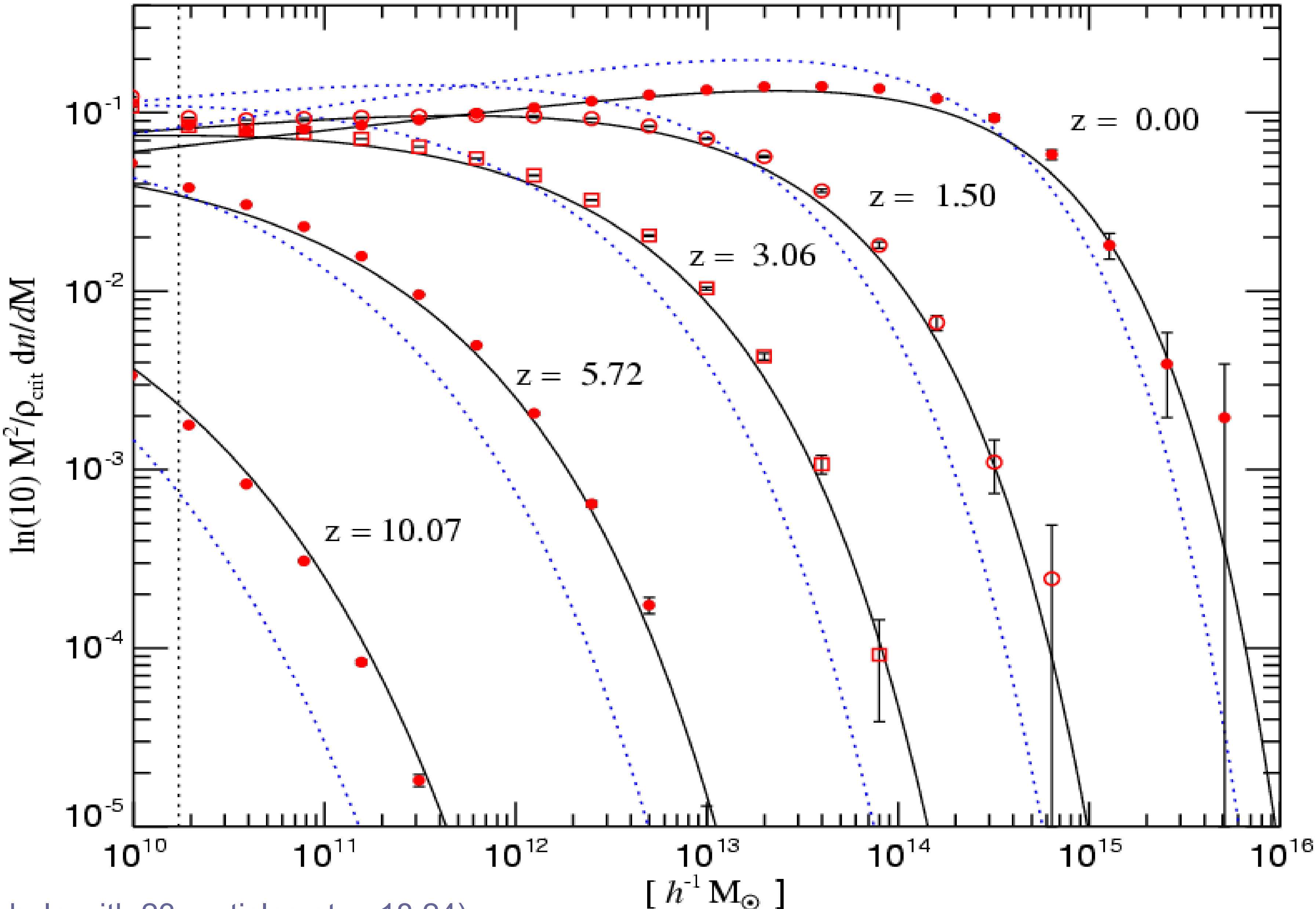

(First halo with 23 particles at z=18.24)

Some of the fundamental cosmological parameters have moved substantially in the third-year data release of WMAP

COSMOLOGICAL PARAMETERS IN THE MILLENNIUM COSMOLOGY COMPARED TO WMAP3

	Millennium Simulation (WMAP1 compatible)	**WMAP3** (best guess CMB only)
Ω_m	0.25	0.24
Ω_Λ	0.75	0.76
n	1.00	0.95
σ_8	0.90	0.74
h	0.73	0.73
Ω_b	0.045	0.042

The tilt delays the formation of small halos

CHANGES IN THE MASS FUNCTION DUE TO INTRODUCTION OF A TILT

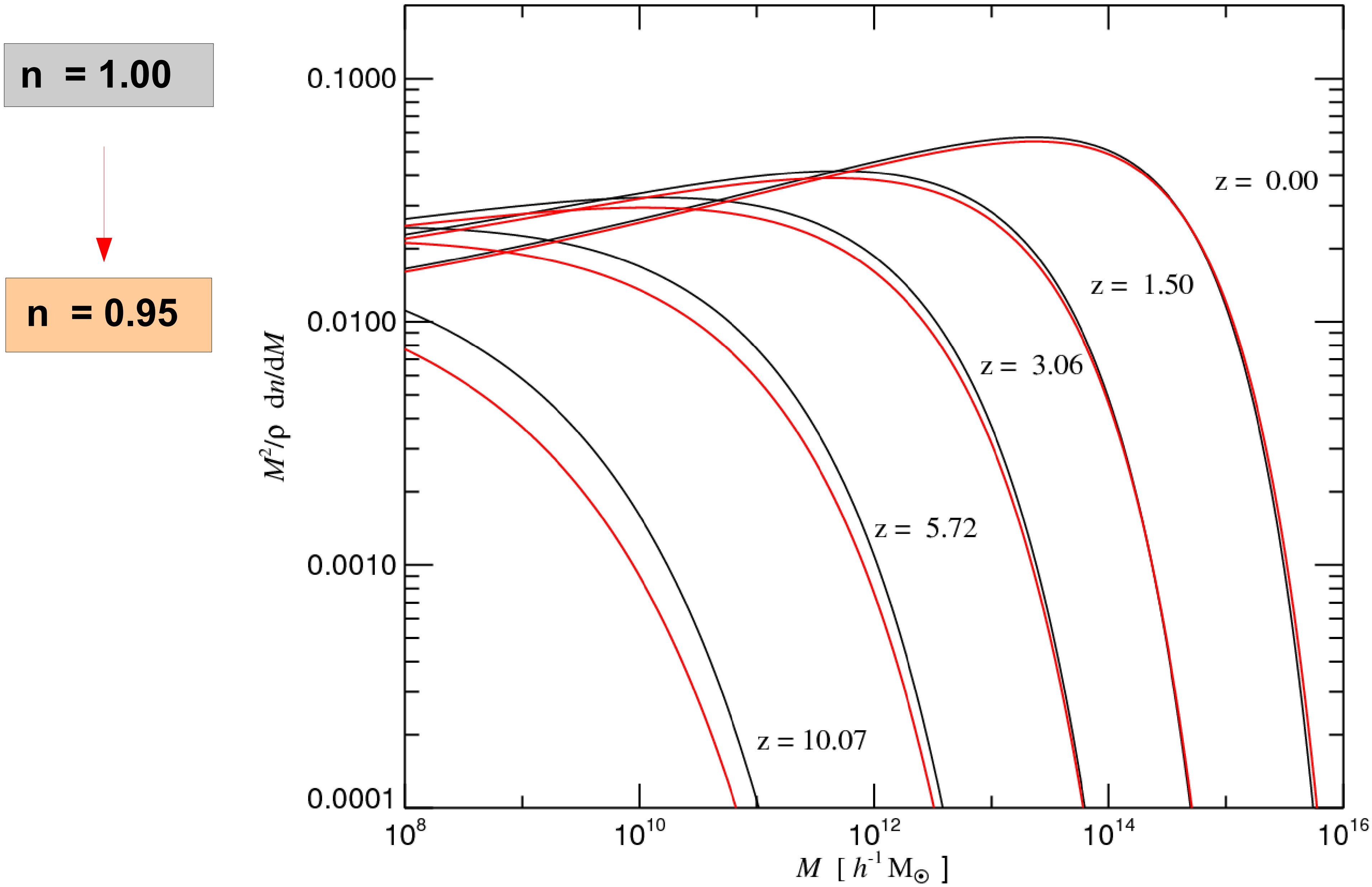

The small reduction in the dark matter density slightly affects the expansion history and the abundance of halos on all mass scales

CHANGES IN THE MASS FUNCTION DUE TO THE CHANGE IN THE MATTER DENSITY

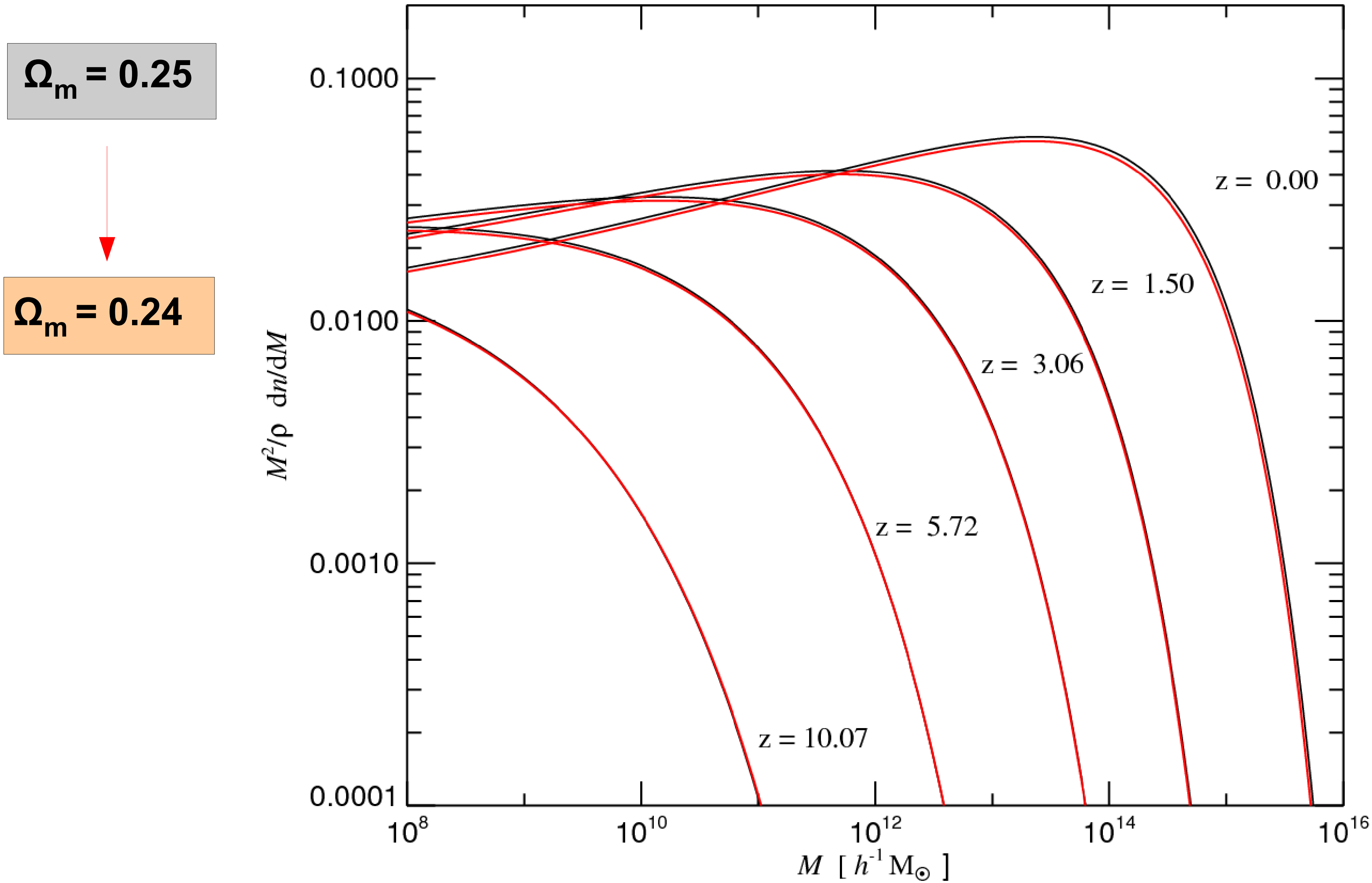

The change in the normalization strongly delays the formation of halos in the exponential tail of the mass function

CHANGES IN THE MASS FUNCTION DUE TO THE SMALLER σ_8

σ_8 = 0.90

σ_8 = 0.74

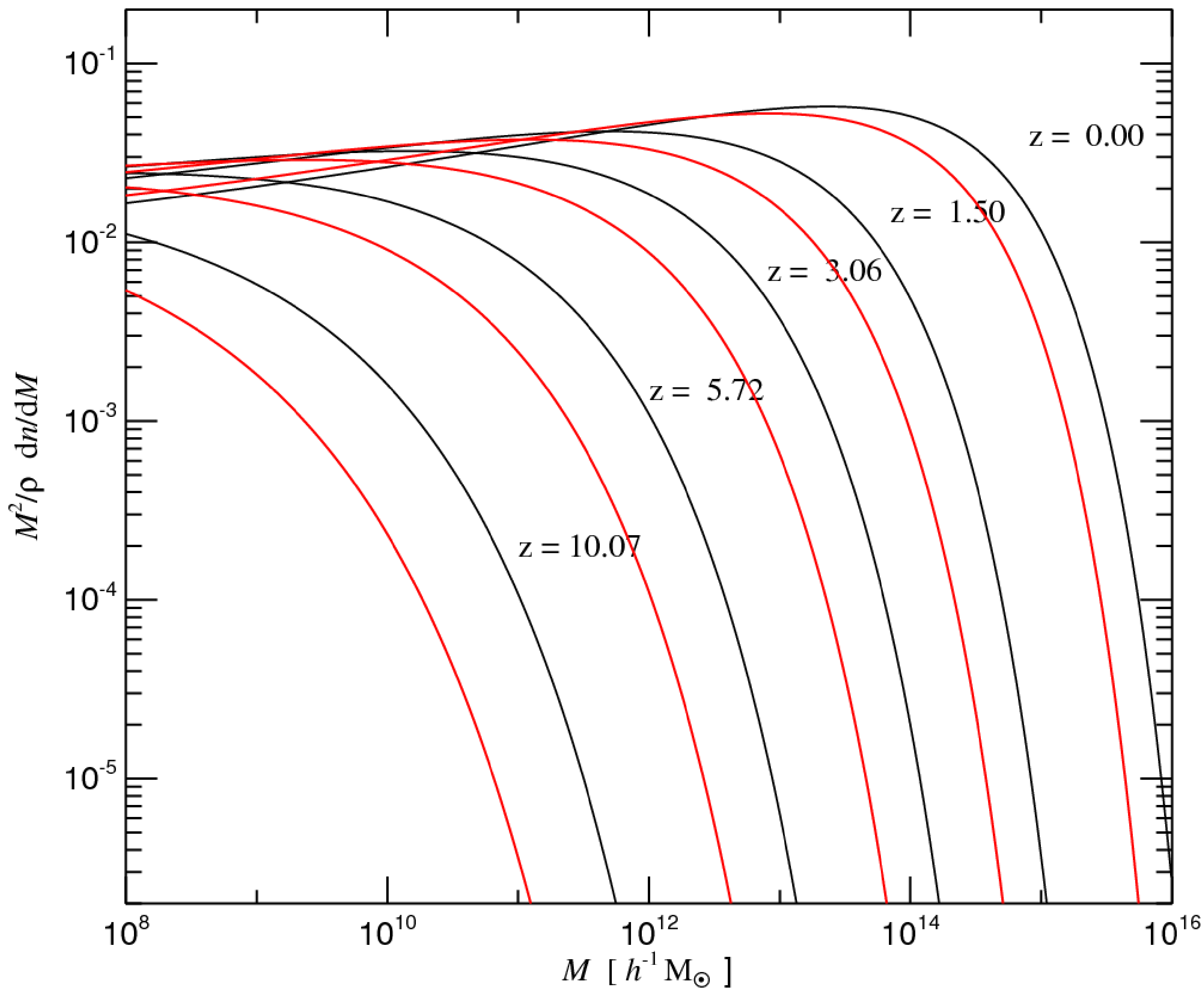

The WMAP3 cosmology leads to a substantial revision of the evolution of the cosmological halo mass function

RELATIVE CHANGE IN THE ABUNDANCE OF HALOS AT Z=0

Ω_m = 0.25
Ω_Λ = 0.75
n = 1.00
σ_8 = 0.90
h = 0.73
Ω_b = 0.045

Ω_m = 0.24
Ω_Λ = 0.76
n = 0.95
σ_8 = 0.74
h = 0.73
Ω_b = 0.042